Universidad de Oviedo

Programa de Doctorado en Biomedicina y Oncología Molecular

New intervention strategies in aging and cancer based on gene edition and proteostasis modulation

Nuevas estrategias de intervención en envejecimiento y cáncer basadas en la edición génica y la modulación de la proteostasis

Doctoral Thesis

Olaya Santiago Fernández

January, 2021

Universidad de Oviedo
Universidá d'Uviéu
University of Oviedo

RESUMEN DEL CONTENIDO DE TESIS DOCTORAL

1.- Título de la Tesis	
Español/Otro Idioma: Nuevas estrategias de intervención en envejecimiento y cáncer basadas en la edición génica y la modulación de la proteostasis	Inglés: New intervention strategies in aging and cancer based on gene edition and proteostasis modulation

2.- Autor	
Nombre: Olaya Santiago Fernández	DNI/Pasaporte/NIE: [redacted]
Programa de Doctorado: Biomedicina y Oncología Molecular	
Órgano responsable: Instituto Universitario de Oncología del Principado de Asturias (IUOPA)	

RESUMEN (en español)

El envejecimiento es un proceso complejo caracterizado por un declive funcional que produce un aumento en la incidencia de enfermedades que finalmente conducen a la muerte. En los últimos años, se ha demostrado que tanto mecanismos celulares autónomos como mecanismos sistémicos pueden contribuir al desarrollo del envejecimiento. Abordar el estudio y tratamiento del envejecimiento y de enfermedades relacionadas, como el cáncer, requiere por lo tanto de aproximaciones integrativas. En la presente Tesis Doctoral, nos hemos valido del uso de modelos murinos y del análisis de especies animales longevas para explorar mecanismos involucrados en el envejecimiento y el cáncer, y proponer nuevas estrategias de intervención. En primer lugar, hemos investigado el uso de la edición génica como posible tratamiento de la progeria de Hutchinson-Gilford (HGPS), una enfermedad rara de envejecimiento acelerado. Para ello, hemos utilizado el sistema CRISPR/Cas9 para evitar la producción de progerina, proteína tóxica causante de esta patología. La administración de este sistema en un modelo murino de HGPS ha demostrado reducir el fenotipo progeroide y alargar la vida de estos ratones. Paralelamente, hemos realizado un análisis bioinformático de genes involucrados en la reparación del ADN en dos especies de tortugas gigantes. De este modo, hemos obtenido potenciales genes candidatos asociados a longevidad y resistencia a cáncer en estas especies. Por último, hemos explorado mecanismos de regulación de la de la proteostasis, a través del factor AIRAPL, y ensayado su posible modulación mediante intervención genética y mediante dietas basadas en el ayuno.

RESUMEN (en Inglés)

Aging is a complex process characterized by a functional decline that leads to an increased vulnerability to several pathologies, which finally drive to death. Over the last years, both cell-autonomous and systemic mechanisms have been proposed to contribute to the development of aging. Integrative approaches are therefore needed to address the study and treatment of aging and age-related diseases, such as cancer. In the present Doctoral Thesis, we have used mouse models and long-lived wild species analysis to explore the mechanisms involved in aging and cancer and propose new intervention strategies. First, we have investigated the use of genetic edition as a potential treatment for Hutchinson-Gilford progeria syndrome (HGPS), a rare premature aging disease. For this purpose, we have used the CRIPSR/Cas9 system to avoid progerin production, a toxic protein causing this disorder. Administration of this system to an HGPS mouse model has demonstrated to reduce the progeroid phenotype and extend lifespan. Secondly, we have carried out a bioinformatic analysis of DNA repair genes in two giant tortoise species. This way, we have obtained potential candidate genes associated to longevity and cancer resistance in both species. Finally, we have explored proteostasis regulatory mechanisms, though AIRAPL factor, and assayed their possible modulation through genetic intervention and fasting-based diets.

SR. PRESIDENTE DE LA COMISIÓN ACADÉMICA DEL PROGRAMA DE DOCTORADO EN BIOMEDICINA Y ONCOLOGÍA MOLECULAR

ABBREVIATIONS

AAV	adeno-associated viruses
ABE	adenine base editor
ATP	adenosine triphosphate
BER	base excision repair
bp	base pair
CBE	cytosine base editors
cDNA	complementary deoxyribonucleic acid
CI	confidence interval
CMA	chaperone-mediated autophagy
CML	chronic myeloid leukemia
CRISPR	clustered regularly interspaced short palindromic repeats
DAPI	4’,6-diamidino-2-phenylindole
DMEM	Dulbecco’s modified Eagle’s medium
DNA	deoxyribonucleic acid
DSS	dextran sulfate sodium
EDTA	ethylenediaminetetraacetic acid
ER	endoplasmic reticulum
ERAD	endoplasmic reticulum-associated protein degradation
ET	essential thrombocythemia
FBS	fetal bovine serum
FTI	farnesyltransferase inhibitor
GH	growth hormone
H&E	hematoxylin and eosin
HDR	homology-directed repair
HGPS	Hutchinson-Gilford progeria syndrome
HR	homologous recombination
HRP	horseradish peroxidase
ICMT	isoprenylcysteine carboxylmethyltransferase
IGF-1	insulin like growth factor 1
IIS	insulin/IGF signaling
iPSCs	induced pluripotent stem cells
kb	kilobase

kDa	kilodalton
KO	knock-out
MCA	3-methylcholanthrene
MEF	mouse embryonic fibroblast
MMR	mismatch repair
MPN	myeloproliferative neoplasms
MPO	myeloperoxidase
mRNA	messenger ribonucleic acid
NER	nucleotide excision repair
NHEJ	non-homologous end-joining
PAM	protospacer-adjacent motif
PBS	phosphate buffered saline
PCR	polymerase chain reaction
PFA	paraformaldehyde
PMF	primary myelofibrosis
PQC	pre-emptitive quality control
PV	polycythemia vera
qRT-PCR	quantitative reverse transcriptase-PCR
RNA	ribonucleic acid
ROS	reactive oxygen species
RT-PCR	reverse transcriptase-PCR
SD	standard deviation
SDS	sodium dodecyl sulfate
SEM	standard error of the mean
SUMO	small ubiquitin-like modifier
TALEN	transcription activator-like effector nucleases
TBE	tris-borate EDTA
TG	transgenic
TUNEL	terminal deoxynucleotidyl transferase dUTP nick end labeling assay
UPR	unfolded protein response
UPS	ubiquitin-proteasome system
WT	wild-type
ZFN	zinc-finger nuclease

CONTENTS

INTRODUCTION

The intriguing phenomenon of aging and the prospects to intervene on it have haunted the human being throughout history. Aging can be defined as a complex process characterized by a physiological decline that leads to an increased vulnerability to several diseases, which ultimately drive to death[1,2]. These pathologies include cardiovascular disorders, neurodegenerative diseases and cancer. At first, cancer appears to be an opposite phenomenon to aging, as cancer implies an aberrant increase in cellular fitness[3] while aging is associated with a loss of this feature[1]. Nevertheless, these two processes share common mechanisms and origins, being their most important cause the accumulation of cellular damage[4].

The phenomenon of aging has been conserved in evolution, occurring in most organisms, and is, at least in part, controlled by classical signaling pathways[5,6]. Over the last few years, research in the field of longevity has benefited from the study of centenarians[7-9] and long-lived organisms[10-12]. Genomics, transcriptomics, proteomics and other multi-omics analysis of both groups can project shared biochemical pathways involved in lifespan extension. On the contrary, progeroid syndromes may offer a model of accelerated aging, allowing the identification of regulatory mechanisms involved in both progeria and physiological aging[13]. Thus, integrative approaches are essential to unravel the keys of the multifaceted process of aging and to develop intervention strategies to prevent or delay some of its associated diseases.

The nine hallmarks of aging

In 2013, the aging research field experienced a breakthrough when the molecular, cellular and systemic features of aging were classified in nine hallmarks[1]. These hallmarks should ideally achieve three principles: they should appear during normal aging; their exacerbation should lead to accelerated aging; and their reduction should delay aging, conducting therefore to a healthier lifespan. Following these criteria, nine hallmarks were proposed: genomic instability, telomere attrition, epigenetic alterations, loss of proteostasis, deregulated nutrient sensing, mitochondrial dysfunction, cellular senescence, stem cell exhaustion, and altered intercellular communication.

These nine candidates have also been grouped into three categories: primary, antagonistic and integrative hallmarks, depending on their characteristics. The primary hallmarks would correspond to the main causes of damage, playing all of them clearly

negative roles. This category includes genomic instability, telomere attrition, epigenetic alterations and loss of proteostasis. The antagonistic hallmarks would comprise those with a compensatory response to damage and have opposing effects depending on their intensity. This category encompasses deregulated nutrient sensing, mitochondrial dysfunction and cellular senescence. Integrative hallmarks result from the previous two groups and are responsible for the decline associated with aging, comprising stem cell exhaustion and altered intercellular communication[1] (**Fig. 1**).

Figure 1. Hallmarks of aging. The nine hallmarks of aging are grouped into primary hallmarks, antagonistic hallmarks and integrative hallmarks. Adapted from López-Otín *et al*., 2013.

Genomic instability

Accumulation of genomic damage throughout life is a well-known hallmark of aging, affecting both nuclear and mitochondrial DNA[4,14]. These genetic lesions, produced by intrinsic or extrinsic agents, include point mutations, translocations, gene disruption, chromosomal gains and losses and telomere shortening. To reduce these alterations,

different DNA repair mechanisms exist in the cell. Interestingly, many premature aging syndromes are caused by mutations in DNA repair genes resulting in an increased accumulation of DNA damage[15]. Besides, promotion of chromosome integrity can delay aging in model organisms[16].

Telomere attrition

Telomerase, the enzyme responsible for chromosome ends replication, remains inactive under most circumstances in somatic cells. This incapacity to replicate DNA terminal ends is responsible for the limited proliferative capacity of cells *in vitro*[17] and leads to a shortening of telomeres during normal aging in mammals[18]. Moreover, it has been suggested that short telomeres are associated with a higher mortality risk[19]. Conversely, experimental induction of telomerase or the increase in telomere length in mice extends longevity and improves several biomarkers of aging[20,21].

Epigenetic alterations

Different epigenetic changes, involving variations in DNA methylation patterns, post-translational modifications of histones and chromatin remodeling, are accumulated during lifetime[22]. This accumulation of specific marks in the epigenome is associated with aging and experimental induction of epigenetic alterations can trigger premature aging phenotypes in animal models. The deacetylase SIRT6 represents an example of how changes in the epigenome can play a role in longevity, as its deficiency leads to premature aging, while its overexpression extends lifespan in mice[23,24].

Loss of proteostasis

Quality control mechanisms in the cell guarantee the stability and functionality of the proteome through chaperone-mediated protein folding, and the autophagy-lysosome and ubiquitin-proteasome proteolytic systems. During aging, there is a decline in the activity of these systems, leading to an accumulation of damaged and misfolded proteins and the consequent loss of protein homeostasis, which can impair tissue function[25]. Moreover, chronic accumulation of aggregates of these misfolded proteins is associated with neurodegenerative pathologies, such as Alzheimer's and Parkinson's disease[26]. Many studies have shown that experimental disruption of proteostasis can lead to aging-

associated pathologies and premature death[27], whereas an increased activity of the proteostasis network increases health and lifespan[28,29].

Deregulated nutrient sensing

Cells respond to fluctuations in the levels of nutrients through different signaling pathways. Among them, the best known is the insulin and IGF-1 signaling (IIS) pathway, which controls the FOXO family of transcription factors and the mTOR complexes, both involved in longevity[30]. Furthermore, there is evidence that anabolic signaling, activated in periods of nutrient abundancy, accelerates aging, whereas reduced nutrient signaling delays it[31]. Accordingly, excessive intake of carbohydrates has a negative impact on health, known as carbotoxicity, which leads to aging-related diseases[32]. By contrast, caloric restriction or pharmacological interventions that mimic a deprivation in nutrients extend longevity and healthspan in different organisms[33,34].

Mitochondrial dysfunction

Aging is generally associated with a gradual dysfunction of mitochondria, characterized by a reduced effectiveness of the respiratory chain due to an increase in electron leakage and a reduction in ATP generation[35]. During aging, a rise in the levels of reactive oxygen species (ROS) and a decrease in the efficiency of mitochondrial energetics are observed. Moreover, mitochondrial dysfunction can also lead to a premature aging phenotype in mice[36,37].

Cellular senescence

As a response to stress, cells can undergo a process of permanent proliferative arrest accompanied by alterations in their phenotype, including chromatin and secretome changes and hyper-activation of tumor suppressor signaling[38]. Although cellular senescence has diverse roles, its main functions in adults seem to be to avoid the spread of damaged cells and to promote tissue repair and oncogenic suppression[39]. However, during aging, there is an increase in the accumulation of senescent cells, which might play a causative role in this process. Accordingly, several studies have shown that elimination of senescent cells in progeroid mice can ameliorate their phenotype[40] and their clearance in wild-type mice attenuates physiological deterioration and extends lifespan[41].

Stem cell exhaustion

A decline in stem cell function is responsible for the decay in the regenerative potential of tissues observed during aging. Stem cell exhaustion has been described in most cell compartments, especially in the hematopoietic system[42], muscle[43] and brain[44]. Being the result of different types of aging-associated damage, attrition of stem cells constitutes an integrative hallmark. Moreover, it has been proposed that stem cell rejuvenation may delay the process of aging[45].

Altered intercellular communication

Intercellular communications, either endocrine, neuroendocrine or neuronal, tend to get deregulated during aging[46,47]. The pro-inflammatory phenotype associated with aging, known as inflammaging, is one of the best studied alterations. In this sense, there are several proofs of the role of the microenvironment in aging. Different studies support both the role of dysfunctional hematologic cells in promoting aging-associated features[48] and the rejuvenating properties of young blood in the organism[49-51]. Recently, the gut microbiome has also been described to exert systemic effects in the organism and its modulation can extend lifespan in progeroid mice[52].

Short-lived and long-lived models of longevity

An enormous diversity in longevity exists in nature as a result of modifications in the genomes of species throughout evolution. Only in the subphylum of vertebrates, more than a 500-fold change in maximal lifespan has been reported[53]. In recent years, comparative genomics of short-lived and long-lived animals has been used to uncover putative genetic variants involved in the modulation of longevity. Analysis of short-lived species, such as the African killifish, can contribute to understand its reduced lifespan and its adaptations to life-threatening environments[54]. In contrast, annotation of the genomes of the bowhead whale[11], the naked mole rat[10], the Brandt's bat[55] and the elephant[56] has allowed the identification of candidate genes contributing to exceptional lifespans and resistance to age-related diseases. Specific variants and copy number variations have been identified in genes involved in all of the hallmarks of aging. Therefore, positive selection and adaptations in several genes involved in DNA repair, proteostasis maintenance or mitochondrial function were described in long-lived species.

Moreover, variants in nutrient-sensing pathways were also underscored, affecting especially the IIS pathway[55,57]. Altogether, data obtained from these comparative analyses can help to understand the modulation of aging, which is crucial for the subsequent development of intervention strategies against its related diseases. However, further analyses including more long-lived species from less explored families, such as giant tortoises, are still needed.

Progeria as a model of the aging process

Over the last years, research on accelerated aging syndromes has led to a deeper knowledge of the molecular mechanisms involved in normal aging. In these disorders, many of the characteristics of physiological aging are manifested prematurely and several of its hallmarks are recapitulated[1,58]. Premature aging syndromes are mainly caused by alterations in the DNA repair machinery or in the nuclear envelope architecture. Defects in DNA repair mechanisms are the principal cause of progeroid syndromes, as occurs in the case of Werner syndrome. This syndrome starts to manifest around the third decade of life with aged facies, cataracts, grey hair, subcutaneous calcification, arteriosclerosis, diabetes mellitus and high incidence of cancer. This finally drives to a premature death at a median age of 54 years[15]. Classical Werner syndrome is caused by null mutations in *WRN* gene, which encodes a protein of the RECQ family[59]. This protein has DNA exonuclease and helicase activities and performs important functions in DNA repair, recombination and replication, as well as in telomere maintenance[60].

The second cause of premature aging disorders —globally known as progeroid laminopathies— is related to defects in the nuclear envelope structure, which ultimately produce accumulation of DNA damage and chromosome instability in the cell. Hutchinson-Gilford progeria syndrome (HGPS) is the best known of these ultrarare disorders. HGPS patients develop aging-associated symptoms early in childhood, such as growth impairment, hair loss, lipodystrophy, joint contractures and cardiovascular disease, which finally drive to their premature death at around 14.5 years of age[61,62]. In 2003, the molecular basis of this syndrome was found to result from a *de novo* point mutation in the *LMNA* gene (c.1824C>T; p.Gly608Gly)[63,64], coding for lamins A and C through alternative splicing. These lamins are two filamentous proteins of the inner nuclear envelope, that provide support to this structure and establish interactions with the

heterochromatin. HGPS mutation induces the activation of a cryptic splice site in exon 11 of this gene that results in the loss of 50 amino acids in the lamin A protein, leading to the production of a pathogenic isoform known as progerin.

Typically, mature lamin A is produced after a multistep posttranslational processing that seems to play a role in its target to the nuclear envelope. Thus, lamin A is initially synthesized as the precursor prelamin A, ending with a CaaX motif. First, the C-terminal cysteine undergoes a farnesylation event by farnesyltransferase. This process is followed by the proteolytic removal of the last three amino acids and the methylation of the newly exposed carboxyl group of the terminal cysteine residue by the isoprenylcysteine carboxylmethyltransferase (ICMT). In the last step, the metalloprotease FACE-1/ZMPSTE24 cleaves the terminal 15 amino acids, including the farnesyl group, finally generating mature lamin A. In progerin —the HGPS isoform of prelamin A— this last cleavage site is missing, leading to the accumulation of the constitutively farnesylated form of the protein (**Fig. 2**). It has been widely demonstrated that this protein acts on a dominant-negative way, triggering the alterations characteristic of HGPS cells and the subsequent symptoms developed by progeria patients[65].

Accumulation of progerin or other forms of altered lamin A in the cell nucleus generates defects in the morphology of the nuclear envelope and produces changes in heterochromatin organization, gene transcription, mitosis and DNA repair. HGPS recapitulates different hallmarks of aging, such as genomic instability due to the nuclear disruption, telomere attrition, epigenetic changes, senescence, alterations in metabolism and increased systemic inflammation that altogether lead to the progeroid phenotype[66]. Interestingly, it has been observed that small amounts of progerin are also produced and accumulated during normal aging through activation of the cryptic splice site altered in progeria, providing additional relevance to the study of HGPS[67].

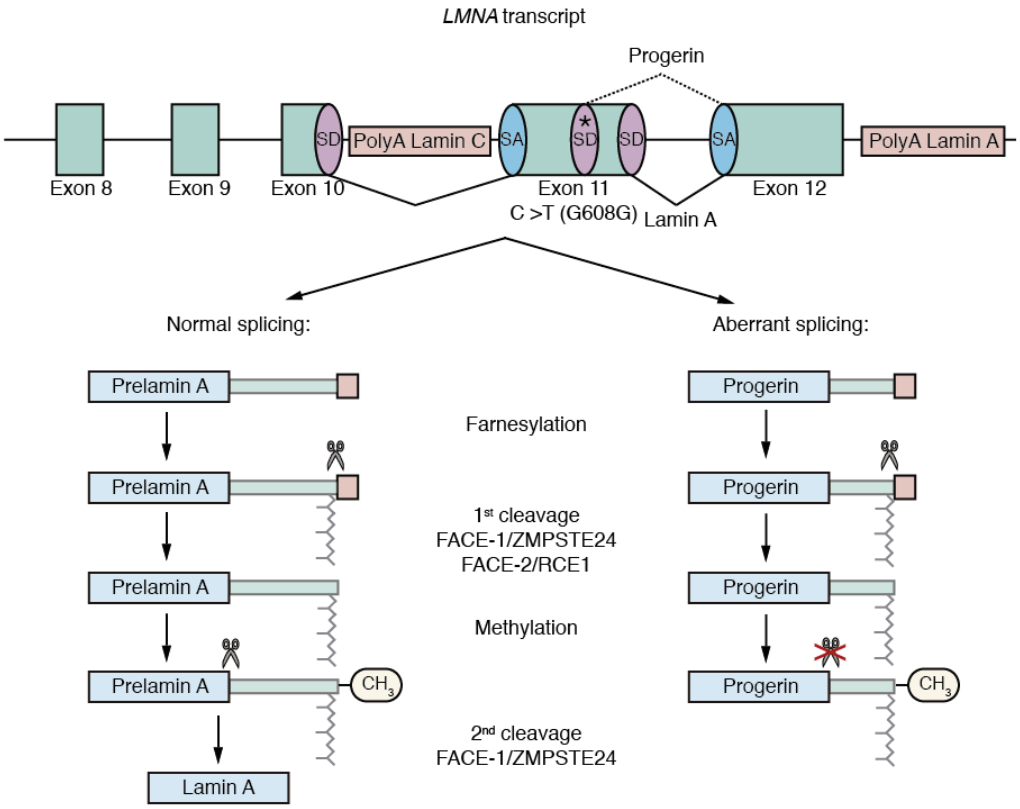

Figure 2. Posttranslational processing of lamin A in normal and HGPS cells. The C-terminal cysteine of the CaaX motif in prelamin A is farnesylated and the aaX peptides are cleaved off afterwards. Then, the farnesylated cysteine suffers a methylation and finally 15 amino acids including this modified cysteine are cleaved off to produce the mature lamin A. Adapted from Osorio *et al*., 2008.

Progeroid mouse models

Over the last years, different progeroid mouse models —and even minipig and monkey models— that phenocopy many of the characteristics of HGPS have been developed[68-72]. These animals represent useful tools to investigate the molecular mechanisms underlying progeroid syndromes and normal aging, and to test therapeutic strategies against these pathologies[73]. Two of these mouse models (*Zmpste24*-deficient mice and *Lmna*$^{G609G/G609G}$ mice) were generated in our laboratory.

Zmpste24-deficient mouse model

The generation of the *Zmpste24*-deficient mouse allowed the identification of the zinc metalloprotease ZMPSTE24 as a critical enzyme in the maturation process of lamin A[68]. Therefore, this mouse model accumulates farnesylated prelamin A in the nuclear envelope, which constitutes another form of unprocessed lamin A with similar effects to progerin. Thus, *Zmpste24*$^{-/-}$ mice phenocopy many of the symptoms of the HGPS patients,

developing growth impairment, lypodystrophy, osteolytic lesions, lordokyphosis, hypoglycemia and heart alterations, and show a shortened lifespan of approximately 5 months of age[68] (**Fig. 3a-d**). This phenotype makes of *Zmpste24*-deficient mouse a valuable model for the study of progeria, but fails to imitate the aberrant splicing of lamin A present in HGPS children.

Nevertheless, the use of *Zmpste24*$^{-/-}$ mouse models has allowed to unravel many of the cellular and systemic alterations caused by prelamin A accumulation[74]. Transcriptional analysis of tissues from these mice revealed a hyperactivation of p53 signaling, which played a role in the premature aging phenotype[75]. Also, the lysosome-autophagy system, which normally declines with age, is markedly activated in these progeroid mice[76]. Stem cell dysfunction was observed in the epidermal stem cells of *Zmpste24*-deficient mice, showing reduced proliferation and increased apoptosis[77]. All of these findings also seem to play a relevant role in the pathology of human HGPS.

Regarding systemic alterations, *Zmpste24*-deficient mice show a marked deregulation in the GH (growth hormone)/IGF-1 (insulin-like growth factor 1) rate pathway, with a gradual reduction in IGF-1 and an increase of GH levels. These alterations in the somatotroph axis could explain some progeroid features of these mice, such as the reduction in body size and muscle development, alopecia and hypoglycemia[78]. Systemic inflammation was also observed in these mice[79]. Furthermore, this mouse model was used to demonstrate that reducing the levels of prelamin A results in a total rescue of its progeroid phenotype[75,80].

Lmna$^{G609G/G609G}$ *mouse model*

The *Lmna*$^{G609G/G609G}$ mouse model imitates the HGPS human mutation and the resulting aberrant *LMNA* splicing, therefore providing a useful tool for the evaluation of strategies focused on the correction of this event[70]. The specific point mutation was introduced in exon 11 of the *Lmna* gene (c.1827C>T; p.Gly609Gly) by using a replacing vector, which produced the activation of the cryptic splice site, then triggering the accumulation of progerin in the cell nucleus. *Lmna*$^{G609G/G609G}$ mice started to develop a progeroid phenotype early in life, with growth retardation, loss of body weight, an apparent lordokyphosis, heart dysfunction, hypoglycemia, and premature death at approximately 4 months of age[70] (**Fig. 3e-h**). Heterozygous *Lmna*$^{G609G/+}$ mice accumulated progerin on a similar way to HGPS patients —producing both lamin A and

the toxic progerin form— but they showed a normal phenotype until 8 months of age. At this age, they started to develop similar features to the homozygous phenotype and died approximately at 9 months[70] (**Fig. 3e-h**). This could be explained by the higher tolerance that mice seem to have to alterations in nuclear lamins. For this reason, homozygous *Lmna*$^{G609G/G609G}$ mice seem to be a better model for the general study of HGPS.

Transcription profiles of *Lmna*$^{G609G/G609G}$ mice revealed similar alterations to those previously detected in the *Zmpste24*-deficient mouse model, such as the hyperactivation of the p53 and the ATM-related pathways, which could be triggering the senescent phenotype in these mice. Likewise, *Lmna*$^{G609G/G609G}$ mice also showed a deregulation in the somatotroph axis, with a significant reduction in IGF-1 and an increase of GH blood levels[70]. These similarities with the *Zmpste24*$^{-/-}$ mice support the existence of common drivers of the progeroid phenotype in these mouse models.

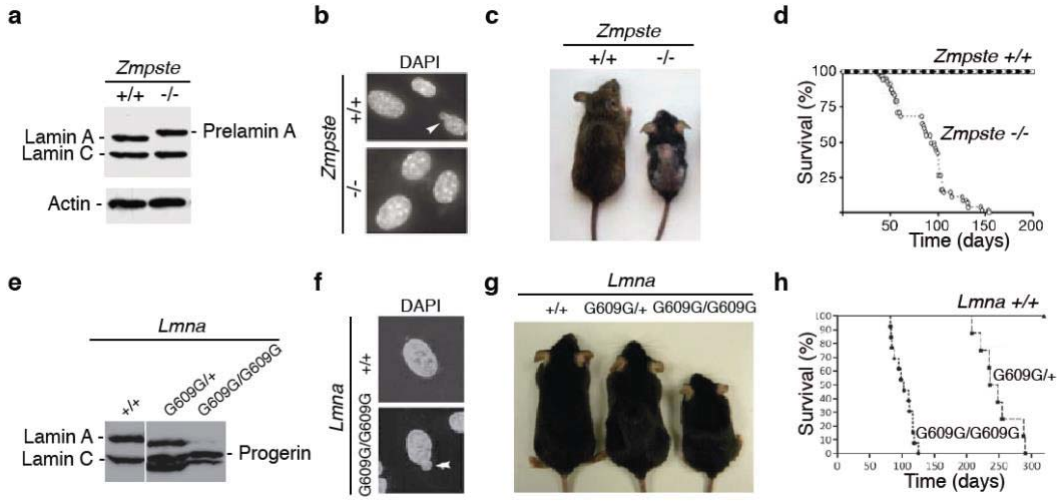

Figure 3. Characterization of two progeroid mouse models. (a) *Zmpste24*$^{-/-}$ mice produce prelamin A instead of lamin A. **(b)** Accumulation of prelamin A in the cell nuclei results in alterations in the nuclear shape, which are indicated with an arrowhead. **(c)** *Zmpste24*-deficient mice show a reduced bodyweight compared to their wild-type (WT) littermates. **(d)** *Zmpste24*$^{-/-}$ mice show a premature death. **(e)** *Lmna*$^{G609G/G609G}$ mice mainly generate progerin, while *Lmna*$^{G609G/+}$ mice produce both lamin A and progerin. **(f)** Accumulation of progerin in the cell nuclei triggers alterations in the nuclear shape, which are indicated with an arrowhead. **(g)** *Lmna*$^{G609G/G609G}$ mice show a smaller size compared to their WT littermates, while *Lmna*$^{G609G/+}$ mice are indistinguishable from WT mice the first months of life. **(h)** Heterozygous *Lmna*$^{G609G/+}$ mice show a reduced lifespan compared to WT mice, which is even shorter in the case of the homozygous *Lmna*$^{G609G/G609G}$ mice. Adapted from Pendás *et al*., 2002; Varela *et al*., 2005; Osorio *et al*., 2011.

Therapeutic strategies in progeria

Since the discovery of the *LMNA* mutation, different therapeutic strategies have been proposed for the treatment of HGPS based mainly on drug development, RNA

intervention and gene therapy approaches[13,81,82] (**Fig. 4**). The rapid development of these therapeutic strategies and the transfer of the most feasible ones to clinical trials has been possible due to the availability of different mouse models and the organization of the very few patients on an efficient progeria network.

Drug and dietary interventions

Due to the farnesylation state of progerin, one of the first drugs assayed in progeria were the farnesyltransferase inhibitors (FTIs), which had previously been approved for cancer treatment. After promising results in HGPS cell cultures[83-87] and progeroid mouse models[88-91], clinical trials were conducted and showed a modest improvement in some of the progeroid symptoms[92-94] (ClinicalTrials.gov: NCT00425607 and NCT03895528). Concurrently, it was discovered that progerin also suffered a process of geranylgeranylation after the treatment with FTIs and this event produced a similar toxic form of progerin[95]. Both processes of geranylgeranylation and farnesylation could be blocked by a combined treatment with statins and aminobisphosphonates. This therapeutic strategy was first assayed in HGPS cells and in the *Zmpste24*-deficient mouse model, with promising results in reducing the progeroid phenotype[95], and is now under clinical trials, alone or in combination with a FTI[96] (ClinicalTrials.gov: NCT00731016, NCT00916747 and NCT00879034).

The mTOR inhibitor rapamycin, known to have a positive impact on retarding aging, was proven to enhance progerin degradation through autophagy, resulting on a reduction of the nuclear alterations and senescence in HGPS cells[97,98] and in aging mouse models[99-101]. Conversely, autophagy has also been reported to be upregulated in an HGPS mouse model, in association with diverse metabolic alterations[76]. A new clinical trial, using rapamycin in combination with a FTI, will unravel the effect of this drug on progeria patients (ClinicalTrials.gov: NCT02579044). Another pro-longevity compound, resveratrol, an activator of SIRT1 which interacts with lamin A, has also been evaluated as a therapy for progeria. In HGPS, SIRT1 shows a reduced deacetylase activity that results in an exhaustion of stem cells. Resveratrol was reported to rescue the stem cell decline and to improve the progeroid phenotype in the *Zmpste24*$^{-/-}$ mouse model[102].

At a systemic level, inhibition of the hyperactivated NF-κB signaling by nonsteroidal anti-inflammatory drugs has also shown promising results in reducing the progeroid symptoms[79]. Furthermore, dietary interventions based on methionine

restriction or magnesium supplementation extended lifespan in different progeroid mouse models by reducing inflammation or increasing ATP availability respectively[103,104]. Correction of intestinal dysbiosis found in HGPS mice also improved their phenotype and lifespan, opening the possibility of microbiome-based approaches for HGPS treatment[52].

RNA therapy

RNA therapy has been widely considered a promising candidate treatment for progeria, as the cause of this syndrome is the activation of a cryptic splice site. In this sense, a strategy based on siRNAs was first developed to eliminate the progerin mRNA in HGPS cells[105]. Likewise, morpholino antisense oligonucleotides were designed to modulate the altered splice site. These antisense approaches were tested in HGPS fibroblasts[106] and mice[70,107], resulting on an important improvement of the progeroid phenotype. Still, the *in vivo* delivery of these agents remains the main challenge for the application of these promising strategies.

Gene therapy

Nowadays, gene therapy is getting more power in addressing the correction of genetic-based diseases due to the discovery and development of Zinc-Finger Nucleases (ZFNs), transcription activator-like effector nucleases (TALENs), and specially Clustered Regularly Interspaced Short Palindromic Repeats (CRISPR) strategies. Due to its genetic origin, HGPS is a potential candidate for the evaluation of gene-editing treatments. As a proof of principle, in 2011, multiple *LMNA* mutations were corrected by homologous recombination in iPSCs derived from patient fibroblasts[108].

The recent development of CRISPR/Cas9 gene editing tools has provided promising alternatives for the treatment of several diseases[109,110]. This system was initially discovered in bacteria, as part of their adaptive immune system, and its modified mechanism for research use involves a programmable Cas9 endonuclease directed by a single-guide RNA (sgRNA). This sgRNA, allows the system to recognize its target region plus a protospacer adjacent motif (PAM) sequence that varies between bacteria. Upon recognition, the nuclease generates a double-strand break in the DNA, which is mainly repaired through non-homologous end-joining (NHEJ) producing insertions and deletions (indels) in the target region that can lead therefore to the disruption of a gene.

Alternatively, the double-strand breaks can be repaired by homology-directed repair (HDR), which can be used to insert specific mutations in the DNA[111].

Since its discovery, the CRISPR system has undergone a rapid evolution to address specific issues, such as the emergence of RNA editing nucleases[112], base-editors[113] and prime editing[114] tools. Nevertheless, specific problems such as the off-target effects or possible toxicity still exist. The system has already been tested for different syndromes in both cell cultures and mouse models, such as Duchenne muscular dystrophy[115], β-hemoglobinopathies[116], myocilin-associated glaucoma[117], metabolopathies[118] or deafness[119], showing very encouraging results in all of them. In HGPS, progerin plays a dominant negative role, thus the potential gene therapy could be focused on either correcting or disrupting the mutated *LMNA* gene. In this sense, the development of lamin A-deficient mouse models showed that the mice that only express lamin C have an apparent normal phenotype and lifespan[70,80], so both options seem feasible.

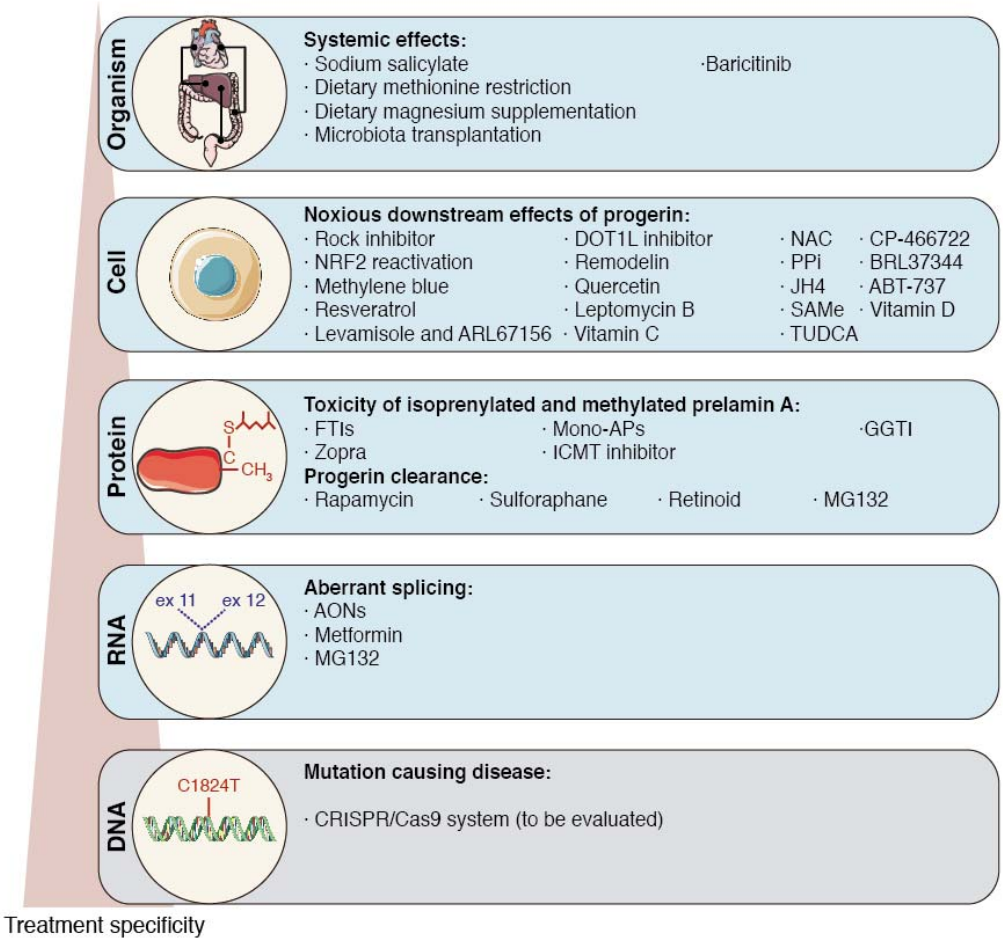

Figure 4. Therapies proposed for HGPS treatment. Therapeutic strategies are ranged from those targeting only the DNA to those having a systemic effect in the organism. Adapted from Gordon *et al*., 2014; Harhouri *et al*., 2018. This figure was made with Servier Medical Art templates, which are licensed under a Creative Commons Attribution 3.0 Unported License: (https://smart.servier.com).

Protein homeostasis in aging and cancer

Maintenance of protein homeostasis, or proteostasis, is guaranteed by a complex network in the cell that prevents and corrects possible alterations of the proteome. Under chronic stress, the proteostasis network gets compromised, which can lead to the development of proteotoxicity in the cell[26]. This loss of proteostasis is a primary hallmark of aging and is associated with many age-related pathologies, such as cancer, type 2 diabetes or neurodegenerative diseases[1]. Conversely, a correct proteostasis maintenance is related to healthy aging. Long-lived animals show a higher proteome stability[120] and interventions that enhance proteostasis in animal models lead to a delay of aging and age-related diseases[121,122].

The wide proteostasis network, which includes approximately 800 proteins, is formed by three main components: molecular chaperones, the autophagy-lysosome system and the ubiquitin-proteasome system (UPS) (**Fig. 5**). Besides these cellular systems, some organelles show specific responses against loss of proteostasis, with the endoplasmic reticulum (ER) standing out among them. Furthermore, recent studies point to the existence of not only cell-autonomous but also systemic proteostasis networks.

Chaperones

Newly synthesized proteins generally need the assistance of molecular chaperones to guarantee their correct folding and to prevent their aggregation. Still, as proteins are dynamic macromolecules, chaperones must surveil them during their lifetime to ensure the maintenance of proteostasis. If a protein becomes misfolded, chaperones can either refold it or target it for degradation, depending on different factors and conditions in the cell[123]. Furthermore, molecular chaperones also play a role in protein trafficking. Chaperones are grouped in different classes forming cooperative pathways and many of them are known as heat-shock proteins (HSPs), as they are upregulated under stress conditions.

During aging, the function of stress-induced chaperones becomes progressively impaired, contributing to the loss of proteostasis. Deficiencies in chaperones have been associated with multiple age-related diseases, particularly with neurodegenerative pathologies[124]. Furthermore, studies in different model organisms have shown that an increase in chaperone induction leads to an extension in longevity. Overexpression of HSP16 triggers lifespan extension and stress resistance in *C. elegans*[122]. On the other

hand, alterations in chaperones are not restricted to the aging process, as these molecules also become dysregulated in oncogenic processes. HSP90 constitutes an example of the role of chaperones in cancer. This chaperone assists the folding of multiple kinases involved in cellular proliferation and has therefore been proposed as a target for cancer treatment[125].

Ubiquitin proteasome system

The ubiquitin-proteasome system is the main mechanism for protein degradation in the cell, playing therefore and important role in proteostasis control. Degradation by the UPS involves two phases. First, the substrate protein is recognized and marked by ubiquitin conjugation and afterwards it is degraded by the proteolytic core of the proteasome in an ATP-dependent manner. Besides degrading misfolded or damaged proteins, the UPS also helps to control the levels of non-defective proteins, regulates a wide variety of cellular processes, is involved in the processing of antigens for their presentation to the immune system, and participates in the generation of amino acids for *de novo* protein biosynthesis[126]. Due to its important role in cellular physiology, alterations in the UPS have been associated with multiple disorders[127-129].

During aging, the activity of the proteasome system diminishes, leading to an increase in the accumulation of misfolded proteins in different tissues[25]. In contrast, centenarians and naked mole rats show high levels of proteasome activity throughout life[130,131]. Regarding cancer, the increase in protein synthesis observed in tumor cells make them particularly sensitive to alterations in proteolytic systems. Hence, proteasome inhibitors have been evaluated as a treatment for different types of tumors, such as the use of bortezomib in multiple myeloma[132,133]. The resulting massive accumulation of misfolded proteins triggers cell death by apoptosis.

Autophagy-lysosome system

Like the UPS, the autophagy-lysosome system also participates in the clearance of misfolded proteins and aggregates. Depending on the mechanisms of protein recognition and delivery to lysosomes, three types of autophagy are distinguished: macroautophagy, microautophagy and chaperone-mediated autophagy (CMA). Microautophagy refers to the degradation of cytosolic components by invagination of the lysosome membrane. In macroautophagy, large portions of the cytoplasm are surrounded by a double membrane

vesicle (autophagosome) and fused then with lysosomes. CMA consists in the selective degradation of specific proteins, which are recognized by the molecular chaperone HSC70 and translocated to the lysosomes by the membrane receptor LAMP2A[134]. Autophagy is constitutively active in the cell, but its activity arises under metabolic stress conditions, in particular during nutrient deprivation.

Similar to other proteostasis systems, autophagy tends to decrease during aging and its promotion is linked to an increase in longevity in humans and other animal species[130,135]. Alterations in CMA functioning have been associated with numerous neurodegenerative disorders[136]. Moreover, genetic interventions that promote autophagy in model organisms, such as the overexpression of Atg5 or the disruption of the beclin 1/Bcl-2 complex in mice, lead to an increase in lifespan[29,121]. A protumorigenic role of CMA has also been described in cancer cells, probably due to its contribution to protein quality control and the degradation of certain regulatory proteins. Blocking CMA decreases tumorigenicity and proliferation of cancer cells[137]. However, under physiological conditions, CMA seems to protect cells against oncogenic transformation partly through degradation of oncoproteins[138].

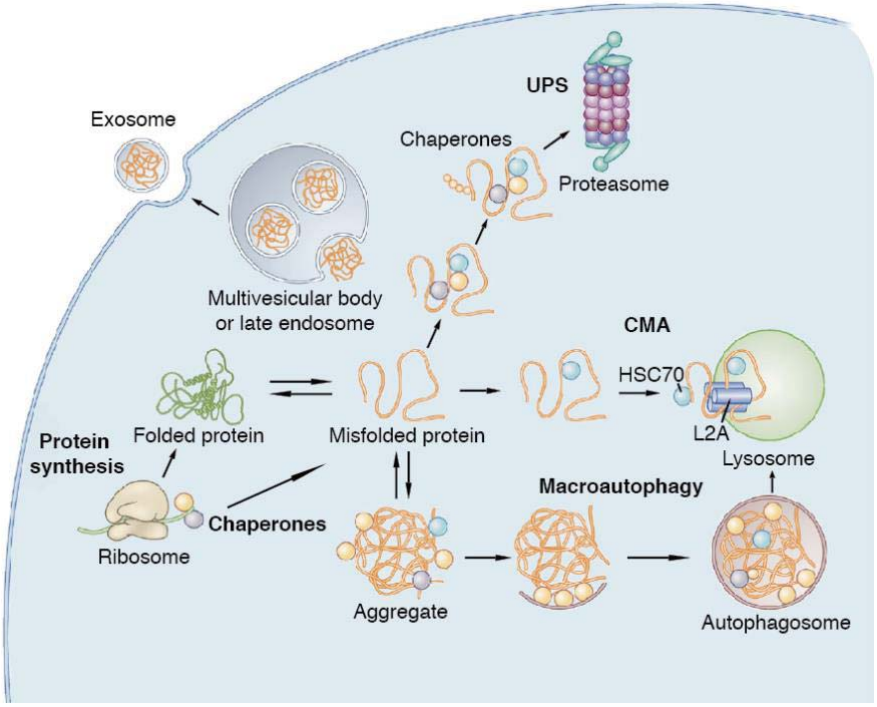

Figure 5. Intracellular proteostasis systems. Chaperones and two proteolytic systems, the ubiquitin-proteasome system (UPS) and the autophagy-lysosome system, are responsible for the maintenance of proteostasis. Adapted from Kaushik & Cuervo, 2015.

Proteostasis in the endoplasmic reticulum

The endoplasmic reticulum is an essential organelle in the control of cellular proteostasis due to its role in regulating protein biosynthesis and protein secretion. Thus, the ER is continuously exposed to a high volume of unfolded proteins. Under certain circumstances, the amount of unfolded proteins can rise, leading to a situation of stress in the ER. Proteostasis maintenance in this organelle is assured by different systems, the unfolded protein response (UPR), the retrotranslocation system or endoplasmic reticulum-associated protein degradation (ERAD), and a specific type of autophagy known as ER-phagy. The UPR is a signaling pathway that senses the folded state of proteins in the lumen by three stress sensors in the ER membrane: IRE1, PERK and ATF6, linked to the BiP chaperone. When the volume of unfolded proteins is high, these sensors get activated, promoting an increase in the folding capacity by inducing transcriptional changes[139]. If the UPR fails to reach proteostasis under these circumstances, unfolded proteins are retrotranslocated to the cytosol and degraded by the proteasome system following the ERAD[140]. In recent years, it has been described that whole regions of the ER can be degraded by a novel form of autophagy known as ER-phagy, which is mediated by the protein FAM134B[141].

During aging, a chronic ER stress is often developed, accompanied by an altered response to unfolded proteins[142]. In neurodegenerative diseases, a dysfunction in the activity of the UPR system has been detected. Accordingly, some studies have observed an overexpression of stress markers in the ER of neural tissues in Alzheimer's disease, and IRE1 deficiency has been suggested to protect against Alzheimer development in a mouse model of the disease[143]. Likewise, the rapid proliferation of tumor cells entails harsh conditions in their microenvironment, which lead to an increase in the load of misfolded proteins in the ER. Therefore, ER stress sensors, such as IRE1 or PERK are activated in tumor cells. Paradoxically, tolerable levels of ER stress promote aggressiveness, metastatic potential and drug-resistance of tumors, which could point ER as a target for cancer treatment[144].

Systemic regulation of proteostasis

Besides cell-autonomous systems, multicellular organisms have developed intercellular networks to control and coordinate the response of tissues and organs to proteotoxicity[145]. Typical intercellular communications, including gap junctions,

exosomes or nanotubes could be used to organize the response and signals of this loss of proteostasis[146,147]. Proteostasis components, such as proteasomes, lysosomes or chaperones, and even misfolded proteins and aggregates could be transferred between cells to resolve proteotoxic stress. Interestingly, reduced levels of the chaperone HSC70 have been observed in neural exosomes in preclinical Alzheimer's disease[148]. On the other hand, it has been proposed that transfer of aggregation-prone proteins across cells can contribute to the propagation of neurodegenerative disease[149].

The proteostasis factor AIRAPL

Diverse studies carried out in the nematode *Caenorhabditis elegans* have allowed the identification of novel regulatory factors of proteostasis involved in aging. An example of this is AIP-1, a protein localized in the endoplasmic reticulum that interacts with the proteasome under stress conditions, playing an important role in proteostasis maintenance. AIP-1-deficient worms show a reduced lifespan and have more difficulties to cope with misfolded proteins compared to wild-type animals[27]. Accordingly, AIP-1 overexpression protects *C. elegans* against the proteotoxicity caused by β-amyloid peptides, involved in Alzheimer's disease[150].

Two orthologues of AIP-1 have been identified in mammals: AIRAP (arsenic-inducible proteasomal 19S regulatory particle-associated protein) and AIRAPL (AIRAP-like). Both of them promote substrate access to the 26S proteasome but it has been suggested that some features shared between AIP-1 and AIRAPL, albeit missing in AIRAP, might be key to preserving lifespan. These traits include their posttranslational regulation, their CaaX farnesylation site and their ubiquitin-interacting motifs (UIMs)[27].

Interestingly, recent results from our laboratory have revealed that mice deficient in AIRAPL develop cell-autonomous alterations in the hematopoietic stem cell (HSC) compartment, finally driving to a myeloproliferative neoplastic process[151]. Likewise, AIRAPL was shown to be downregulated in human myeloproliferative syndromes as a result of microRNA miR-125a-3p overexpression. Proteomic analysis also determined that AIRAPL interacts with newly synthesized IGF-1 receptor in the endoplasmic reticulum, promoting its degradation through the ubiquitin-proteasome system. Genetic and pharmacological inhibition of this receptor in AIRAPL-deficient mice prevented the neoplastic transformation of hematopoietic cells, offering a new target for the treatment of these myeloid disorders. Collectively, all these data support the role of proteostasis

deregulation in both the aging process[27] and the oncogenic transformation of hematopoietic cells[152,153].

Intervention strategies modulating proteostasis in aging and age-related diseases

Aging has long been considered an irremediable phenomenon. Nevertheless, strategies to delay it have started to arise, proving the plasticity of this process[154]. Interestingly, most of these approaches are based on proteostasis modulation.

Diverse drugs, such as rapamycin, resveratrol, metformin and spermidine, have gained importance due to their effects on extending lifespan and delaying the onset of age-related diseases[155]. All these drugs exert their function by activating autophagy[135], but other mechanisms can be involved. Rapamycin is a small molecule produced by a soil bacterium which inhibits the nutrient-sensing mTOR (mechanistic target of rapamycin), resulting on a strong induction of autophagy. This molecule has been proven to extend lifespan and healthspan in several species[33,156]. Although it is approved for immunosuppressive use, long-term treatment may cause adverse effects in humans[157]. Interestingly, treatment of a mouse model of Alzheimer's disease with rapamycin delays the cognitive and molecular manifestations of the disease by reducing proteotoxicity[158]. Likewise, spermidine —a polyamine produced by the body—activates autophagy in multiple organs. Its administration to animal models also prolongs lifespan and delays neurodegeneration[159]. Another pro-longevity component is metformin, widely used as a treatment against type 2 diabetes. This drug has been reported to extend lifespan through different signaling pathways and to attenuate some of the hallmarks of aging such as deregulated nutrient sensing and loss of proteostasis[160]. Furthermore, resveratrol is a polyphenolic compound of grapes can that also stimulate autophagy through different stress-related targets like SIRT1[161]. This drug promotes longevity and induce protection in some models of age-related diseases[102,162].

Other non-pharmacological interventions can also have a positive impact in protein homeostasis and longevity. Physical activity has also been reported to promote the proteostasis network by increasing the activity of molecular chaperones, the proteasome and autophagy[163-165]. Although it does not seem to extend lifespan, exercise plays a critical role in reducing the risk of morbidity and mortality in both mice and humans.

Besides exercise, some types of food such as coffee[166] and olive oil[167] have reported positive effects in proteostasis maintenance and aging.

Moreover, the effects of calorie restriction on lifespan extension were already reported in 1939[168]. This type of regimen consists in a reduction of approximately 30% on the calories consumed, but always avoiding malnutrition. Restriction of caloric intake seems to exert its effect by modulating nutrient signaling pathways, such as AMPK, SIRT1 and MTORC1, subsequently activating autophagy[169]. However, this type of diet can be hard to maintain and has some side effects. Alternatively, different forms of fasting have been proposed as having similar effects on aging and age-related pathologies[170]. Interestingly, these fasting interventions also seem to play a role in the prevention and treatment of some types of cancer. Tumor cells are highly dependent on nutrient availability and specific metabolites. Therefore, fasting and related diets can contribute to reduce their survival[171]. Moreover, it has also been reported that fasting-based diets can help to protect against chemotherapy side effects by specifically increasing the resistance of normal cells[172]. In general, most of this research has been centered in solid malignancies[173-175]. However, a remarkable study has also described that intermittent fasting has an effect on blocking the initiation and progression of acute lymphoblastic leukemia[176]. Although further studies are needed, particularly in the field of hematopoietic neoplasms, preclinical data suggest that combined chemotherapeutic treatments with fasting diets could be useful to fight some types of cancer.

In summary, in this section I have tried to outline part of the vast knowledge gained in the last few years in the mechanisms involved in aging and age-related diseases, such as HGPS or cancer. As a result of this growing information and the development of new technologies, novel therapeutic strategies have arisen as possible treatments for these pathologies. Still, many of them remain to be explored *in vivo* in the field of aging.

OBJECTIVES

In recent years, the idea that not only cell-autonomous but also systemic alterations contribute to the aging phenotype has gained importance. Both processes should be considered for the development of new anti-aging approaches and the study of mechanisms contributing to the hallmarks of aging. In order to unravel some of these regulators of longevity and evaluate possible intervention strategies, we focused on the mechanisms that protect the cell from damage through genome stability maintenance and proteostasis enhancement. For this purpose, we explored both accelerated aging and loss of proteostasis mouse models, as well as long-lived animal species. First, we evaluated strategies based on gene-editing to extend lifespan in a premature aging disease. Furthermore, we performed an analysis of DNA repair genes that could be associated with lifespan extension in long-lived species. Finally, we explored regulatory mechanisms of protein homeostasis through the proteostasis factor AIRAPL, and how it can contribute to age-related pathologies.

The specific objectives of this Doctoral Thesis were:

- Identification and targeting of genes involved in genome protection in aging and age-related diseases through comparative genomics and gene-edition.
    - Development of an *LMNA* gene-editing strategy for aging and progeria based on the CRISPR/Cas9 system.
    - Analysis of DNA repair-related genes in giant tortoises as a long-lived model organism.

- Modulation of factors involved in proteostasis regulation in aging and cancer by using cell-intrinsic and cell-extrinsic strategies.

EXPERIMENTAL PROCEDURES

Molecular biology methods

DNA genotyping

DNA was extracted from mouse tail biopsies by alkaline lysis. In all cases, PCR was performed using Platinum™ *Taq* DNA polymerase (Invitrogen) under the following conditions: denaturalization at 95 ºC for 30 seconds, annealing at 60 ºC for 30 seconds and extension at 72 ºC for 45 seconds, with 35 cycles of amplification. *Lmna*$^{G609G/G609G}$ mice genotyping was performed with the following oligonucleotides: 5'-AAGGGGCTGGGAGGACAGAG-3', 5'-AGTAGAAGGTGGCGCGAAGG-3' and 5'-AGCATGCAATAGGGTGGAAGGA-3'. PCR products consisted in a band of 240 bp for the mutant allele and a band of 100 bp for the wild-type allele.

DNA extraction and genomic qPCR analysis

DNA was extracted from liver, heart, muscle and lung for CRISPR delivery experiments. Extraction was performed by following the phenol-chloroform protocol. Then, samples were quantified using a NanoDrop ND-1000 spectrophotometer (NanoDrop Technologies) and evaluated for purity (260/280 nm ratio). Quantitative PCR analyses were performed using 4.5 ng of DNA by triplicate for each sample in the Applied Biosystems 7300HT Real-Time PCR System. We used SYBR® green PCR Universal Master Mix (Applied Biosystems) and the following oligonucleotides: AAV_fwd (5'-GAAGCTGTTGTCGAAGGACAC-3') and AAV_rev (5'-GACATGCAGGAAGGCA AGTG-3') for CRISPR delivery assessment, and Hxq_rev (5'-GGGAACACAAAAGA CCTCTTCTGG-3') for hexokinase-2 amplification, used as a reference in both cases.

RNA preparation and RT-qPCR

Collected cells or tissues were homogenized in TRIzol reagent (Life Technologies) and RNA was extracted with the RNeasy Mini kit (QIAGEN) following the manufacturer's instructions. After extraction, samples were quantified using a NanoDrop ND-1000 spectrophotometer (NanoDrop Technologies) and evaluated for purity (260/280 nm ratio). cDNA was synthesized with the QuantiTect Reverse Transcription kit (QIAGEN) using 1 μg of total RNA and following the manufacturer's instructions. Quantitative RT-PCR analysis was performed in triplicate for each sample with 20 ng of cDNA using an Applied Biosystems 7300HT Real-Time PCR System. For progerin

analysis, TaqMan™ PCR Universal Master Mix (Applied Biosystems) was used. In the case of progerin, we used the following oligonucleotides and probe: MmProgerin_fwd (5'-TGAGTACAACCTGCGCTCAC-3'), MmProgerin_rev (5'-TGGCAGGTCCCAGA TTACAT-3') and MmProgerin_probe (5'-CGGGAGCCCAGAGCTCCCAGAA-3'). For lamin C analysis, we used SYBR® green PCR Universal Master Mix (Applied Biosystems) and the oligonucleotides Lmnc_fwd (5'-CGACGAGGATGGAGAAGAGC -3') and Lmnc_rev (5'-AGACTTTGGCATGGAGGTGG-3') for lamin C; or Actb_Fwd (5'-CTGAGGAGCACCCTGTGCT-3') and Actb_Rev (5'-GTTGAAGGTCTCAAACA TGATCTG-3') for β-actin as endogenous control. Relative expression was calculated by $RQ=^{2-\Delta\Delta Ct}$.

Protein isolation and Western blot analysis

For progerin analyses, fibroblasts or tissues were homogenized in RIPA lysis buffer containing 100 mM Tris pH 7.4, 150 mM NaCl, 10 mM EDTA pH 8, 1% sodium deoxycholate, 1% Triton X-100 and 0.1% SDS, supplemented with protease inhibitor cocktail (Complete, EDTA-free, Roche) and phosphatase inhibitors (PhosSTOP, Roche). For repair studies, HEK-293T cells were lysed in NP-40 lysis buffer containing 50 mM Tris-HCl pH 7.4, 150 mM NaCl, 10 mM EDTA pH 8 and 1% NP-40, and supplemented with protease inhibitor cocktail (cOmplete, EDTA-free; Roche), as well as phosphatase inhibitors (PhosSTOP; Roche/NaF; Merck). Protein concentration was determined with the bicinchoninic acid technique (Pierce BCA Protein Assay Kit) and equal amounts of proteins were loaded onto SDS-polyacrylamide gels for electrophoresis. Gels were then electrotransferred onto nitrocellulose or polyvinylidene fluoride (PVDF) membranes (GE Healthcare Life Sciences), blocked with 5% nonfat dry milk in TBS-T buffer (20 mM Tris pH 7.4, 150 mM NaCl and 0.05% Tween 20) and incubated overnight at 4 ºC with primary antibodies: 1:500 mouse monoclonal anti-lamin A/C (Manlac-1; provided by Prof. G.E. Morris; Wolfson Centre for Inherited Neuromuscular Disease, UK) for experiments involving mouse cells, 1:1,000 rabbit polyclonal anti-lamin A/C (Santa Cruz Biotechnology, sc-20681) for experiments involving human cells, anti-phospho-Histone H2AX (Ser139) (EMD Millipore; 05-636, clone JBW301), anti-PARP (Cell Signaling Technology; 9542S, rabbit polyclonal), anti-FLAG (Cell Signaling Technology; 2368S, rabbit polyclonal), anti-β-actin (Sigma–Aldrich, A5441, clone AC-15) and anti-α–tubulin (Sigma–Aldrich, T6074, clone B-5-1-2). For progerin analyses, blots were incubated with 1:10,000 goat anti-mouse (Jackson ImmunoR) or 1:3,000 goat anti-rabbit horseradish

peroxidase (HRP) (Cell Signaling) in 1.5% nonfat dry milk in TBS-T and washed with TBS-T. The immunoreactive bands were developed with Immobilon Western chemiluminescent HRP substrate (Millipore) in a LAS-3000 Imaging System (Fujifilm). For repair studies, membranes were incubated with secondary antibodies conjugated with IRDye 680RD (LI-COR Biosciences; 926-68071, polyclonal goat-anti-rabbit; and 926-32220, polyclonal goat-anti-mouse) or IRDye 800CW (LI-COR Biosciences; 926-32211, polyclonal goat-anti-rabbit; and 926-32210, polyclonal goat-anti-mouse) for 1 h at room temperature. Protein bands were scanned on an Odyssey infrared scanner (LI-COR Biosciences). Band intensities were quantified using ImageJ.

Plasmids and sgRNA cloning

All sgRNA-LCS were designed to target exon 11 of the *LMNA* gene by using the Benchling CRISPR Design tool. For the infections involving HGPS human and mouse fibroblasts, we used the lentiviral vector lentiCRISPRv2 developed by Dr. F. Zhang (MIT, Boston, USA)[177] (Addgene, #52961), where we cloned the sgRNA-control (5'-GGAGACGGGATACCGTCTCT-3') or the sgRNA-LCS1 (5'-AGCGCAGGTTGTAC TCAGCG-3'). For AAV injection, we cloned the sgRNA-control or the sgRNA-LCS2 (5'-GTGCAGCGGCTCGGGGGACCCCG-3') in the pX601-AAV-CMV::NLS-SaCas9-NLS-3xHA-bGHpA;U6::BsaI-sgRNA vector from Dr. F. Zhang (MIT, Boston, USA)[178] (Addgene, #61591), containing the Cas9 nuclease from *S. aureus*. For DNA repair experiments, *NEIL* or *RMI2* cDNA was cloned in a pCDH vector.

Capillary electrophoresis-based fragment analysis

In the case of Cas9-transduced cells, we performed a PCR amplification of the target region with the forward oligonucleotide labelled with 6FAM fluorophore in the 5' position, allowing the fragment analysis of the resulting products by capillary electrophoresis. For human cells, we used the oligonucleotides LMNA_Fwd: [6FAM]GCACAGAACCACACCTTCCT and LMNA_Rev: TGACCAGATTGTCCCC GAAG, while for mouse cells we used Lmna_Fwd: [6FAM]GTCCCCATCACTTGGTT GTC and Lmna_Rev: TGACTAGGTTGTCCCCGAAG. Capillary electrophoresis-based fragment analysis was performed at Servicios Científico-Técnicos of Universidad de Oviedo.

Sanger sequencing

We validated the relevant variants found in *Chelonoidis abingdonii* and *Aldabrachelys gigantea* by Sanger sequencing using DNA samples from these species as well as from other tortoises from Galapagos Islands, including the islands of Santa Cruz (*Chelonoidis porteri*), Española (*Chelonoidis hoodensis*), Isabela (*Chelonoidis becki* and *Chelonoidis vicina*) and Pinzón (*Chelonoidis duncanensis*). We also included in the analysis two continental outgroups: *Chelonoidis chilensis*, *Chelonoidis carbonaria* and *Chelonoidis denticulata* for Galapagos Islands tortoises, and *Stigmochelys pardalis* for Aldabra tortoise. We first performed a PCR amplification of the region of interest by using the following oligonucleotides: NEIL1_fwd: GGTCAGCTTGATCTCCTTGC, NEIL1_rev: CTTCATTTGGGCAGGTGTCT; RMI2_copyA_fwd: GCTCCATGTGCT CCTGTGTA, RMI2_copyA_rev: GATGCAGGGCACGGTACT; RMI2_copyB_fwd: TTTCTGGCATCTGCAAAAATAA, RMI2_copyB_rev: CAAACCCACCTGGAGTCC T; DCLRE1B_fwd: AGAGCCCATCCTCTCTCCTG; DCLRE1B_rev: TCTGCCTGCA GACTGAGAAA; XRCC6_fwd: TAAACCCTGCATGCTTCCTT, XRCC6_rev: AAGT TTTGCAGTGTTTTCCCTA; XRCC5_fwd: GGGAGGTTGGTTTGTTTTGA, XRCC5 _rev: AGTCCCCAAGGGAAGGTCTA. Sanger sequencing was performed at Servicios Científico-Técnicos of Universidad de Oviedo.

Cell biology methods

Cell culture

We maintained HEK-293T cell cultures in Dulbecco's modified Eagle's medium supplemented with 10% fetal bovine serum (FBS), 1% penicillin-streptomycin-L-glutamine and 1% antibiotic-antimycotic (Gibco) at 37 ºC in 5% CO_2. In the case of human and mouse fibroblasts, 1x non-essential amino acids, 10 mM HEPES buffer, 100 μM 2-mercaptoethanol and 1x sodium pyruvate (Gibco) were also added to the previous medium and 15% FBS was used.

Viral packaging and cell transduction

For lentiviral infection, HEK-293T cells were transfected with the corresponding lentiCRISPRv2 or pCDH vector together with second-generation packaging plasmids using Lipofectamine reagent (Life Technologies). Supernatants were filtered through

0.45 μm polyethersulfone filters to collect the viral particles and added in a 1:3 dilution to previously seeded human and mouse fibroblasts, supplemented with 0.8 μg/ml polybrene (Millipore). Puromycin selection (2 μg/ml) was done two days after infection and the editing efficiency, nuclear morphology or repair studies were performed one week later.

Immunofluorescence and nuclear morphology analysis

For immunofluorescence assays, cells were fixed in 4% paraformaldehyde solution, rinsed in PBS and permeabilized with 0.5% Triton X-100. Afterwards, they were blocked with 15% goat serum solution and incubated overnight at 4 ºC with a rabbit polyclonal anti-progerin antibody in PBS (1:200). Next, slides were washed with TBS-T and incubated with 1:500 anti-rabbit secondary antibody Alexa Fluor 488 (Life Technologies). Nuclei were stained with 4',6-diamidino-2-phenylindole (DAPI, Invitrogen). To determine the percentage of progerin-positive cells and nuclei with aberrations, five random fields per culture or tissue sample were blindly analyzed. For tissue samples, in each field a pre-established grid was used and five random areas were quantified.

Stress induction studies

For repair studies, HEK-293T cells were transduced with pCDH, pCDH-NEIL1, pCDH-RMI2 or pCDH-NEIL1 + pCDH-RMI2. Then, we isolated clones from these cells with proper expression levels of NEIL1 and RMI2 and expanded them. Cells were exposed either to ultraviolet light at 20 J/m^2 in the CL1000 UV Crosslinker UPV or to H_2O_2 at 500 μM (Sigma aldrich) 24 and 48 h before being lysed for Western blot analysis.

Animal model methods

Animal experiments

All animal experiments were performed in accordance with institutional guidelines and approved by the Committee of Animal Experimentation of University of Oviedo (Oviedo, Spain). All animals were housed in a facility with a photoperiod of 12 hours light/12 hours dark, at 22 ± 2 ºC, 50 ± 10% of relative humidity and fed *ad libitum* with

standard diet. All gene-editing and phenotypic analyses involving *Lmna*$^{G609G/G609G}$ mice were performed at 3.5 months of age.

AAV production and injection

pX601-sgRNA-control or pX601-sgRNA-LCS2 plasmids were packaged in AAV serotype 9 by The Viral Vector Production Unit (UPV) of the Universitat Autònoma de Barcelona (Barcelona, Spain), followed by PEG precipitation and iodixanol gradient purification. Aliquots of $2x10^{11}$ genome copies in 60 μL of PBS-MK were prepared for the injections and stored at -80 °C. For AAV injection, postnatal day 3 (P3) *Lmna*$^{G609G/G609G}$ mice were injected intraperitoneally with either sgRNA-control- or sgRNA-LCS2-containing vectors.

Histological analysis and TUNEL staining

Tissues were collected in 4% PFA in PBS and embedded in paraffin. H&E staining was performed in transversal sections of stomach. The atrophy of the gastric mucosa was blindly assessed in three different sections per mouse, establishing a pathological score (0, normal; 1, mild; 2, moderate; 3, severe atrophy).

TUNEL staining in mouse kidneys was done according to the manufacturer's instructions (In-Situ Cell Death Detection Kit, TMR red, Roche). To determine the number of TUNEL-positive nuclei, ten random fields per mouse were blindly analyzed using ImageJ. H&E with Gomori's trichrome staining was performed in heart and quadriceps muscle and five random fields per tissue were quantified with a FIJI plugin provided by Dr. A.M. Nistal (Servicios Científico-Técnicos, Universidad de Oviedo).

Immunohistochemistry

Tissues were fixed in 4% PFA and incubated with Target Retrieval Solution at 95 ºC for 20 minutes, a Peroxidase Blocking Solution for 5 minutes and a Protein Block Serum Free (all from Dako) for 20 minutes before the incubation with primary antibody for 1 hour. An HRP-conjugated polyclonal anti-rabbit was applied for 30 minutes and then 3,3'-diaminobenzidine (DAB) for 10 minutes. Tissues were counterstained with hematoxylin (Dako) and visualized by light microscopy. For progerin analysis, a rabbit anti-progerin polyclonal antibody was used in a 1:300 dilution. This antibody was generated using peptide immunogens and standard immunization procedures (S.

Nourshargh et al., manuscript in preparation). The specificity of the antibody was confirmed by nuclear staining of *Lmna*$^{G609G/G609G}$ mice-derived fibroblasts, which was negative in the case of wild-type cells

Bioinformatics and statistical methods

Statistical analysis

Animals of the same age were used for the comparisons between mice groups and no statistical method was used to predict sample size. For statistical analysis of differences between mouse cohorts, normality was assessed using a Shapiro-Wilk test in those cases were n>10. In the rest of the cases, normality was assumed based on previous data and we performed two-tailed Student's *t*-test to study the statistical significance. For survival comparisons, we used the Log-rank test. In the case of gene-editing experiments, differences in maximum lifespan were calculated using the one-tailed Fisher exact test comparing the number of alive control- and LCS2-transduced mice at the age corresponding to the 80th percentile of lifespan in the joint survival distribution. We used Microsoft Excel or GraphPad Prism software for the analysis and significant differences were considered when $*P < 0.05$, $**P < 0.01$, $***P < 0.001$.

Gene editing assessment

To assess the efficiency of our CRISPR/Cas9 strategy, we performed DNA amplification and Illumina sequencing of the target region in the *Lmna* gene. First, DNA was isolated from liver, heart, muscle and lung from mice transduced with sgRNA-control or sgRNA-LCS2-encoding AAVs to prepare the library. Next, we amplified the target region of the Cas9 nuclease with the *Pfu* DNA polymerase (Promega) adding the Illumina adapters by two PCRs: NGS1_fwd: ACACTCTTTCCCTACACGACGCTCTTCCGAT CTNNNNTGTGACACTGGAGGCAGAAG and NGS1_rev: GTGACTGGAGTTCAG ACGTGTGCTCTTCCGATCTCAAGTCCCCATCACTTGGTT for the first PCR, and NGS2_fwd: AATGATACGGCGACCACCGAGATCTACACTCTTTCCCTACACGA CGCTCTTCCGATCT and NGS2_rev: CAAGCAGAAGACGGCATACGAGATXXX XXXGTGACTGGAGTTC for the second PCR. The N represents random bases and the X the sequence used for the index. MiSeq DNA sequencing was performed by Macrogen, Inc. using the Illumina 300bpPE. Genomic reads in FASTQ format were aligned to the

GRCm38.p6 assembly of the mouse genome using BWA v. 0.7.5a-r405[179]. Then, reads spanning the genomic region putatively affected by the CRISPR/Cas9 action (chr3: 88482555-88482615) were extracted with Samtools v. 1.3.1[180] and analyzed using in-house Perl scripts. Briefly, these scripts isolate the part of each read spanning the chosen region, highlight small insertions/deletions and output a count of each regional sequence. Then, we analyzed the percentage of the sequences showing regional differences in sgRNA-control and sgRNA-LCS2-transduced mouse samples.

Genome sequencing and assembly in giant tortoises

We obtained DNA from a blood sample from Lonesome George, the last member of *C. abingdonii*. This DNA was sequenced, using the Illumina HiSeq 2000 platform, from a 180-base pair-insert paired-endlibrary, a 5-kilobase (kb)-insert mate-pair library and a 20-kb-insert mate-pair library. These libraries were assembled with the AllPaths algorithm[181] for a draft genome contigs with SSPACE version 3.0[182] using the long-insert mate-pair libraries. Finally, we filled the gaps with PBJelly version 15.8.24[183] using the reads obtained from 18 BioPac cells. This step yielded 10,623 scaffolds with an N50 of 1.27 megabases, for a final assembly 2.3 gigabases long. Then, we soft-masked repeated regions using RepeatMasker (http://www.repeatmasker.org) with a database containing chordate repeated elements (included in the software) as a reference. Additionally, we assessed the completeness of assembly by their estimated gene content, using Benchmarking Universal Single-Copy Orthologs (BUSCO version 3.0.0)[184], which tested the status of a set of 2,586 vertebrata genes from the comprehensive catalogue of orthologues[185]. We also performed RNA-Seq from *C. abingdonii* blood and *A. gigantea* granuloma, and aligned the resulting reads to the assembled genome using TopHat[186] (version 2.0.14). Finally, we obtained whole-genome data from *A. gigantea* with one Illumina lane of a 180-base pair paired-end library. The resulting reads were aligned to the *C. abingdonii* genome with BWA[179] (version 0.7.5a). Raw reads from *C. abingdonii* were also aligned to the genome for manual curation of the results. All work on field samples was conducted at Yale University under Institutional Animal Care and Use Committee permit number 2016-10825, Galapagos Park Permit PC-75-16 and Convention on International Trade in Endangered Species number 15US209142/9.

Genome annotation

Using the genome assembly of *C. abingdonii* and the RNA-Seq reads from *C. abingdonii* and *A. gigantea*, we performed de novo annotation with MAKER2. The algorithm was also fed both human and *P. sinensis* reference sequences, and performed two runs in a Microsoft Azure virtual machine. In parallel, we used selected genes from the human protein database in Ensembl as a reference to manually predict the corresponding homologues in the genome of *C. abingdonii* using the BATI algorithm (Blast, Annotate, Tune, Iterate)[187]. Briefly, this algorithm allows a user to annotate the position and intron/exon boundaries of genes in novel genomes from tblastn results. In addition, tblastn results are integrated to search for novel homologues in the explored genome. Sequencing data have been deposited at the Sequence Read Archive (https://www.ncbi.nlm.nih.gov/sra), with comments showing which regions were filled with the BioPac reads and therefore may contain frequent errors

RESULTS

1. Development of an *LMNA* gene-editing strategy for aging and progeria based on the CRISPR/Cas9 system

New therapies based on the CRISPR/Cas9 editing system hold a great promise for the treatment of genetic diseases. Among these, Hutchinson-Gilford progeria syndrome (HGPS) stands out as a potential candidate, due to its genetic cause lying in a point mutation in the *LMNA* gene. This change in a splicing site leads to the accumulation of the pathogenic protein known as progerin. Patients suffering from this condition develop an accelerated aging phenotype, which normally leads to a premature death at childhood. Besides this critical condition, treatments against this disease are not effective enough, thus the finding of a more definitive cure is crucial[13]. In this section, we explore the efficacy of a CRISPR/Cas9-based approach reverting several alterations in both HGPS cells and a progeroid mouse model by introducing frameshift mutations in *LMNA*.

The initial idea that prompted us to develop this approach was based on three previous findings. First, mice lacking lamin A (lamin C-only mice or $Lmna^{LCO/LCO}$ mice) apparently have a normal lifespan and phenotype, without evidence of muscle or bone alterations[70,80]. Consistent with this, lamin A also seems to be dispensable in human cells, indicating that it could be possible to treat HGPS by avoiding the synthesis of prelamin A. Second, $Zmpste24^{-/-}$ mice with reduced levels of prelamin A ($Zmpste24^{-/-}Lmna^{+/-}$ mice) presented a normal phenotype, not showing the premature death and growth retardation characteristic of these progeroid mice[75,80]. Finally, the *Zmpste24* mosaic mouse model, in which prelamin A-accumulating cells and regular cells coexist in similar proportions, shows a completely normal phenotype, without the altered levels of systemic parameters characteristic of progeroid mice[188]. This suggests that a partial reduction of progerin accumulation, even in a lower ratio than 50% of cells, could be sufficient for an important phenotype relief. On these bases, we were prompted to develop a CRISPR/Cas9-based strategy against HGPS aimed at avoiding accumulation of lamin A or progerin.

1.1. Design of a CRISPR/Cas9-based strategy against HGPS

The *LMNA* gene encodes two nuclear proteins, lamin C (from exon 1 to 10) and lamin A (from exon 1 to 12), through alternative splicing and polyadenylation. Since lamin A seems to be dispensable[70,80], our strategy is focused on disrupting the last part of the *LMNA* gene, impeding lamin A/progerin production without affecting lamin C.

Maintaining the integrity of lamin C is crucial, as it plays an important role in the nuclear envelope architecture and the correct functioning of skeletal and cardiac muscles. Elimination of both proteins triggers aberrations and weakening of the nuclear envelope in cells and leads to a premature death by 5-6 weeks of age and a muscular dystrophy phenotype in mice[189]. To only disrupt lamin A/progerin-coding region of the gene, we designed a sgRNA (sgRNA-LCS1), followed by the 5'-NGG-3' PAM sequence of the *Streptococcus pyogenes* Cas9, to target *LMNA* exon 11. The target sequence is upstream of the HGPS mutation, in a region conserved across human and mouse (**Fig. 6**).

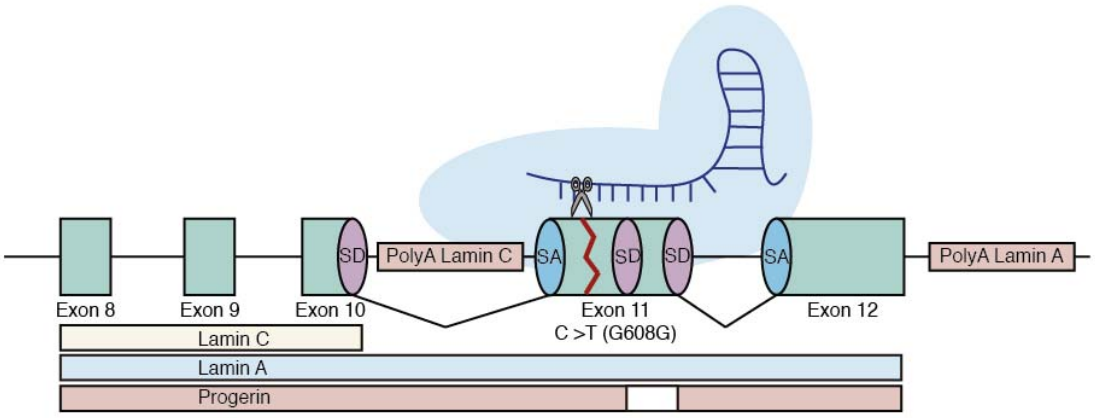

Figure 6. Diagram showing the CRISPR/Cas9-based strategy. Our sgRNA-LCS1 directs Cas9 nuclease against exon 11 of *LMNA* gene upstream of the HGPS mutation, disrupting therefore lamin A and progerin without altering lamin C (SA, splice acceptor; SD, splice donor).

1.2. CRISPR/Cas9 in vitro testing in HGPS cellular models

To test the efficacy of this approach, we first cloned the sgRNA-LCS1 or the sgRNA-control in a lentiviral vector containing the *S. pyogenes* Cas9 (lentiCRISPRv2) and transduced *Lmna*$^{+/+}$ and *Lmna*$^{G609G/G609G}$ murine fibroblasts. As a result, indels of variable lengths were produced in sgRNA-LCS1-transduced cells, as assessed by capillary electrophoresis-based fragment analysis (**Fig. 7a**). As expected, Western blot analysis showed a significant decrease in the accumulation of progerin and lamin A, while lamin C levels were not affected (**Fig. 7b**). Likewise, immunofluorescence analysis demonstrated that progerin-positive nuclei were reduced by 74% in sgRNA-LCS1-transduced cells compared to control-transduced cells (**Fig. 7c**).

A large number of HGPS cells present morphological anomalies in their nuclei, including blebbings and invaginations, produced by the accumulation of progerin[65]. It has

been previously demonstrated that a reduction in the progerin levels by antisense oligonucleotides produces a decrease in the number of aberrations in HGPS cell nuclei[70]. To explore the effect of progerin disruption by CRISPR/Cas9 in the nuclear shape, we analyzed the number of nuclear aberrations, staining nuclei with DAPI and counting anomalies on a blinded way. Accordingly, we found a 65% decrease in the number of nuclear alterations in *Lmna*$^{G609G/G609G}$ cells transduced with sgRNA-LCS1 compared to sgRNA-control-transduced cells (**Fig. 7c**).

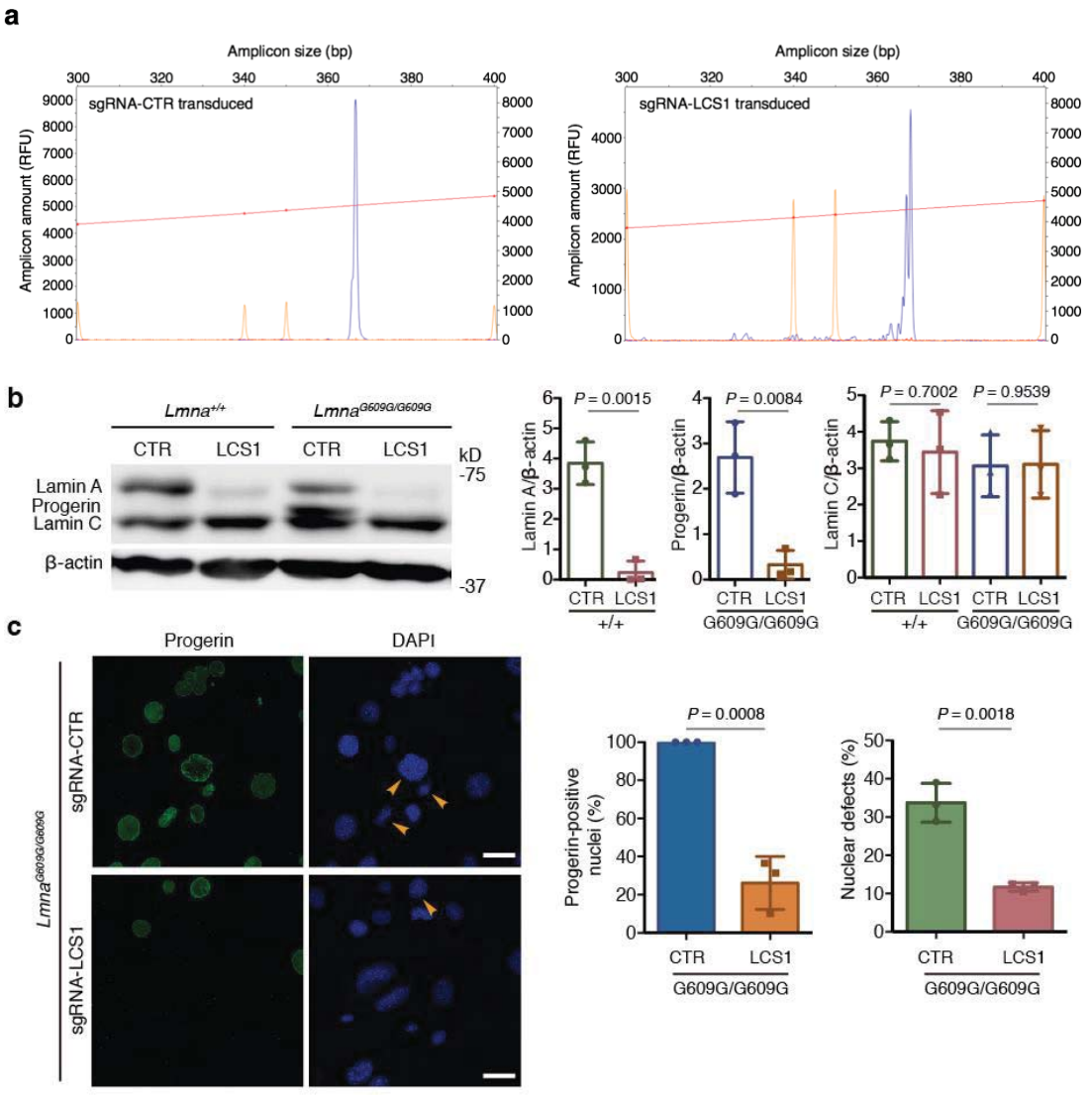

Figure 7. CRISPR/Cas9 testing in HGPS mouse embryonic fibroblasts (MEFs). (a) Representative capillary electrophoresis-based fragment analysis of sgRNA-control and sgRNA-LCS1-transduced *Lmna*$^{G609G/G609G}$ mouse embryonic fibroblasts (n=3 independent infections and MEF lines). Red line and orange peaks correspond to size standards. **(b)** Cropped Western blot of lamin A, progerin and lamin C in MEFs transduced with sgRNA-control or sgRNA-LCS1 (n=3 independent infections and MEF lines; two-tailed Student's t-test). **(c)** Immunofluorescence analysis of progerin-positive nuclei and quantification of nuclear alterations by DAPI staining (n=3 independent infections and MEF lines; two-tailed Student's t-test). Arrowheads indicate nuclear aberrations. Bar plots represent mean ± SD and individual values are overlaid. Scale bars, 40 µm.

At the same time, we tested this system in human cells, infecting *LMNA*$^{G608G/+}$ fibroblasts from HGPS patients and *LMNA*$^{+/+}$ fibroblasts with these lentiviral vectors. Similar to mouse fibroblasts, we observed different indels in the DNA by capillary electrophoresis-based fragment analysis (**Fig. 8a**). Likewise, a decrease of progerin and lamin A was also observed by Western blot (**Fig. 8b**) and by immunofluorescence (**Fig. 8c**), with an 83% decrease in progerin-positive nuclei. In HGPS human fibroblasts, analysis of nuclear alterations revealed a 39% reduction in the number of aberrant nuclei in sgRNA-LCS1 *versus* sgRNA-control-transduced cells (**Fig. 8c**).

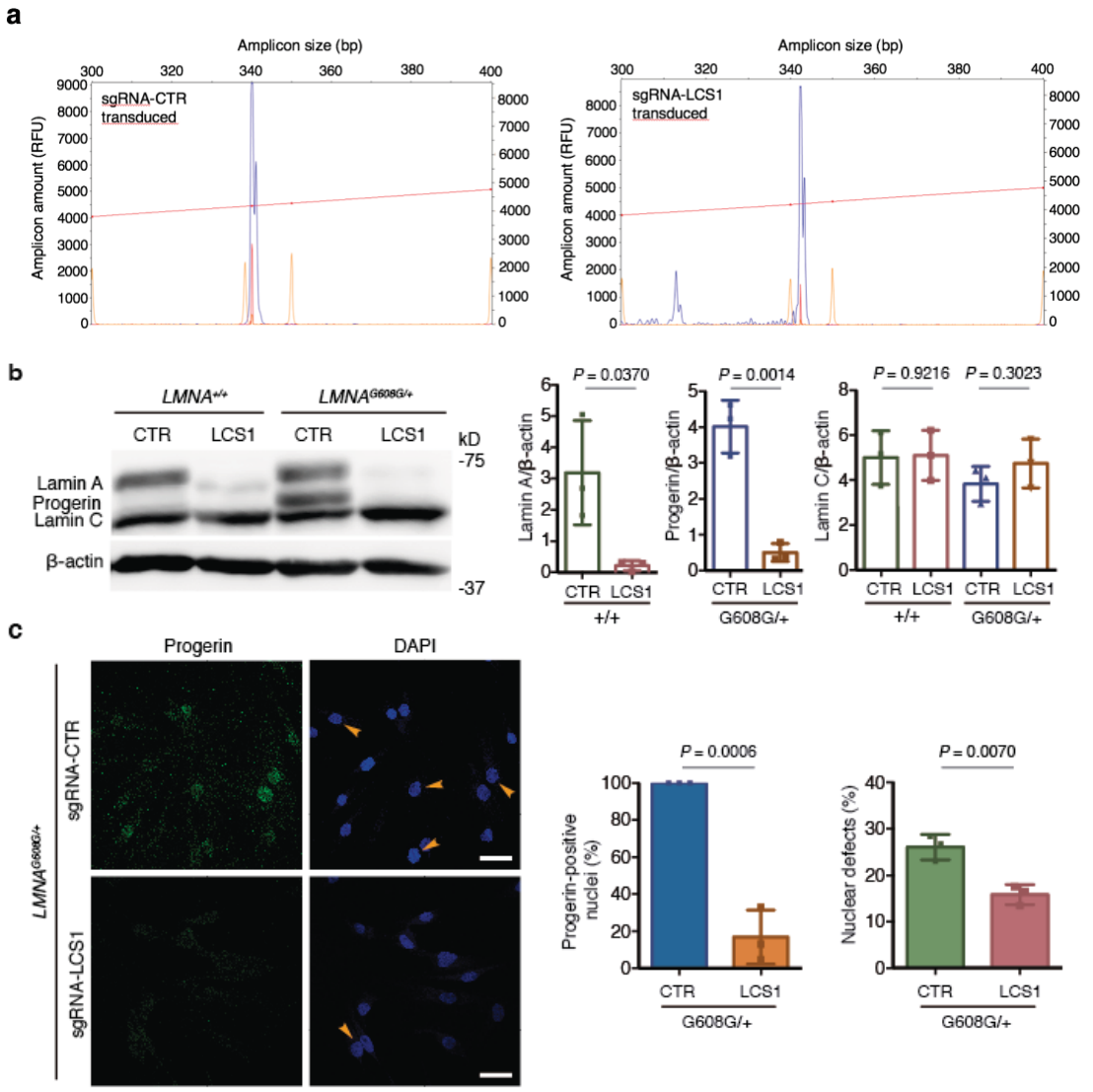

Figure 8. CRISPR/Cas9 testing in HGPS human fibroblasts. (a) Representative capillary electrophoresis-based fragment analysis of sgRNA-control and sgRNA-LCS1-transduced *LMNA*$^{G608G/+}$ human fibroblasts (n=3 independent infections). Red line and orange peaks correspond to size standards. **(b)** Cropped Western blot of lamin A, progerin and lamin C in human fibroblasts transduced with sgRNA-control or sgRNA-LCS1 (n=3 independent infections; two-tailed Student's t-test). **(c)** Progerin immunofluorescence and analysis of nuclear aberrations by DAPI staining (n=3 independent infections; two-tailed Student's t-test). Arrowheads indicate blebbings and invaginations. Bar plots represent mean ± SD and individual values are overlaid. Scale bars, 40 µm.

1.3. Cas9 delivery to Lmna$^{G609G/G609G}$ mice by adeno-associated viral infection

With the aim of further evaluating this genome editing approach as an eventual treatment for HGPS patients, we decided to test this system *in vivo*. For this purpose, we chose *Lmna$^{G609G/G609G}$* mice as the animal model of progeria[70], since it is the one that best imitates the mutation and general pathophysiology of HGPS patients. As a delivery vector, we decided to use adeno-associated viruses (AAVs) of serotype 9 due to their safety, broad tissue tropism and long-term expression in dividing and non-dividing cells[190,191]. Given the packaging limit of these viruses (approximately 4.8 kb), we turned to the *Staphylococcus aureus* Cas9 nuclease[111] (SaCas9; 3,16 kb) and designed a new sgRNA directed against the same region in exon 11 with the 5'-NNGRRT-3' PAM sequence (sgRNA-LCS2). After packaging the vectors, either with sgRNA-LCS2 or the sgRNA-control, we injected intraperitoneally $2x10^{11}$ AAV9 genome copies in postnatal day 3 (P3) *Lmna$^{G609G/G609G}$* mice (**Fig. 9a)**. The following qPCR analysis performed in genomic DNA extracted from different tissues of these mice revealed the main presence of AAVs in liver, followed by heart and muscle and a small amount in lungs (**Fig. 9b)**.

Next, to assess the editing efficiency, we performed Illumina sequencing of the target region in DNA extracted from four of the AAV9 main target organs —liver, heart, muscle and lung— of injected mice. Analysis was performed using in-house Perl scripts, highlighting small insertions and deletions in the Cas9 target region. Notably, *Lmna* contained indels in 13.6% ± 2.6 of the genome copies in liver, 5.3 ± 1.0% in heart, 4.1 ± 0.6% in muscle, and 1.1 ± 0.2% in lung (**Fig. 9c,d; Tables 1-4**). As a consequence of the introduction of frameshift mutations we would expect an RNA decay in the levels of progerin. However, given the modest fraction of cells edited *in vivo*, the global decrease of progerin mRNA was too low to be reliably detected by RT-qPCR, although a tendency was observed in liver tissue (**Fig. 9e**).

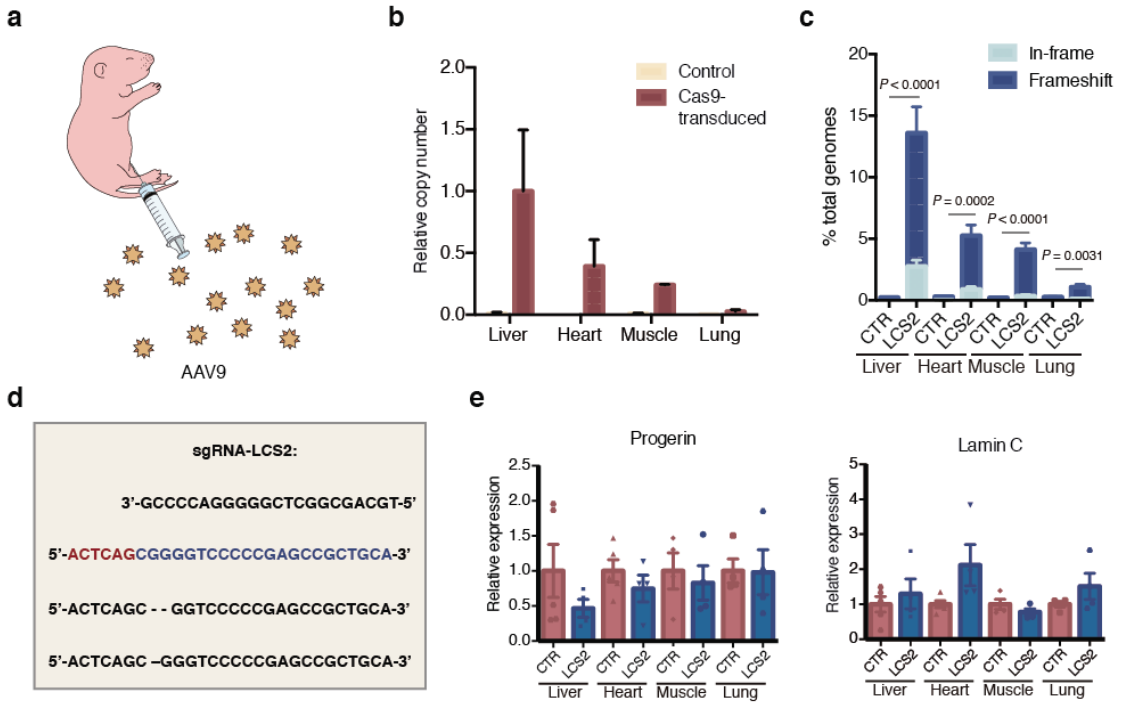

Figure 9. CRISPR/Cas9 delivery in *Lmna*$^{G609G/G609G}$ mice. (a) Diagram of the intraperitoneal injection of AAV9 in P3 mice. **(b)** qPCR analysis of AAV copies in liver, heart, muscle and lung from control and Cas9-transduced mice. Data are mean ± SD (n=2 mice per group). **(c)** Percentage of in-frame and frameshift mutations in the *Lmna* target region at liver, heart, muscle and lung. Data are mean ± SEM (n=10 tissues per group, except n=9 LCS2-transduced liver; two-tailed Student's t-test for total indels). **(d)** Alignment of the most common indels found in LCS2-transduced mice. Blue, target sequence; red, PAM sequence. **(e)** RT-qPCR analysis of progerin and lamin C in tissues from *Lmna*$^{G609G/G609G}$ sgRNA-control-transduced and *Lmna*$^{G609G/G609G}$ sgRNA-LCS2-transduced mice. Data are mean ± SEM (n=4 tissues per group, except sgRNA-control-transduced liver and heart where n=5; two-tailed Student's t-test).

In addition, we also performed progerin immunohistochemistry in tissue sections from various organs to determine the editing effect at a protein level. These analyses revealed a significant reduction of progerin-positive nuclei in liver, heart and skeletal muscle from sgRNA-LCS2-transduced mice compared to control-transduced animals (**Fig. 10**). Remarkably, these results concurred with the DNA sequencing data.

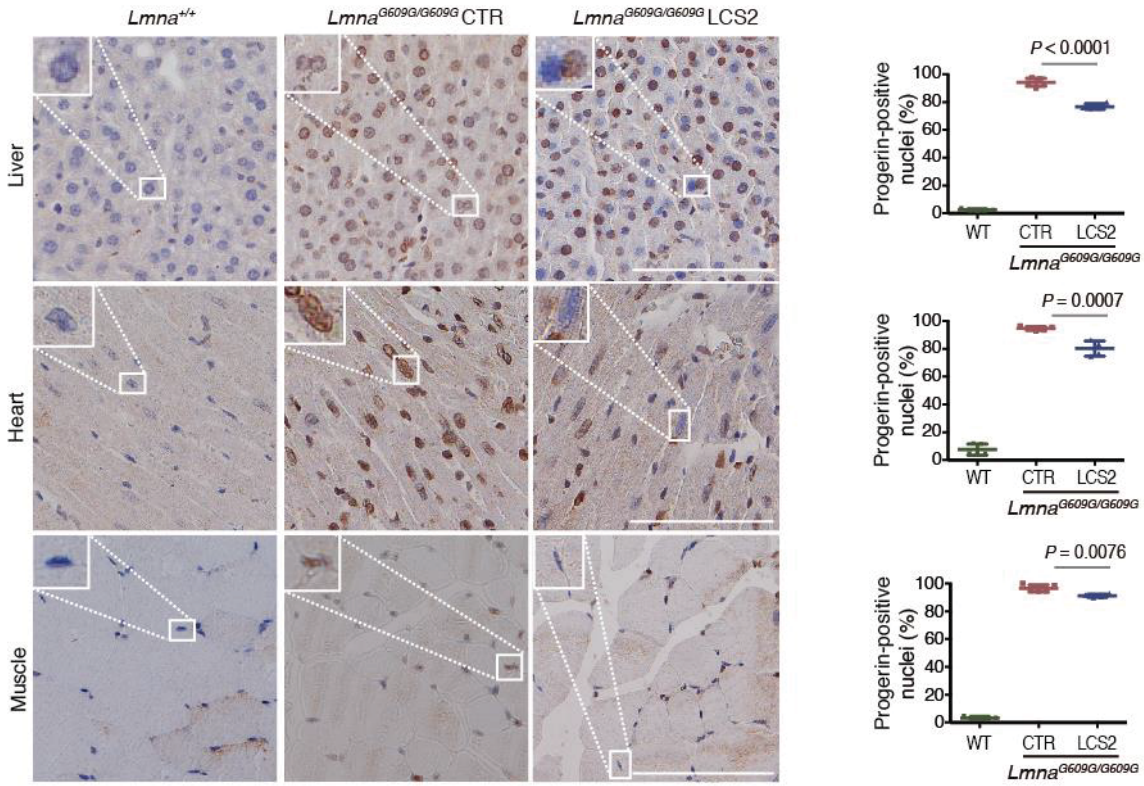

Figure 10. Progerin reduction in treated *Lmna*$^{G609G/G609G}$ mice. Progerin immunohistochemistry in liver, heart and muscle from control and LCS2-transduced mice. Data are mean ± SD (n=5 wild-type and sgRNA-control-transduced mice; n=4 sgRNA-LCS2-transduced mice; two-tailed Student's t-test). Insets, digital magnification of a selected area. Scale bars, 100 μm.

However, in lung, kidney and aorta, no reduction in the number of progerin-positive nuclei was observed, possibly due to the lower tropism of the AAV9 in these tissues (**Fig. 11**). Given the importance of vascular alterations in HGPS, the lack of noticeable direct effects on aorta is a setback of the approach tested. Nevertheless, vascular pathologies characteristic of HGPS such as atherosclerosis are strongly influenced by systemic factors. Therefore, a reliable assessment of potential vascular benefits will ideally require the use of more susceptible mouse models carrying additional genetic alterations, such as *Apoe* or *Ldlr* inactivation[192].

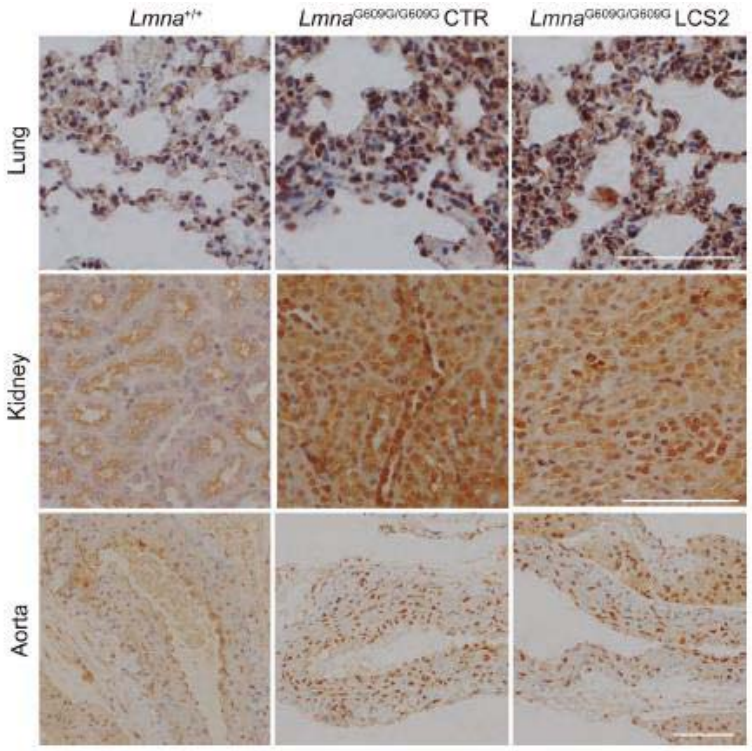

Figure 11. Progerin immunohistochemistry in lung, kidney and aorta. Progerin immunohistochemistry in tissues from WT, *Lmna*$^{G609G/G609G}$ sgRNA-control-transduced and *Lmna*$^{G609G/G609G}$ sgRNA-LCS2-transduced mice (lung and kidney, n=5 for WT and sgRNA-control-transduced mice and n=4 for sgRNA-LCS2-transduced mice; aorta, n=2 for WT and n=3 for sgRNA-control- and sgRNA-LCS2-transduced *Lmna*$^{G609G/G609G}$ mice). Scale bar, 100 μm.

1.4. Phenotype characterization of Lmna$^{G609G/G609G}$ mice after AAV9 CRISPR/Cas9 treatment

We next explored the effect of progerin reduction in lifespan and healthspan of treated mice. Importantly, progerin reduction in AAV9-sgRNA-LCS2-transduced mice was translated into an increase in their median survival of 33.5 days, from 127 to 160.5 days, compared to the control-transduced cohort, which represents a 26.4% lifespan increase (**Fig. 12a**). Mean survival was extended from 128.1 days (SD 15.73; 95% CI 116.8-139.4) to 167.4 days (SD 30.41; 95% CI 145.6-189.2). Likewise, the maximum survival was extended from 151 to 212 days ($P < 0.05$; one-tailed Fisher exact test). Phenotypically, sgRNA-LCS2-transduced *Lmna*$^{G609G/G609G}$ mice were more active and presented a healthier appearance, with retarded loss of grooming, improved posture and a slight increase in body weight (**Fig. 12b,c**). Progeroid mice progressively lose weight as they age. To evaluate this trait, we monitored their weight from week 9 and observed a reduced weight loss in sgRNA-LCS2-transduced mice. These animals also showed

increased blood glucose levels in comparison with control mice, partially rescuing the hypoglycemia characteristic of progeroid mice (**Fig. 12d**).

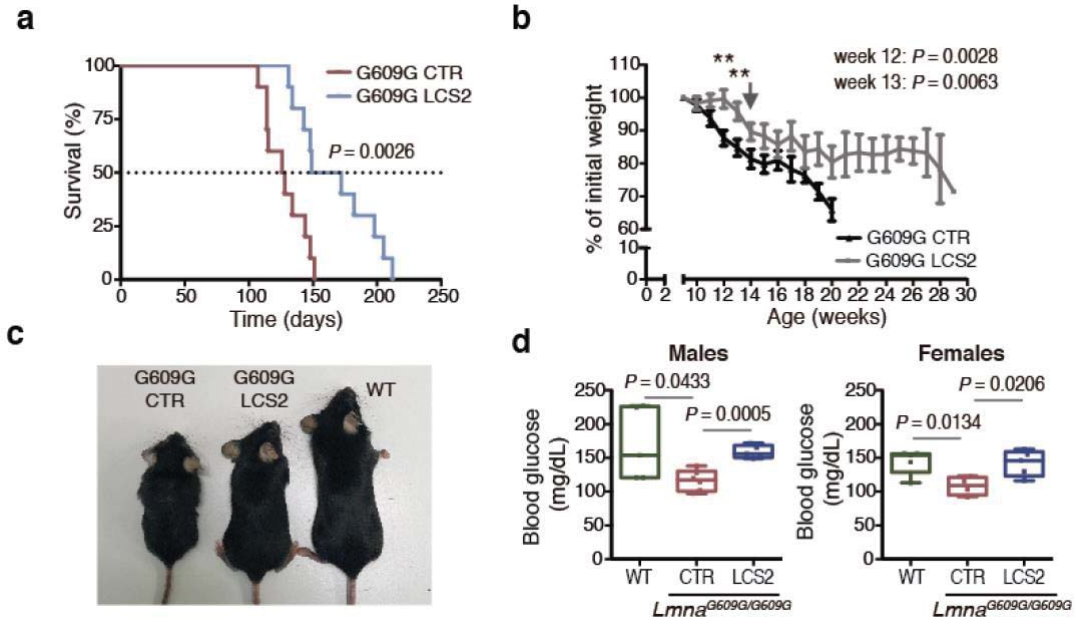

Figure 12. Phenotype amelioration of *Lmna*$^{G609G/G609G}$ mice. (a) Kaplan-Meier survival plot of sgRNA-control *versus* sgRNA-LCS2-transduced *Lmna*$^{G609G/G609G}$ mice (n=10 mice per group; two-sided Log-rank test). **(b)** Progression of body weight of mice transduced with sgRNA-control or sgRNA-LCS2, expressed as percentage of weight at 9 weeks. Vertical arrow, time point (3.5 months) at which the cohort destined for histological studies (4-5 mice per group) was sacrificed. Mean values ± SEM are represented (initial n=15 sgRNA-control-transduced mice; n=14 sgRNA-LCS2-transduced mice; two-tailed Student's t-test). **(c)** Representative photograph of *Lmna*$^{G609G/G609G}$ control-transduced, sgRNA-LCS2-transduced and *Lmna*$^{+/+}$ female mice at 3.5 months of age. **(d)** Blood glucose levels in *Lmna*$^{+/+}$ (males, n=5; females, n=5), sgRNA-control-transduced (males, n=6; females, n=4) and sgRNA-LCS2-transduced *Lmna*$^{G609G/G609G}$ mice (males, n=5; females, n=5). Data are represented by box plots and whiskers are minimum to maximum values (two-tailed Student's t-test).

Furthermore, TUNEL analysis revealed that the sgRNA-LCS2-transduced group presented significantly less apoptotic cells in the kidney (**Fig. 13a)**. Since progerin reduction was not detected in this organ, this result suggests an effect dependent on systemic factors. Cardiac and skeletal muscles are also altered in HGPS mouse models, showing a fibrosis phenotype. To assess it in these tissues, we performed Gomori's trichrome staining, which revealed a reduced focal and perivascular fibrosis in heart and quadriceps muscle in sgRNA-LCS2-transduced mice, which was in accordance with their higher mobility **(Fig. 13b)**. Finally, we analyzed gastric tissue by histology, as it shows degeneration in progeroid mice, and observed a decrease in gastric mucosa atrophy in sgRNA-LCS2-transduced compared to sgRNA-control-transduced animals **(Fig. 13c)**.

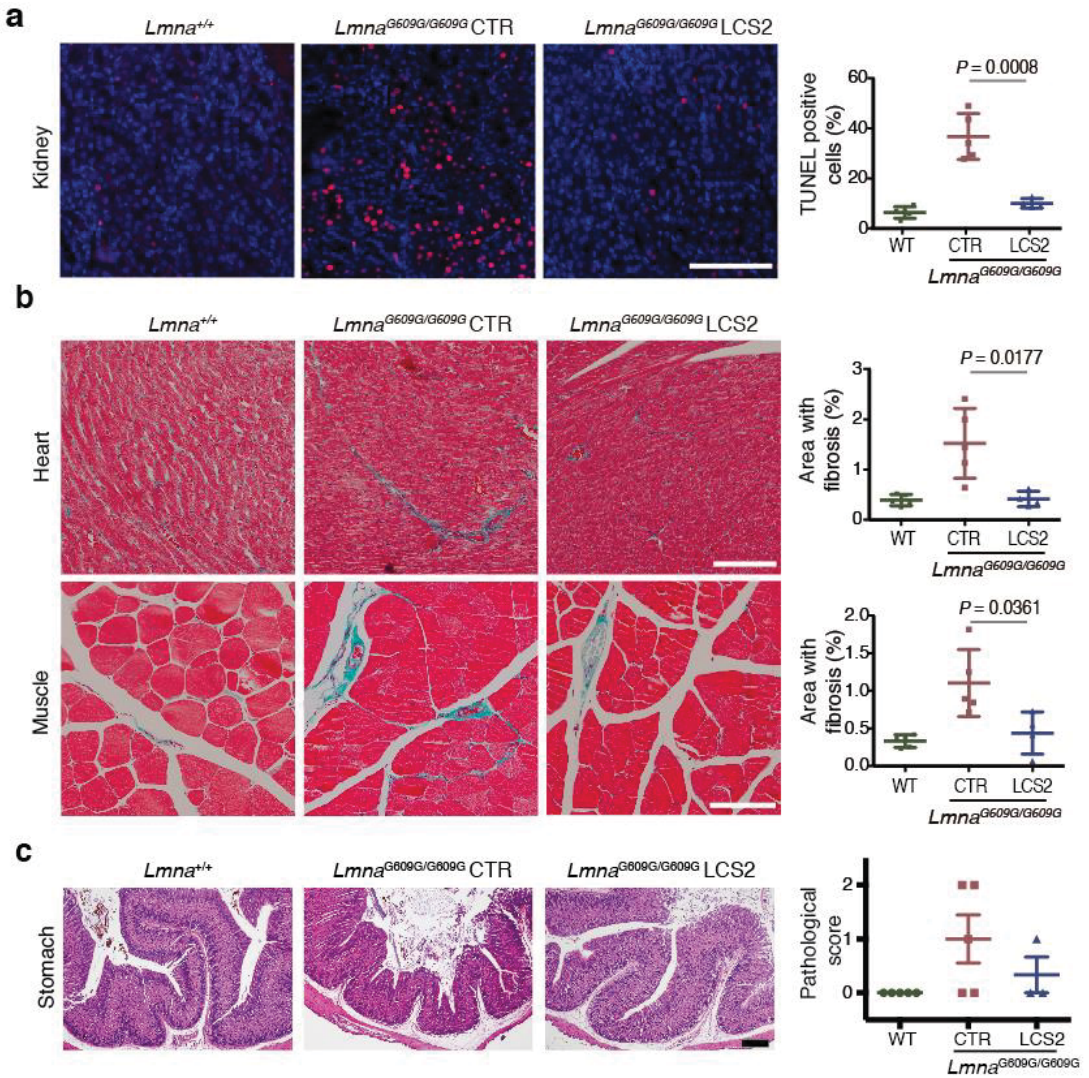

Figure 13. Histological studies in *Lmna*$^{G609G/G609G}$ mice. (a) TUNEL assay in kidney of 3.5-month-old mice. Data are mean ± SD (n=5 wild-type and sgRNA-control-transduced mice; n=4 sgRNA-LCS2-transduced mice; two-tailed Student's t-test). **(b)** Gomori's trichrome staining in 3.5-month-old mouse tissues showing moderate perivascular and interstitial fibrosis in heart and quadriceps muscle of *Lmna*$^{G609G/G609G}$ mice (blue areas). Data are mean ± SD (n=5 wild-type and sgRNA-control-transduced mice; n=4 sgRNA-LCS2-transduced mice; two-tailed Student's t-test). Scale bars, 100 μm.

In summary, we have provided herein some data that support the efficacy of our genome editing strategy both in HGPS cells and in the *Lmna*$^{G609G/G609G}$ mouse experimental model of the disease. The CRISPR/Cas9 system can reduce the progerin load in cells and relieve therefore the phenotype of progeroid mice, which is translated into an extension of their lifespan. We have proposed the use of AAV9 as an effective delivery method, due to their safety in clinical trials and their wide organ tropism, especially in cardiac tissue, which is one of the most affected tissues in HGPS pathology. On the whole, this supports the potential use of gene-editing approaches for the treatment of HGPS patients. Furthermore, as the Cas9 endonuclease is not directed specifically

against the p.Gly608Gly point mutation, which is the most common HGPS mutation, this strategy would also permit the treatment of other less frequent *LMNA* mutations causing HGPS or type A laminopathies.

Table 1. Illumina sequencing reads with indels in the liver of a mouse transduced with sgRNA-LCS2 by AAV9 delivery. Percentage of each indel is shown.

Sequence	bp	Type	% of total indels
CGGTGCGTGAGCGCAGGTTGTACTCAGC--GGTCCCCCGAGCCGCTGCAGTGGGAACCCT	-2	Frameshift	15.64
CGGTGCGTGAGCGCAGGTTGTACTCAGC-GGGTCCCCCGAGCCGCTGCAGTGGGAACCCT	-1	Frameshift	10.38
CGGTGCGTGAGCGCAGGTTGTACTC----------AGCCGCTGCAGTGGGAACCCT	-14	Frameshift	4.22
CGGTGCGTGAGCGCAGGTTGTACTCAG----------CGAGCCGCTGCAGTGGGAACCCT	-10	Frameshift	2.68
CGGTGCGTGAGCGCAGGTT----------GTCCCCCGAGCCGCTGCAGTGGGAACCCT	-12	In-frame	2.42
CGGTGCGTGAGCGCAGGTTGTAC---------TCCCCCGAGCCGCTGCAGTGGGAACCCT	-9	In-frame	1.95
CGGTGCGTGAGCGCAGGTTGTACTCA----GGTCCCCCGAGCCGCTGCAGTGGGAACCCT	-4	Frameshift	1.89
CGGTGCGTGAGCGCAGGTTGTA----------CCCGAGCCGCTGCAGTGGGAACCCT	-13	Frameshift	1.87
CGGTGCGT----------GAGCCGCTGCAGTGGGAACCCT	-30	In-frame	1.80
CGGTGCGTGAGCGCAGGTTGTACTCA----------GCTGCAGTGGGAACCCT	-17	Frameshift	1.47
CGGTGCGTGAGC----------GCAGTGGGAACCCT	-34	Frameshift	1.16
CGGTGCGTGAGCGCAGGTTGTACTCAGCGGGGT-CCCCGAGCCGCTGCAGTGGGAACCCT	-1	Frameshift	1.12
CGGTGCGTGAGCGCAGGTTGTACTCAGCGG----CCCCGAGCCGCTGCAGTGGGAACCCT	-4	Frameshift	1.03
CGGTGCGTGAGCGCAGGTTGTACTCAGCGGTGGTCCCCCGAGCCGCTGCAGTGGGAACCCT	1	Frameshift	0.96
CGGTGCGTGAGCGCA----------GGTCCCCCGAGCCGCTGCAGTGGGAACCCT	-15	In-frame	0.96
CGGTGCGTGAGCGCAGGTTGTACTCAGCG----------GCTGCAGTGGGAACCCT	-14	Frameshift	0.82
CGGTGCGTGAGCGCAGGTTGTACTCAGCGGAGGTCCCCCGAGCCGCTGCAGTGGGAACCCT	1	Frameshift	0.79
CGGTGCGTGAGCGCAGGTTGTACT----------CCGAGCCGCTGCAGTGGGAACCCT	-12	In-frame	0.78
CGGTGCGTGAGCGCAGGTTGTACT----------CCCCGAGCCGCTGCAGTGGGAACCCT	-10	Frameshift	0.68

Table 2. Illumina sequencing reads with indels in the heart of a mouse transduced with sgRNA-LCS2 by AAV9 delivery. Percentage of each indel is shown.

Sequence	bp	Type	% of total indels
CGGTGCGTGAGCGCAGGTTGTACTCAGC--GGTCCCCCGAGCCGCTGCAGTGGGAACCCT	-2	Frameshift	23.37
CGGTGCGTGAGCGCAGGTTGTACTCAGC-GGGTCCCCCGAGCCGCTGCAGTGGGAACCCT	-1	Frameshift	17.87
CGGTGCGTGAGCGCAGGTTGTACTCAGCGGGGT-CCCCGAGCCGCTGCAGTGGGAACCCT	-1	Frameshift	3.57
CGGTGCGTGAGCGCAGGTT----------GTCCCCCGAGCCGCTGCAGTGGGAACCCT	-12	In-frame	2.31
CGGTGCGTGAGCGCAGGTTGTACTCA----GGTCCCCCGAGCCGCTGCAGTGGGAACCCT	-4	Frameshift	2.15
CGGTGCGTGAGCGCAGGTTGTACTCAG---------CGAGCCGCTGCAGTGGGAACCCT	-10	Frameshift	1.63
CGGTGCGTGAGCGCAGGTTGTACTCAG------CCCCCGAGCCGCTGCAGTGGGAACCCT	-6	In-frame	1.21
CGGTGCGTGAGCGCAGGTTGTACTCAGCGG----CCCCGAGCCGCTGCAGTGGGAACCCT	-4	Frameshift	1.05
CGGTGCGTGAGCGCAGGTTGTACTCAGCGGAGGTCCCCCGAGCCGCTGCAGTGGGAACCCT	1	Frameshift	0.86
CGGTGCGTGAGCGCAGGTTGTACTC----------AGCCGCTGCAGTGGGAACCCT	-14	Frameshift	0.82
CGGTGCGTGAGCGCAGGTTGTACTCAGCGGTGGTCCCCCGAGCCGCTGCAGTGGGAACCCT	1	Frameshift	0.70
CGGTGCGTGAGCGCAGGTTGTACTCA---GGGTCCCCCGAGCCGCTGCAGTGGGAACCCT	-3	In-frame	0.70
----------GTCCCCCGAGCCGCTGCAGTGGGAACCCT	-44	Frameshift	0.68
CGGGGCGTGAGCGCAGGTTGTACTCAGC-GGGTCCCCCGAGCCGCTGCAGTGGGAACCCT	-1	Frameshift	0.68
CGGTGCGTGAGCGCAGGTTGTACT---------CCCCGAGCCGCTGCAGTGGGAACCCT	-10	Frameshift	0.65
CGGTGCGGGAGCGCAGGTTGTACTCAGC-GGGTCCCCCGAGCCGCTGCAGTGGGAACCCT	-1	Frameshift	0.61
CGGTGCGTGAGCGCAGGTTGTACTCA----------GCTGCAGTGGGAACCCT	-17	Frameshift	0.60
CGGTGCGTGAGCGCAGGTTGTACTCA-----GTCCCCCGAGCCGCTGCAGTGGGAACCCT	-5	Frameshift	0.60
CGGTGCGTGAGCGCAGGTTGTAC---------TCCCCCGAGCCGCTGCAGTGGGAACCCT	-9	In-frame	0.57

Table 3. Illumina sequencing reads with indels in the muscle of a mouse transduced with sgRNA-LCS2 by AAV9 delivery. Percentage of each indel is shown.

Sequence	bp	Type	% of total indels
CGGTGCGTGAGCGCAGGTTGTACTCAGC--GGTCCCCCGAGCCGCTGCAGTGGGAACCCT	-2	Frameshift	39.75
CGGTGCGTGAGCGCAGGTTGTACTCAGC-GGGTCCCCCGAGCCGCTGCAGTGGGAACCCT	-1	Frameshift	24.08
CGGTGCGTGAGCGCAGGTTGTACTCAGCGGGGT-CCCCGAGCCGCTGCAGTGGGAACCCT	-1	Frameshift	2.77
CGGTGCGTGAGCGCAGGTTGTACTCAG----------CGAGCCGCTGCAGTGGGAACCCT	-10	Frameshift	2.46
CGGTGCGTGAGCGCAGGTTGTACT------GGTCCCCCGAGCCGCTGCAGTGGGAACCCT	-6	In-frame	1.94
CGGGGCGTGAGCGCAGGTTGTACTCAGC-GGGTCCCCCGAGCCGCTGCAGTGGGAACCCT	-1	Frameshift	1.28
CGGTGCGTGAGCGCAGGTTGTACTCAGCG----------GTGGGAACCCT	-20	Frameshift	1.14
CGGTGCGTGAGCGCAGGTT----------GCTGCAGTGGGAACCCT	-24	In-frame	1.07
CGGTGCGTGAGCGCAGGTTGTACTCAGCGGTGGTCCCCCGAGCCGCTGCAGTGGGAACCCT	1	Frameshift	0.73
CGGTGCGTGAGCGCAGGTT----------CGGTCCCCCGAGCCGCTGCAGTGGGAACCCT	-10	Frameshift	0.73
CGGTGCGTGAGCGCAGGTTGTACTC----------AGCCGCTGCAGTGGGAACCCT	-14	Frameshift	0.72
CGGTGCGTGAGCGCAGGTTGTACTCAGC-AGGTCCCCCGAGCCGCTGCAGTGGGAACCCT	-1	Frameshift	0.68
CGGTGCGTGAGCGCAGGTTGTACTCAGCGG----CCCCGAGCCGCTGCAGTGGGAACCCT	-4	Frameshift	0.65
CGGTGCGTGAGCGCAGGTTGTACTCAGCGG--------GACCCGCTGCAGTGGGAACCCT	-8	Frameshift	0.61
CGGTGCGGGAGCGCAGGTTGTACTCAGC-GGGTCCCCCGAGCCGCTGCAGTGGGAACCCT	-1	Frameshift	0.61
CGGTGCGT----------GAGCCGCTGCAGTGGGAACCCT	-30	In-frame	0.59
CGGTGCGTGAGCGCAGGTTGTACTCAGCGGGGGTCCCCCGAGCCGCTGCAGTGGGAACCCT	1	Frameshift	0.54
CGGTGCGTGGGCGCAGGTTGTACTCAGC-GGGTCCCCCGAGCCGCTGCAGTGGGAACCCT	-1	Frameshift	0.51
CGGTGCG----------TGCAGTGGGAACCCT	-38	Frameshift	0.44

Table 4. Illumina sequencing reads with indels in the lungs of a mouse transduced with sgRNA-LCS2 by AAV9 delivery. Percentage of each indel is shown.

Sequence	bp	Type	% of total indels
CGGTGCGTGAGCGCAGGTTGTACTCAGC--GGTCCCCCGAGCCGCTGCAGTGGGAACCCT	-2	Frameshift	18.74
CGGTGCGTGAGCGCAGGTTGTACTCAGCGGGGT-CCCCGAGCCGCTGCAGTGGGAACCCT	-1	Frameshift	15.94
CGGTGCGTGAGCGCAGGTTGT----------	-79	Frameshift	13.25
CGGTGCGTGAGCGCAGGTTGT----------ACCCT	-34	Frameshift	7.94
CGGTGCGTGAGCGCAGGTTGTACTCAG----------CGAGCCGCTGCAGTGGGAACCCT	-10	Frameshift	7.79
CGGTGCGTGAGCGCAGGTTGTACT----------CCCT	-32	Frameshift	4.71
CGGTGCGTGAGCGCAGGTTGTA--------GGTCCCCCGAGCCGCTGCAGTGGGAACCCT	-8	Frameshift	4.67
CGGTGCGTGAGCGCAGGTTGTACTC----------AGCCGCTGCAGTGGGAACCCT	-14	Frameshift	4.02
CGGTGCGTGAGCGCAGGTTGTACTCAGC-GGGTCCCCCGAGCCGCTGCAGTGGGAACCCT	-1	Frameshift	3.27
CGGTGCGTGAGCGCAGGTTGTAC---------TCCCCCGAGCCGCTGCAGTGGGAACCCT	-9	In-frame	0.77
CGGGGCGTGAGCGCAGGTTGTACTCAGCGGGGT-CCCCGAGCCGCTGCAGTGGGAACCCT	-1	Frameshift	0.60
CGGTGCGTGAGCGCAGGTTGTACTCAGCGGGGTCCCCCGAGCCGCTGCAGT-GGAACCCT	-1	Frameshift	0.58
CGGTGCGTGAGCGCAGGTTGTACTCAGC-GGGTCCCCCGAGCCGCTGCAGCGGGAACCCT	-1	Frameshift	0.41
CGGTGCGTGGGCGCAGGTTGTACTCAG----------CGAGCCGCTGCAGTGGGAACCCT	-10	Frameshift	0.37
CGGTGCGTGAGCGCAGGTTGTACTCAGCGGGGTCCCCCCGAGCCGCTGCAGTGGGAACCCT	1	Frameshift	0.32
CGGCGCGTGAGCGCAGGTTGTACTCAG----------CGAGCCGCTGCAGTGGGAACCCT	-10	Frameshift	0.26
CGGTGCGTGAGCGCAGGGTGTACTCAGC--GGTCCCCCGAGCCGCTGCAGTGGGAACCCT	-2	Frameshift	0.24
CGGTGTGTGAGCGCAGGTTGTAC---------TCCCCCGAGCCGCTGCAGTGGGAACCCT	-9	In-frame	0.24
CGGTGCGTGAGCGCAGGTTGT-CTCAGCGGGGTCCCCCGAGCCGCTGCAGTGGGAACCCT	-1	Frameshift	0.22

2. Analysis of DNA repair-related genes in giant tortoises as a long-lived model organism

Genomic instability is related with a higher incidence of cancer in multicellular organisms and constitutes one of the primary hallmarks of aging[1], although the impact of its reduction in lifespan extension is yet to be established. Comparative genomic analyses of some long-lived organisms point to a positive selection of numerous DNA repair genes. In this sense, giant tortoises represent an interesting model for the study of genomic stability maintenance in the context of longevity and cancer resistance, as they are among the longest-lived animals. Unfortunately, genomic data on giant tortoises is still scarce, with the exception of the Agassiz's desert tortoise (*Gopherus agassizii*) whose draft genome has been recently annotated[193].

In this section, we provide a deep comparative analysis of DNA repair genes of the last member of *Chelonoidis abingdonii*, a Galapagos giant tortoise commonly known as Lonesome George, and an individual of *Aldabrachelys gigantea*, the Aldabra giant tortoise. Accordingly, we performed manually supervised annotation and analysis of 178 genes involved in different mechanisms of DNA repair, including base excision repair (BER), mismatch repair (MMR), nucleotide excision repair (NER), non-homologous end joining (NHEJ) and homologous recombination (HR) **(Fig. 14; Table 5)**. Manual annotation takes a bigger effort than automatic analysis, which is more used nowadays. However, it allows a better identification of genes and relevant variants. Novel variants were identified when compared with mammal species (*Homo sapiens*, *Loxodonta africana*, *Mus musculus*, *Heterocephalus glaber*, *Microtus oeconomus*), fishes (*Danio rerio*, *Barbus barbus*) cephalopods (*Loligo forbesi*), birds (*Gallus gallus*) and reptiles, including lizards (*Anolis carolinensis*), turtles (*Pelodiscus sinensis*, *Chelonia mydas*, *Chrysemys picta belli*) and the tortoise *G. agassizii*. These variants were first validated by RNA-Seq data, obtained from a blood sample in the case of *C. abingdonii* and a granuloma in *Aldabrachelys gigantea*. The most interesting variants, involving gene duplications or those affecting key motifs, were confirmed by PCR amplification and Sanger sequencing and compared with DNA samples obtained from other 11 tortoise species.

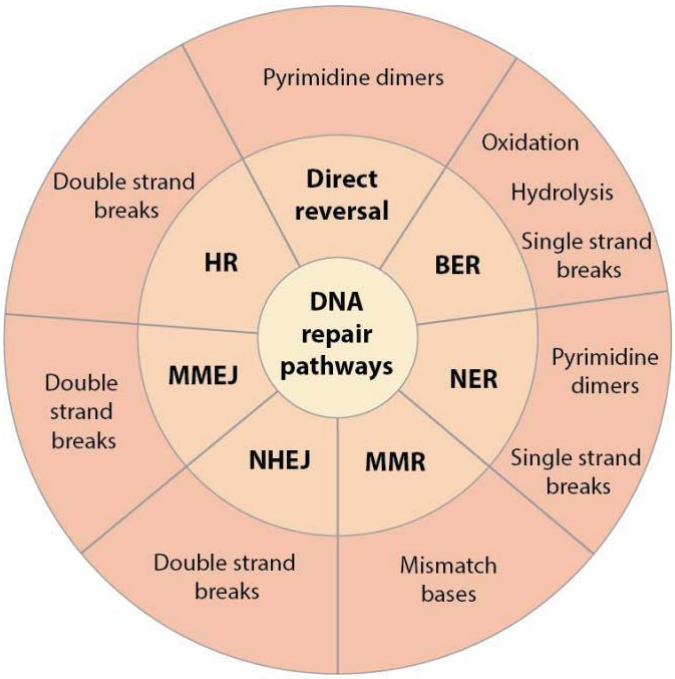

Figure 14. DNA repair pathways depending on the type of damage. BER, base excision repair; NER, nucleotide excision repair; MMR, mismatch repair; NHEJ, non-homologous end joining; MMEJ, microhomology-mediated end joining; HR, homologous recombination.

2.1. Search of relevant variants in C. abingdonii and A. gigantea

A first overall analysis revealed that DNA repair genes appear highly conserved in giant tortoises, with the exception of some rapidly evolving genes, such as the Werner syndrome gene (*WRN*) **(Table 5)**. This fact underlies the importance of DNA repair and genome integrity in long-lived species. Still, point variants and duplications with a potential relevance were found in some of these genes, which could suggest differences in the expression, regulation or interactions of the DNA repair factors in *C. abingdonii* and *A. gigantea*.

Specifically, we observed a variant in the DNA damage response gene *TP53* in both giant tortoises. p53 is a transcription factor with different functions in regulating cell cycle, apoptosis and energy metabolism, and has a major role in tumor suppression[194]. This important transcription factor presents one functional copy in *C. abingdonii, A. gigantea* and in the rest of Reptilia[195,196], essential for DNA stability and cancer protection. However, *C. abingdonii* shares with the other Testudines (including the other giant tortoises analyzed herein) a modification at codon 106 (p.S106E), which had been previously identified in root vole (*Microtus oeconomus*)[197] **(Fig. 15)**. This variant had

been described as an adaptation to hypoxia in the Tibet plateau niche and it is also found in four fish species (*Barbus barbus*, *Tetraodon miurus*, *Platichthys flesus* and *Xiphophorus hellerii*) and a squid species (*Loligo forbesi*). It has been observed that p.S106E variant avoids activation of the apoptotic genes *IGFBP3*, *APAF1*, *BAX*, *NOXA*, *PUMA* and *HDM* by p53, without affecting cell-cycle genes. As a result, cell apoptosis by p53 is suppressed under stress conditions[197]. This variant in *TP53* could suggest a process of convergent evolution in the adaptation to hypoxia, likely driven by an ancestral aquatic environment, which left this footprint in the genomes of terrestrial giant tortoises. Interestingly, giant tortoises also show the p.R72P ancestral variant in *TP53*, which has been associated with longevity and improved cancer prognosis in human populations[198].

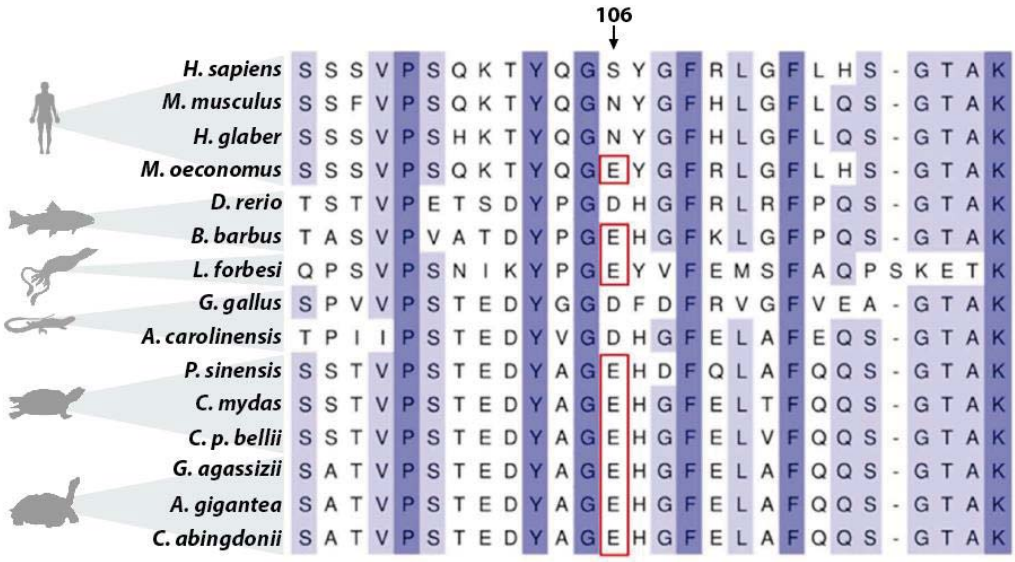

Figure 15. Partial amino acid alignment of the *TP53* sequence in *C. abingdonii*, *A. gigantea* and other vertebrate species. Codon 106 changes from serine (S) to glutamic acid (E) are highlighted with red boxes.

Then, we also identified and validated a duplication in *C. abingdonii* and *A. gigantea* affecting *NEIL1*, a DNA glycosylase involved in the pre-replicative removal of oxidized DNA bases by BER[199] **(Fig. 16)**. Duplications in *NEIL1* were also found in *C. p. bellii*, and in the tortoise *G. agassizii*, as well as in the other Galápagos tortoises, Aldabra Island tortoises, and their corresponding continental outgroups. According to RNA-Seq data, both copies are expressed and no evidence of a positive selection process was found in either of them, based on their dN/dS value. Previous studies have associated a higher expression of *NEIL1* in naked mole rats with their extended longevity compared to mice[200]. Moreover, downregulation of this gene has been reported in cancer[201]. These

results suggest that *NEIL1* could be a candidate gene for longevity and cancer protection through maintenance of genomic stability.

Likewise, we found another duplication affecting *RMI2*, which has a major role in processing homologous recombination intermediates to limit DNA crossover formation in cells[202]. Interestingly, loss of *RMI2* leads to increased genome instability and cancer predisposition[203]. In giant tortoises, both copies seem to be expressed, as confirmed by RNA-Seq. Other Sauropsida, such as *C. p. bellii*, *P. sinensis* or *A. carolinensis*, present a second pseudogenized copy although it does not seem to be functional. Duplication in *RMI2* might suggest an enhanced ability to resolve homologous recombination intermediates, which can lead to a higher genome integrity.

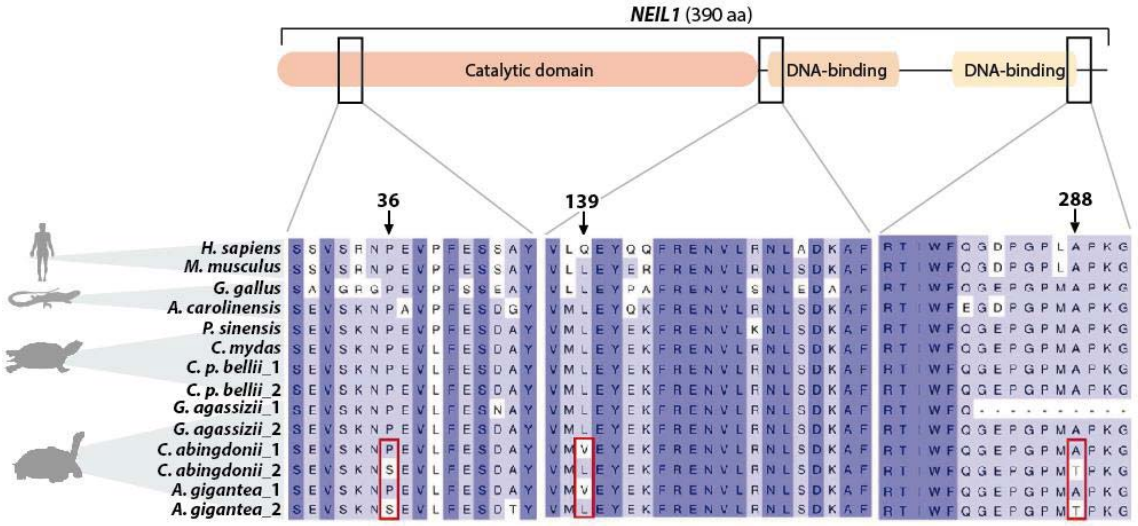

Figure 16. Partial amino acid alignment of *NEIL1* sequence in *C. abingdonii*, *A. gigantea*, and other vertebrate species. Copy-specific variants present in *C. abingdonii* and *A. gigantea* are highlighted with a red rectangle.

In addition, some alterations were identified in genes involved in non-homologous end-joining (NHEJ), an essential pathway that repairs double-strand breaks in DNA. This way, variants affecting sumoylation sites were found in *XRCC6* (p.K556R) and *XRCC5* (p.K568N), two ssDNA-dependent ATP-dependent helicases involved in NHEJ[204,205]. The variant affecting *XRCC6* is present in *C. abingdonii*, *A. gigantea* and other giant tortoises used for Sanger sequencing validation **(Fig. 17)**, and the mutation affecting *XRCC5* was also found in *C. p. belli*, and *P. sinensis*. Unexpectedly, the naked mole rat, the longest-living rodent, also presented a similar variant in *XRCC6* (p.K556N)[10]. Sumoylation is the post-translational covalent addition of a small ubiquitin-like modifier (SUMO) to certain lysine residues and can play a role in genomic stability and

transcription by regulating protein-protein interactions[206]. Consequently, alterations in this process may have an effect in the DNA repair response.

On the other hand, protection against NHEJ is important in telomeres, as they can be mistaken with DNA breaks. To avoid this, DCLRE1B, together with other proteins, has an important role in the protection of telomeres by forming the telomeric loop (T-loop) after being recruited by TERF2[207]. We found a modification in DCLRE1B in the heterodimer interface binding TERF2 (p.R498C) in *C. abingdonii*, *A. gigantea* and the other giant tortoises used in the validation **(Fig. 17)**. Interestingly, TERF2 also had several modifications in the binding domain to DCLRE1B (p.S161T, p.M164T, p.N176G and p.M180L), which was also shared by other turtles. These variants in key binding residues could affect the interactions between these two proteins and therefore vary the T-loop formation. Moreover, the aforementioned variants in *XRCC5* and *XRCC6*, could also impinge on telomere dynamics in tortoises[208,209].

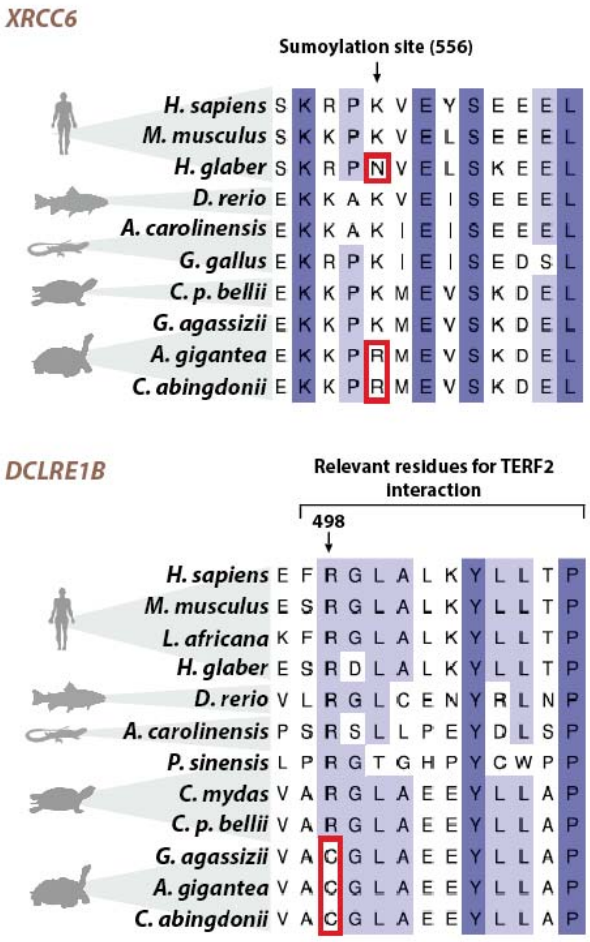

Figure 17. Partial amino acid alignment of *XRCC6* and *DCLRE1B* sequences in *C. abingdonii*, *A. gigantea*, and other vertebrate species. Codon changes are highlighted with red boxes.

2.2. Functional analysis of NEIL1 and RMI2 duplications

To complete this study, we aimed to explore if the duplications affecting *NEIL1* and *RMI2* could play a role in modulating the DNA repair response to induced stress. As a proof of principle, we cloned the corresponding cDNAs on a pCDH vector and transduced HEK-293T cells with them, individually and in combination —pCDH, pCDH-NEIL1, pCDH-RMI2 and pCDH-NEIL1+pCDH-RMI2— to evaluate their combined effect. Next, we isolated clones from each condition overexpressing reasonable levels of these genes, and exposed cells to sub-lethal doses of either UV light (20 J/m^2) or H_2O_2 stress (500 μM). The activation of DNA damage response pathways was analyzed by Western blot 24 or 48 hours after the exposition to damage. We observed a reduction in histone H2AX phosphorylation and in the cleavage of poly (ADP-ribose) polymerase (PARP) in all different conditions **(Fig. 18)**, suggesting a decrease in the levels of DNA damage in the cell. Hence, duplications in *NEIL1* and *RMI2* existing in giant tortoises could provide them with a quicker and improved DNA-repair response, consequently contributing to their extended longevity and cancer protection.

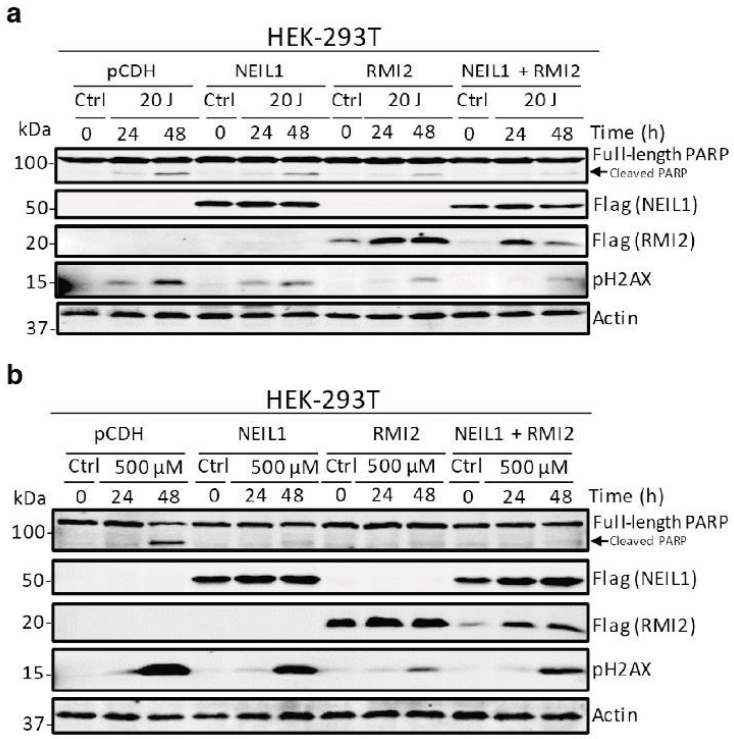

Figure 18. Effect of *NEIL1* and *RMI2* overexpression in the DNA damage response in HEK-293T cells. (a) Western blot analysis of the phosphorylation of histone H2AX at serine 139, and cleaved PARP in cells exposed to UV light (20 J/m^2), after 24 and 48 hours. Note that Flag (RMI2) was detected on the same samples used for the remaining Western-blots shown in this panel, run in parallel on an identical blot. **(b)** Western blot analysis of H2AX phosphorylated at serine 139, and cleaved PARP in cells exposed to H_2O_2 treatment (500 μM), after 24 and 48 hours. The Western-blots shown were carried out with the same

samples run in parallel in three identical blots (one for PARP and actin, a second blot for Flag (NEIL1 and RMI2), and a third blot for pH2AX).

On the whole, the data shown herein suggest a high conservation and, in some cases, even expansion of DNA repair genes in both *C. abingdonii* and *A. gigantea*. Minor variants could also point to small differences in the interaction or regulation of DNA repair proteins, in particular those involved in NHEJ. Interestingly, *TP53* analysis showed a specific variant shared with other Testudines which had been described as an adaptation to hypoxia. As these giant tortoises did not live in an environment with low levels of oxygen, this adaptation could be considered as a residual trace of evolution. Furthermore, duplications in some DNA damage response genes could promote genome integrity, contributing to the prolonged lifespan and cancer protection of giant tortoises and turtles.

Table 5. DNA repair genes analyzed and variants found in *C. abingdonii*.

Gene name	Activity	*C. abingdonii*
Base excision repair (BER)	**Major altered base released**	
UNG	U	No relevant variants
SMUG1	U	No relevant variants
MBD4	U or T opposite G at CpG sequences	No relevant variants
TDG	U, T or ethenoC opposite G	No relevant variants
OGG1	8-oxoG opposite C	No relevant variants
MUTYH (MYH)	A opposite 8-oxoG	No relevant variants
NTHL1 (NTH1)	Ring-saturated or fragmented pyrimidines	No relevant variants
MPG	3-meA, ethenoA, hypoxanthine	No relevant variants
NEIL1	Removes thymine glycol	Duplication
NEIL2	Removes oxidative products of pyrimidines	K154R
NEIL3	Removes oxidative products of pyrimidines	No relevant variants
Other BER and strand break joining factors		
APEX1 (APE1)	AP endonuclease	No relevant variants
APEX2	AP endonuclease	No relevant variants
LIG3	DNA Ligase III	No relevant variants
XRCC1	LIG3 accessory factor	No relevant variants
PNKP	Converts some DNA breaks to ligatable ends	No relevant variants
APLF (C2ORF13)	Accessory factor for DNA end-joining	No relevant variants
Poly(ADP-ribose) polymerase (PARP) enzymes that bind to DNA		
PARP1 (ADPRT)	Protects strand interruptions	No relevant variants
PARP2 (ADPRTL2)	PARP-like enzyme	No relevant variants
PARP3 (ADPRTL3)	PARP-like enzyme	No relevant variants
Direct reversal of damage		
MGMT	O6-meG alkyltransferase	No relevant variants
ALKBH2 (ABH2)	1-meA dioxygenase	No relevant variants
ALKBH3 (DEPC1)	1-meA dioxygenase	E248D
Repair of DNA-topoisomerase crosslinks		
TDP1	Removes 3'-tyrosylphosphate and 3'-phosphoglycolate from DNA	No relevant variants
TDP2 (TTRAP)	5'- and 3'-tyrosyl DNA phosphodiesterase	No relevant variants
Mismatch excision repair (MMR)		
MSH2	Mismatch and loop recognition	No relevant variants
MSH3	Mismatch and loop recognition	No relevant variants
MSH6	Mismatch recognition	Missense variants
MLH1	MutL homologs, forming heterodimer	No relevant variants
PMS2	MutL homologs, forming heterodimer	No relevant variants
MSH4	MutS homologs specialized for meiosis	No relevant variants
MSH5	MutS homologs specialized for meiosis	No relevant variants
MLH3	MutL homologs of unknown function	No relevant variants
PMS1	MutL homologs of unknown function	No relevant variants
PMS2L3	MutL homologs of unknown function	No relevant variants
Nucleotide excision repair (NER)		
XPC	Binds DNA distortions	No relevant variants
RAD23B	Binds DNA distortions	No relevant variants
CETN2	Binds DNA distortions	No relevant variants

Table 5. DNA repair genes analyzed and variants found in *C. abingdonii* (Continuation).

Gene name	Activity	*C. abingdonii*
RAD23A	Substitutes for RAD23B	No relevant variants
XPA	Binds damaged DNA in preincision complex	No relevant variants
DDB1	Complex defective in XP group E	No relevant variants
DDB2 (XPE)	Complex defective in XP group E	No relevant variants
RPA1	Binds DNA in preincision complex	No relevant variants
RPA2	Binds DNA in preincision complex	No relevant variants
RPA3	Binds DNA in preincision complex	No relevant variants
ERCC3 (XPB)	3' to 5' DNA helicase	No relevant variants
ERCC2 (XPD)	5' to 3' DNA helicase	No relevant variants
GTF2H1	Core TFIIH subunit p62	No relevant variants
GTF2H2	Core TFIIH subunit p44	No relevant variants
GTF2H3	Core TFIIH subunit p34	No relevant variants
GTF2H4	Core TFIIH subunit p52	No relevant variants
GTF2H5 (TTDA)	Core TFIIH subunit p8	No relevant variants
CDK7	Kinase subunits of TFIIH	No relevant variants
CCNH	Kinase subunits of TFIIH	No relevant variants
MNAT1	Kinase subunits of TFIIH	No relevant variants
ERCC5 (XPG)	3' incision	No relevant variants
ERCC1	5' incision DNA binding subunit	No relevant variants
ERCC4 (XPF)	5' incision catalytic subunit	No relevant variants
LIG1	DNA ligase	No relevant variants
ERCC8 (CSA)	Cockayne and UV-Sensitive Syndrome	No relevant variants
ERCC6 (CSB)	Cockayne and UV-Sensitive Syndrome	No relevant variants
UVSSA (KIAA1530)	UV-Sensitive Syndrome	No relevant variants
XAB2 (HCNP)	Cockayne syndrome	No relevant variants
MMS19	Iron-sulfur cluster loading and transport	No relevant variants
Homologous recombination		
RAD51	Homologous pairing	No relevant variants
RAD51B	Rad51 homolog	S194T
RAD51D	Rad51 homolog	S197L
DMC1	Rad51 homolog, meiosis	No relevant variants
XRCC2	DNA break and crosslink repair	No relevant variants
XRCC3	DNA break and crosslink repair	No relevant variants
RAD52	Accessory factors for recombination	No relevant variants
RAD54L	Accessory factors for recombination	No relevant variants
RAD54B	Accessory factors for recombination	No relevant variants
BRCA1	Accessory factor for transcription and recombination	S308N
SHFM1 (DSS1)	BRCA2 associated	No relevant variants
RAD50	ATPase in complex with MRE11A, NBS1	No relevant variants
MRE11A	3' exonuclease, defective in ATLD (ataxia-telangiectasia-like disorder)	No relevant variants
NBN (NBS1)	Mutated in Nijmegen breakage syndrome	No relevant variants
RBBP8 (CtIP)	Promotes DNA end resection	No relevant variants
MUS81	Subunits of structure-specific DNA nuclease	No relevant variants
EME1 (MMS4L)	Subunits of structure-specific DNA nuclease	Absent

Table 5. DNA repair genes analyzed and variants found in *C. abingdonii*. (Continuation)

Gene name	Activity	*C. abingdonii*
EME2	Subunits of structure-specific DNA nuclease	No relevant variants
GIYD1 (SLX1A)	Subunit of SLX1 structure-specific nuclease	No relevant variants
GIYD2 (SLX1B)	Subunit of SLX1 structure-specific nuclease	Absent
GEN1	Nuclease cleaving Holliday junctions	No relevant variants
Fanconi anemia		
FANCA	Repair of DNA crosslinks and other adducts	No relevant variants
FANCB	Repair of DNA crosslinks and other adducts	No relevant variants
FANCC	Repair of DNA crosslinks and other adducts	No relevant variants
BRCA2 (FANCD1)	Cooperation with RAD51	S491V; S755V; S2095Q; T3387P
FANCD2	Target for monoubiquitination	No relevant variants
FANCE	Repair of DNA crosslinks and other adducts	No relevant variants
FANCF	Repair of DNA crosslinks and other adducts	No relevant variants
FANCI (KIAA1794)	Target for monoubiquitination	No relevant variants
BRIP1 (FANCJ)	DNA helicase, BRCA1-interacting	No relevant variants
FANCL	Repair of DNA crosslinks and other adducts	No relevant variants
FANCM	Helicase/translocase	No relevant variants
PALB2 (FANCN)	Co-localizes with BRCA2	No relevant variants
RAD51C (FANCO)	Rad51 homolog FANCO	No relevant variants
BTBD12 (SLX4) (FANCP)	Nuclease subunit/scaffold BTBD12 (SLX4)	No relevant variants
FAAP20 (C1orf86)	FANCA - associated	Absent
FAAP24 (C19orf40)	Repair of DNA crosslinks and other adducts	No relevant variants
Non-homologous end-joining		
XRCC6 (Ku70)	DNA end binding subunit	K556R
XRCC5 (Ku80)	DNA end binding subunit	K568N
PRKDC	DNA-dependent protein kinase catalytic subunit	S2612T
LIG4	Ligase	No relevant variants
XRCC4	Ligase accessory factor	No relevant variants
DCLRE1C (Artemis)	Nuclease	No relevant variants
NHEJ1 (XLF, Cernunnos)	End-joining factor	No relevant variants
Modulation of nucleotide pools		
NUDT1 (MTH1)	8-oxoGTPase	No relevant variants
DUT	dUTPase	No relevant variants
RRM2B (p53R2)	p53-inducible ribonucleotide reductase small subunit 2 homolog	No relevant variants
DNA polymerases (catalytic subunits)		
POLB	BER in nuclear DNA	No relevant variants
POLG	BER in mitochondrial DNA	No relevant variants
POLD1	NER and MMR	No relevant variants
POLE	NER and MMR	No relevant variants
PCNA	Sliding clamp for pol delta and pol epsilon	No relevant variants
REV3L (POLZ)	DNA pol zeta catalytic subunit	No relevant variants
MAD2L2 (REV7)	DNA pol zeta subunit	No relevant variants
REV1L (REV1)	dCMP transferase	No relevant variants
POLH	Xeroderma pigmentosum (XP) variant	No relevant variants

Table 5. DNA repair genes analyzed and variants found in *C. abingdonii*. (Continuation)

Gene name	Activity	*C. abingdonii*
POLI (RAD30B)	Lesion bypass	No relevant variants
POLQ	Sensitivity to ionizing radiation	No relevant variants
POLK (DINB1)	Lesion bypass and NER	No relevant variants
POLL	Gap-filling during NHEJ	No relevant variants
POLM	Gap filling during NHEJ	No relevant variants
POLN (POL4P)	DNA crosslink repair	No relevant variants
Editing and processing nucleases		
FEN1 (DNase IV)	5' nuclease	Duplication
FAN1 (MTMR15)	5' nuclease interacting with FANCD2	No relevant variants
TREX1 (DNase III)	3' exonuclease	Absent
TREX2	3' exonuclease	No relevant variants
EXO1 (HEX1)	3' exonuclease	S610G
APTX (aprataxin)	Processing of DNA single-strand interruptions	No relevant variants
SPO11	Endonuclease	No relevant variants
ENDOV	Incision 3' of hypoxanthine and uracil in DNA and inosine in RNA	No relevant variants
Ubiquitination and modification		
UBE2B (RAD6B)	Ubiquitin-conjugating enzyme	No relevant variants
RAD18	E3 ubiquitin ligase	No relevant variants
SHPRH	E3 ubiquitin ligase, SWI/SNF related	No relevant variants
HLTF (SMARCA3)	E3 ubiquitin ligase, SWI/SNF related	No relevant variants
RNF168	E3 ubiquitin ligase for DSB repair	R57W
SPRTN (c1orf124)	Reads ubiquitylation	No relevant variants
RNF8	E3 ubiquitin ligase for DSB repair	No relevant variants
RNF4	E3 ubiquitin ligase	No relevant variants
UBE2V2 (MMS2)	Ubiquitin-conjugating complex	No relevant variants
UBE2N (UBC13)	Ubiquitin-conjugating complex	No relevant variants
Chromatin Structure and Modification		
H2AFX (H2AX)	Histone, phosphorylated after DNA damage	No relevant variants
CHAF1A (CAF1)	Chromatin assembly factor	No relevant variants
SETMAR (METNASE)	DNA damage-associated histone methylase and nuclease	No relevant variants
Genes defective in diseases associated with sensitivity to DNA damaging agents		
BLM	Bloom syndrome helicase	No relevant variants
WRN	Werner syndrome helicase / 3' - exonuclease	Q536E; V586I; K632R; L867F
RECQL4	Rothmund-Thompson syndrome	No relevant variants
ATM	Ataxia telangiectasia	V2873I
TTDN1 (C7orf11) MPLKIP	Non-photosensitive form of trichothiodystrophy	No relevant variants
Other identified genes with known or suspected DNA repair function		
DCLRE1A (SNM1)	DNA crosslink repair	No relevant variants
DCLRE1B (SNM1B)	Related to SNM1	R498C
RPA4	Similar to RPA2	Absent
PRPF19 (PSO4)	DNA crosslink repair; binding to SETMAR	No relevant variants
RECQL (RECQ1)	DNA helicase	No relevant variants

Table 5. DNA repair genes analyzed and variants found in *C. abingdonii*. (Continuation)

Gene name	Activity	*C. abingdonii*
RECQL5	DNA helicase	No relevant variants
HELQ (HEL308)	DNA helicase	No relevant variants
RDM1 (RAD52B)	Similar to RAD52	No relevant variants
OBFC2B (SSB1)	Single-stranded DNA binding protein	No relevant variants
RMI2	Processing of homologous recombination intermediates	Duplication
Other conserved DNA damage response genes		
ATR	ATM- and PI-3K-like essential kinase	No relevant variants
ATRIP	ATR-interacting protein	No relevant variants
MDC1	Mediator of DNA damage checkpoint	No relevant variants
RAD1	Subunits of PCNA-like sensor of damaged DNA	Duplication
RAD9A	Subunits of PCNA-like sensor of damaged DNA	No relevant variants
HUS1	Subunits of PCNA-like sensor of damaged DNA	No relevant variants
RAD17 (RAD24)	RFC-like DNA damage sensor	No relevant variants
CHEK1	Effector kinases	No relevant variants
CHEK2	Effector kinases	No relevant variants
TP53	Regulation of the cell cycle	R72P; S106E; R290C
TP53BP1 (53BP1)	Chromatin-binding checkpoint protein	T543I
RIF1	Suppressor of 5'-end-resection	No relevant variants
TOPBP1	DNA damage checkpoint control	No relevant variants
CLK2	S-phase check point and biological clock protein	No relevant variants
PER1	S-phase check point and biological clock protein	No relevant variants

DISCUSSION

In the last decades, the improvement of diet, hygiene and health services has enhanced human life expectancy. Concomitantly, aging-associated diseases, such as cancer, neurodegenerative disorders and cardiovascular pathologies have substantially increased. Hence, aging research has become a growing field, not with the main objective of extending lifespan but to achieve healthy aging by minimizing the risk of disease. Integrative approaches are being applied to elucidate the mechanisms of aging and to propose novel therapeutic approaches against age-related diseases. In this Doctoral Thesis, we have evaluated new intervention strategies against age-related diseases, studied potentially anti-aging features of the DNA repair machinery in long-lived species, and explored the regulatory mechanisms involved in loss of proteostasis.

Over the last years, different therapeutic approaches against Hutchinson-Gilford progeria syndrome (HGPS) have been tested in cellular and animal models of the disease. These potential therapies include strategies designed to avoid progerin farnesylation[88], some anti-inflammatory compounds[79], or antisense oligonucleotides that block the aberrant splicing of *LMNA*[70], among several others. However, when some of these therapies were moved to clinical trials, they provided limited benefits in patients[94,96]. Besides, these drugs required continuous administration, which represented in some cases an offset[70]. Since HGPS is associated with a significant decrease in the quality of life and premature death of patients —in most cases during childhood or adolescence— the development of new therapeutic strategies with longer-term effects are still urgently needed. Furthermore, due to their common mechanisms, physiological aging could also benefit from the development of some of these therapeutic strategies, increasing the importance of HGPS research.

In this work, we have presented a CRISPR/Cas9-based gene editing approach that targets exon 11 of *LMNA*, interfering permanently and specifically with lamin A and progerin expression (**section 1**). A single dose of one sgRNA together with the *Staphylococcus aureus* Cas9 was administered to P3 $Lmna^{G609G/G609G}$ mice by using adeno-associated viruses. As a result, a reduction in their progeroid phenotype and an extension of in their lifespan was obtained. Remarkably, a concurrent study by Beyret and colleagues described a very similar gene-editing strategy against HGPS[210]. In their case, the CRISPR/Cas9 system was similarly tested in neonatal progeroid mice using the

AAV9 delivery method. Though, they crossed our *Lmna*$^{G609G/G609G}$ mouse model with *Streptococcus pyogenes* Cas9 transgenic mice, so these experimental animals already expressed the nuclease constitutively, and consequently they only had to deliver their sgRNAs by the AAV system. This way, a higher efficiency was achieved with their approximation, but as a counterbalance, its direct translation to humans would not possible. However, comparable encouraging results were obtained in both studies. A lifespan extension of a 26%, and a reduction in body weight loss and in gastric mucosa atrophy was reported in both cases. Besides, Beyret and colleagues found a higher grip strength in treated progeroid mice, while we observed a decrease in muscular fibrosis. These similar and complementing results obtained in two independent laboratories strength the hypothesis of the use of CRISPR/Cas9-based strategies as a potential treatment for HGPS.

Noteworthy, it was earlier published that the coexistence of progeroid and normal cells at an approximately 50/50 ratio in a mosaic mouse model results in a completely normal phenotype and lifespan expectancy[188]. In the current work, the editing efficiency was lower and not achieved in all organs, observing a 13.6% of edition in genome copies in liver, 5.3% in heart, 4.1% in muscle, and 1.1% in lung. Still, significant phenotype amelioration and lifespan extension were obtained in progeroid mice (**Fig. 28**). This indicates that edition of the total number of cells in the organism would not be necessary for an important amelioration of HGPS symptoms in patients. Besides, the higher edition rates obtained in the liver, together with the general phenotype amelioration —including non-edited organs, such as the kidney— could point to a systemic effect of this approach. This might be supported by the multifactorial condition of aging. Other groups have shown that clearance of senescent cells in certain tissues of a progeroid mouse model can delay premature aging phenotypes in other organs in a non-cell-autonomous manner[40]. On the other hand, it is important to point out that we have proved that progerin clearance is efficient when the CRISPR/Cas9 system is administered to neonatal mice, but we do not know the effects in older animals. As HGPS is normally diagnosed between 3.5 months and 4 years[61], the establishment of a timeframe when elimination of progerin has positive effects in the aging-associated phenotypes is also desirable.

It is important to point out that lamin A seems to be dispensable in cells and mice, but it surely plays a role in the cell nucleus and the consequences of abolishing its expression in humans remain still unexplored. Some studies have attributed important

functions to lamin A related to targeting specific proteins to the nuclear envelope. Notwithstanding these preliminary observations, cells lacking lamin A show very little nuclear alterations and mice deficient in this protein show an apparent normal phenotype[70,80]. However, these mice are not completely identical to their wild-type littermates. They present extended lifespan (about 10% longer than normal mice), decreased energy metabolism with weight gain, slight insulin resistance, fewer mitochondria and higher incidence of some types of tumors[211] (**Fig. 28**). Thus, the different *LMNA* isoforms may play antagonistic roles in energy metabolism. It is also necessary to highlight that mice seem to be more resistant to alterations in lamins A and C, proven by the milder phenotypes obtained with strong mutations, so extrapolation of these results to humans has to be taken with precaution. Nevertheless, given the severe phenotypes caused by progerin accumulation, at present it seems more preferable to eliminate lamin A in patients than to allow progerin accumulation in the cell nucleus.

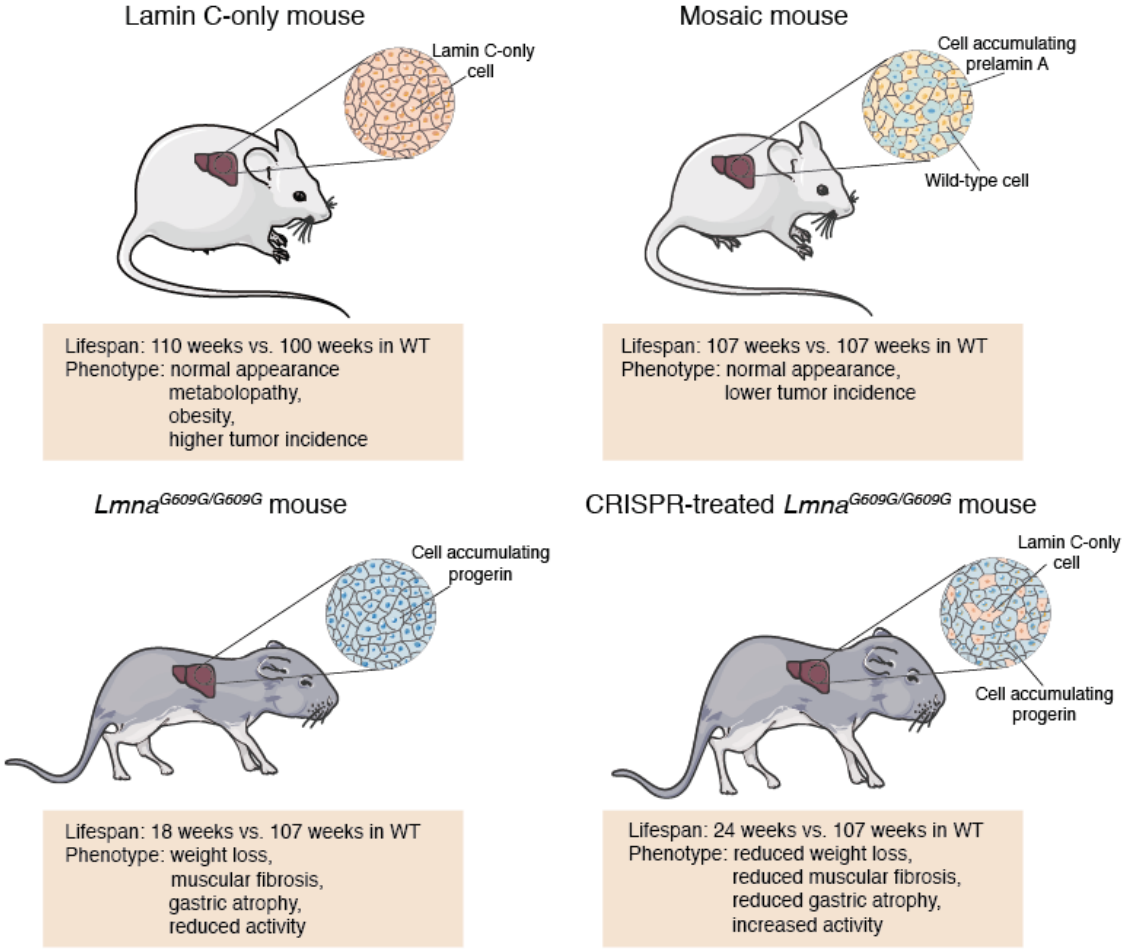

Figure 19. Comparison of mouse models accumulating different isoforms of lamin A. Lamin C-only mouse do not express lamin A in their cells and they live longer than wild-type mice. However, they develop obesity and show a higher incidence of some types of tumors. The prelamin A mosaic mouse model has a 50% of prelamin A-accumulating cells and a 50% of wild-type cells. They have a normal lifespan and show

a higher resistance to some types of tumors induced by chemical carcinogenesis. *Lmna*$^{G609G/G609G}$ mice accumulate progerin in all their cells and show a progeroid phenotype, with weight loss and muscular fibrosis. Lamin A and progerin production was suppressed in a low percentage of cells in this mouse model upon treatment with our CRISPR strategy. These mice show an extended lifespan and a reduced progeroid phenotype compared to the non-treated *Lmna*$^{G609G/G609G}$ mice. This figure was made with Servier Medical Art templates, which are licensed under a Creative Commons Attribution 3.0 Unported License: (https://smart.servier.com).

After publication of our results, Suzuki and colleagues developed a novel knock-in CRISPR/Cas9-based system known as "intercellular linearized single homology arm donor mediated intron-targeting integration (SATI)"[212]. This tool requires a double-strand break induction and a single homology arm donor and relies on both HDR and NHEJ repair pathways in the cell. To prove its potential as a gene therapy, they also tested this system in P1 *Lmna*$^{G609G/G609G}$ progeroid mice by AAV9 delivery. The efficiency of gene correction was a 2.07% in liver and 0.14% in heart, being more common the introduction of small indels at exon 10. Despite this low correction rate, a noteworthy lifespan extension of 44% and an amelioration of the progeroid phenotype in different organs was observed. This could be again explained by a systemic effect of progerin elimination on other non-edited cells or organs, and supports our previous data. Interestingly, Suzuki and colleagues also tested the system in the skeletal muscle of 10-week-old progeroid mice by local injection with positive results. This suggests that progerin clearance could have therapeutic beneficial effects beyond the neonatal stage[212]. Nevertheless, a more profound exam of the consequences of *LMNA* edition in adult mice is still desired.

Over the last two years, a diverse new group of genome editing tools have evolved from the original CRISPR/Cas9 systems, offering the possibility of introducing a wide variety of genetic changes at multiple positions in the genome[213]. This rapid development has given rise to potential methods to treat genetic diseases by replacing the mutated base with a relative high efficiency, which could likewise be relevant for HGPS treatment. One of these novel techniques is the use of base editors, which can install specific point mutations avoiding the introduction of double-strand breaks or the necessity of a donor DNA template[113]. This can be achieved by their two main components, a catalytically inactive Cas nuclease and a deaminase enzyme. Depending on their activity, these base editors can be grouped into adenine base editors (ABEs), converting A•T into G•C base pairs, and cytosine base editors (CBEs), converting C•G into T•A base pairs. The high size of the base editors could represent a major setback for *in vivo* administration, but split ABEs and CBEs have already been engineered for their delivery as dual AAVs and

their later reconstitution by trans-splicing inteins in the cell[214]. In HGPS, the most common mutation occurs by the conversion of a cytosine into a thymine at position c.1824 of the *LMNA* gene. Due to the existence of different PAM sequences nearby, this change could in principle be reverted by using the ABE system. An even more recent tool is the prime editing system, which can introduce any point mutation as well as small insertions and deletions[114]. This tool is based on a chimeric protein with Cas9 nickase and reverse transcriptase activities that is guided by a prime editing guide RNA (pegRNA), containing both the target site and the template sequence for the desired modification. Still, prime editing tool has yet to be adapted for *in vivo* delivery but it could also constitute another promising pathway for HGPS treatment. Certainly, both alternative systems need to be tested in HGPS mouse models and it is tempting to speculate that they could reverse at least part of the progeroid phenotype by specifically correcting the mutation. Besides, another interesting approximation would be to edit the cryptic splice site of *LMNA*. By using this "geroediting" approach, progerin accumulation would also be avoided under normal conditions, and could finally unravel the role of this protein in physiological aging.

There seems to be no doubt that constant improvement of these editing tools will lead to more efficient and safer ways to treat diseases by gene edition. Further research on putative off-target events and adverse effects of these genome editing systems is needed to ensure the safety of these interventions. Nevertheless, an encouraging clinical trial has been initiated using SaCas9 for the treatment of Leber congenital amaurosis 10 (LCA10), a vision disorder affecting the retina (ClinicalTrials.gov: NCT03872479). Altogether, our study and the works from Beyret, Suzuki and colleagues, show preclinical efficacy of genome editing in a mouse model of progeria and pave the way for the use of CRISPR/Cas9 in HGPS and other currently incurable systemic diseases.

Apart from accelerated aging syndromes, geroscience can also benefit from the study of long-lived species. Multi-omic analyses of these species can shed some light on the evolution of longevity, as it has been already exemplified in the genomic and transcriptomic analysis of the bowhead whale[11,215], the African elephant[56] or the naked mole rat[10]. These mammals have a relatively long lifespan and lack an aging phenotype most of their lives, with a comparative reduced risk of cancer. Improvements in different hallmarks of aging, such as enhanced proteostasis or improved mitochondrial function

were reported in some of them. Moreover, positive selection was also observed in genes involved in genomic stability, especially in DNA repair genes. Impairments in DNA repair mechanisms have been thoroughly described in both progeroid syndromes and cancer[4]. To deepen into the mechanisms of extended longevity and cancer protection of some animal species, the second objective of this Doctoral Thesis was focused on manually analyzing repair-related genes in two giant tortoises, *Chelonoidis abingdonii*, represented by the iconic Lonesome George, and *Aldabrachelys gigantea* (**section 2**). Both tortoises are estimated to live more than 100 years, being among the longest-living reptiles, and present a low risk of cancer.

The transcription factor p53 —encoded by *TP53*— is commonly known as the guardian of the genome. It has a major role in tumor suppression and DNA damage response by enhancing cell cycle arrest, senescence and apoptosis[216]. *TP53* is mutated in most types of cancer inducing aggressive proliferation[194]. Noteworthy, multiple retrogenes of *TP53* have been identified in the African and Asian elephants, which lead to higher levels of p53 and enhanced apoptosis in cells as a response to DNA damage[56,217]. The blind mole rat *Spalax* shows two variants in *TP53* (p.R174K and p.R209K compared to humans). These p53 variants were described to upregulate cell cycle arrest genes and downregulate apoptosis[218]. Our analysis of p53 uncovered a specific variant in *C. abingdonii* and *A. gigantea* (p.S106E), shared with other Testudines and some species of fish. This variant has also been described in the root vole *Microtus oeconomus* as an adaptation to hypoxia[197]. This mammal lives in the Tibet plateau and shows altered transcriptional regulation as a response to extreme conditions, suppressing the expression of proapoptotic genes[197]. Since neither *C. abingdonii* nor *A. gigantea* lived in an anoxic or cold environment, this variant could be explained as a conserved residual trace of evolution. Still, it is interesting how different adaptations in p53 have a pro-apoptotic or anti-apoptotic response to stress in long-lived organisms. Interestingly, another adaptation to hypoxia has been found in giant tortoises, the presence of globin X (GbX), which is present in red blood cells and can effectively reduce nitrite[219,220]. It would be noteworthy to consider how these adaptations to stress can contribute to longevity. In this sense, functional analyses would be necessary to determine the relevance of these variants in giant tortoise's response to DNA damage. Nevertheless, the central role of p53 in maintaining genome integrity remains highlighted by the fact that certain variants can contribute to cancer resistance and environmental adaptations in wild animals.

Besides *TP53*, changes in genes involved in NHEJ also stood out in giant tortoises. These species presented variants in two in X-ray repair cross complementing genes, *XRCC5* (p.K568N) and *XRCC6* (p.K556N), which affected sumoylation sites. Interestingly, the long-lived naked mole rat *Heterocephalus glaber* also presented the p.K556N variant in *XRCC6*, and this gene was described to be upregulated in this species as well[200]. Sumoylation occurs in over 1,600 proteins, including important DNA repair factors such as PCNA, BRCA1 and 53BP1[221]. This process plays a key role in DNA repair response by modulating specific protein-protein interactions, localization or activity of its substrates[206]. Therefore, variants found on these sumoylation sites could have an effect in the function of these repair proteins.

Copy number variations can easily affect the levels and function of specific proteins in the cell and can lead to innovations in the frame of evolution[222]. Duplications in DNA repair genes have been identified in different long-lived species, being tempting to relate them with their extended longevity. For instance, a duplication in the *PCNA* gene was described in the bowhead whale[11]. In our study, we identified a duplication affecting *NEIL1*, a DNA glycosylase involved in base excision repair[199]. Remarkably, previous studies have identified an elevated expression of *NEIL1* in naked mole rats and humans compared to mice, which can contribute to their extended longevity[200]. Besides, naked mole rat cells show higher excision repair than mouse cells[223]. Another duplication was observed affecting *RMI2*, which is involved in processing double Holliday junctions during DNA replication to prevent genome instability[202]. Our initial functional studies indicated that human cells overexpressing *RMI2* and *NEIL1* could respond better to induced stress. Although additional studies involving cells from turtles and tortoises are required, these preliminary results add *NEIL1* and *RMI2* to the list of DNA repair candidate genes in long-lived species involved in longevity extension and cancer protection.

An early study has explored the link between longevity and DNA repair in cells from different vertebrate species without observing any association[224]. However, important technical issues could have hindered the interpretation of its results. To further understand DNA repair mechanisms in long-lived reptiles, additional studies are needed. Our first analysis points to a high preservation of DNA damage response genes in giant tortoises compared to humans. However, specific variants found in *TP53*, *XRCC5*, *XRCC6* and *DCLRE1B*, together with the duplications in *NEIL1* and *RMI2* could suggest

small differences in the regulation, function or interaction of certain repair factors. These disparities in DNA repair mechanisms compared to other organisms could explain the extended longevity observed in giant tortoises. Altogether, these results support the idea that genomic analysis of wild animal species can contribute to identify biomarkers of aging an aged and age-related diseases, but besides, they can also help to protect endangered species.

In summary, in this Doctoral Thesis, we have explored different approximations to further understand the mechanisms involved in aging and age-related diseases and propose new therapies based on them. First, we evaluated a novel gene editing approach as a therapy for HGPS with encouraging preclinical results. Elimination of progerin in a modest percentage of mouse cells promoted lifespan and ameliorated the progeroid phenotype in a possibly systemic way. Interestingly, this system could also be relevant to elucidate the role of progerin in normal aging. Besides, our bioinformatic work has provided new candidate genes for longevity extension involved in genome integrity maintenance. Finally, we have further investigated the role of proteostasis in both aging and cancer and explored its modulation through genetic and dietary interventions. Hopefully, our work will contribute to unravel the multifaceted mechanisms involved in aging and to progress in the development of new intervention approaches against its associated diseases.

CONCLUSIONS

1. CRISPR/Cas9-editing of exon 11 of *LMNA* reduces lamin A and progerin expression, and prevents nuclear abnormalities in HGPS cells.
2. *In vivo* delivery of a *Lmna*-specific CRISPR/Cas9 system in HGPS mice extends lifespan and alleviates the progeroid phenotype.
3. DNA repair genes show specific changes in long-lived tortoises, involving copy number variations and missense variants.

CONCLUSIONES

1. El sistema CRISPR/Cas9 dirigido contra el exón 11 de *LMNA* reduce los niveles de lamina A y progerina, y previene las anormalidades nucleares en células HGPS.
2. La administración *in vivo* de un sistema CRISPR/Cas9 específico de *Lmna* en ratones HGPS extiende su esperanza de vida y atenúa su fenotipo progeroide.
3. Los genes de reparación del DNA muestran cambios específicos en las tortugas gigantes longevas, incluyendo variaciones en el número de copias y variantes de cambio de sentido.

BIBLIOGRAPHY

1. López-Otín, C., Blasco, M.A., Partridge, L., Serrano, M. & Kroemer, G. The hallmarks of aging. *Cell* **153**, 1194-1217 (2013).

2. Fulop, T., Larbi, A., Khalil, A., Cohen, A.A. & Witkowski, J.M. Are we ill because we age? *Front Physiol* **10**, 1508 (2019).

3. Hanahan, D. & Weinberg, R.A. Hallmarks of cancer: the next generation. *Cell* **144**, 646-674 (2011).

4. Hoeijmakers, J.H. DNA damage, aging, and cancer. *N Engl J Med* **361**, 1475-1485 (2009).

5. Flatt, T. & Partridge, L. Horizons in the evolution of aging. *BMC Biol* **16**, 93 (2018).

6. Campisi, J.*, et al.* From discoveries in ageing research to therapeutics for healthy ageing. *Nature* **571**, 183-192 (2019).

7. Eisenstein, M. Centenarians: Great expectations. *Nature* **492**, S6-8 (2012).

8. Xiao, F.H.*, et al.* Transcriptome evidence reveals enhanced autophagy-lysosomal function in centenarians. *Genome Res* **28**, 1601-1610 (2018).

9. Santos-Lozano, A.*, et al.* Successful aging: insights from proteome analyses of healthy centenarians. *Aging (Albany NY)* **12**, 3502-3515 (2020).

10. Kim, E.B.*, et al.* Genome sequencing reveals insights into physiology and longevity of the naked mole rat. *Nature* **479**, 223-227 (2011).

11. Keane, M.*, et al.* Insights into the evolution of longevity from the bowhead whale genome. *Cell Rep* **10**, 112-122 (2015).

12. Huang, Z.*, et al.* Longitudinal comparative transcriptomics reveals unique mechanisms underlying extended healthspan in bats. *Nat Ecol Evol* **3**, 1110-1120 (2019).

13. Gordon, L.B., Rothman, F.G., López-Otín, C. & Misteli, T. Progeria: a paradigm for translational medicine. *Cell* **156**, 400-407 (2014).

14. Niedernhofer, L.J.*, et al.* Nuclear genomic instability and aging. *Annu Rev Biochem* **87**, 295-322 (2018).

15. Oshima, J., Sidorova, J.M. & Monnat, R.J., Jr. Werner syndrome: Clinical features, pathogenesis and potential therapeutic interventions. *Ageing Res Rev* **33**, 105-114 (2017).

16. Baker, D.J.*, et al.* Increased expression of BubR1 protects against aneuploidy and cancer and extends healthy lifespan. *Nat Cell Biol* **15**, 96-102 (2013).

17. Hayflick, L. & Moorhead, P.S. The serial cultivation of human diploid cell strains. *Exp Cell Res* **25**, 585-621 (1961).

18. Shay, J.W. & Wright, W.E. Telomeres and telomerase: three decades of progress. *Nat Rev Genet* **20**, 299-309 (2019).

19. Boonekamp, J.J., Simons, M.J., Hemerik, L. & Verhulst, S. Telomere length behaves as biomarker of somatic redundancy rather than biological age. *Aging Cell* **12**, 330-332 (2013).

20. Bernardes de Jesus, B., *et al.* Telomerase gene therapy in adult and old mice delays aging and increases longevity without increasing cancer. *EMBO Mol Med* **4**, 691-704 (2012).

21. Muñóz-Lorente, M.A., Cano-Martín, A.C. & Blasco, M.A. Mice with hyper-long telomeres show less metabolic aging and longer lifespans. *Nat Commun* **10**, 4723 (2019).

22. Cheung, P., *et al.* Single-cell chromatin modification profiling reveals increased epigenetic variations with aging. *Cell* **173**, 1385-1397 e1314 (2018).

23. Mostoslavsky, R., *et al.* Genomic instability and aging-like phenotype in the absence of mammalian SIRT6. *Cell* **124**, 315-329 (2006).

24. Kanfi, Y., *et al.* The sirtuin SIRT6 regulates lifespan in male mice. *Nature* **483**, 218-221 (2012).

25. Hipp, M.S., Kasturi, P. & Hartl, F.U. The proteostasis network and its decline in ageing. *Nat Rev Mol Cell Biol* **20**, 421-435 (2019).

26. Kaushik, S. & Cuervo, A.M. Proteostasis and aging. *Nat Med* **21**, 1406-1415 (2015).

27. Yun, C., *et al.* Proteasomal adaptation to environmental stress links resistance to proteotoxicity with longevity in Caenorhabditis elegans. *Proc Natl Acad Sci U S A* **105**, 7094-7099 (2008).

28. Zhang, C. & Cuervo, A.M. Restoration of chaperone-mediated autophagy in aging liver improves cellular maintenance and hepatic function. *Nat Med* **14**, 959-965 (2008).

29. Fernández, A.F., *et al.* Disruption of the beclin 1-BCL2 autophagy regulatory complex promotes longevity in mice. *Nature* **558**, 136-140 (2018).

30. Johnson, S.C. Nutrient sensing, signaling and ageing: The role of IGF-1 and mTOR in ageing and age-related disease. *Subcell Biochem* **90**, 49-97 (2018).

31. López-Otín, C., Galluzzi, L., Freije, J.M.P., Madeo, F. & Kroemer, G. Metabolic control of longevity. *Cell* **166**, 802-821 (2016).

32. Kroemer, G., López-Otín, C., Madeo, F. & de Cabo, R. Carbotoxicity-noxious effects of carbohydrates. *Cell* **175**, 605-614 (2018).

33. Harrison, D.E., *et al.* Rapamycin fed late in life extends lifespan in genetically heterogeneous mice. *Nature* **460**, 392-395 (2009).

34. Mattison, J.A., *et al.* Caloric restriction improves health and survival of rhesus monkeys. *Nat Commun* **8**, 14063 (2017).

35. Green, D.R., Galluzzi, L. & Kroemer, G. Mitochondria and the autophagy-inflammation-cell death axis in organismal aging. *Science* **333**, 1109-1112 (2011).

36. Vermulst, M., *et al.* DNA deletions and clonal mutations drive premature aging in mitochondrial mutator mice. *Nat Genet* **40**, 392-394 (2008).

37. Edgar, D., *et al.* Random point mutations with major effects on protein-coding genes are the driving force behind premature aging in mtDNA mutator mice. *Cell Metab* **10**, 131-138 (2009).

38. Muñoz-Espín, D. & Serrano, M. Cellular senescence: from physiology to pathology. *Nat Rev Mol Cell Biol* **15**, 482-496 (2014).

39. Gorgoulis, V., *et al.* Cellular senescence: defining a path forward. *Cell* **179**, 813-827 (2019).

40. Baker, D.J., *et al.* Clearance of p16Ink4a-positive senescent cells delays ageing-associated disorders. *Nature* **479**, 232-236 (2011).

41. Baker, D.J., *et al.* Naturally occurring p16(Ink4a)-positive cells shorten healthy lifespan. *Nature* **530**, 184-189 (2016).

42. Maryanovich, M., *et al.* Adrenergic nerve degeneration in bone marrow drives aging of the hematopoietic stem cell niche. *Nat Med* **24**, 782-791 (2018).

43. Muñoz-Cánoves, P., Neves, J. & Sousa-Victor, P. Understanding muscle regenerative decline with aging: new approaches to bring back youthfulness to aged stem cells. *FEBS J* **287**, 406-416 (2020).

44. Navarro Negredo, P., Yeo, R.W. & Brunet, A. Aging and rejuvenation of neural stem cells and their niches. *Cell Stem Cell* **27**, 202-223 (2020).

45. Neves, J., Sousa-Victor, P. & Jasper, H. Rejuvenating strategies for stem cell-based therapies in aging. *Cell Stem Cell* **20**, 161-175 (2017).

46. Russell, S.J. & Kahn, C.R. Endocrine regulation of ageing. *Nat Rev Mol Cell Biol* **8**, 681-691 (2007).

47. Zhang, G., *et al.* Hypothalamic programming of systemic ageing involving IKK-beta, NF-kappaB and GnRH. *Nature* **497**, 211-216 (2013).

48. Desdin-Mico, G., *et al.* T cells with dysfunctional mitochondria induce multimorbidity and premature senescence. *Science* **368**, 1371-1376 (2020).

49. Conboy, I.M., *et al.* Rejuvenation of aged progenitor cells by exposure to a young systemic environment. *Nature* **433**, 760-764 (2005).

50. Loffredo, F.S., *et al.* Growth differentiation factor 11 is a circulating factor that reverses age-related cardiac hypertrophy. *Cell* **153**, 828-839 (2013).

51. Kang, S., Moser, V.A., Svendsen, C.N. & Goodridge, H.S. Rejuvenating the blood and bone marrow to slow aging-associated cognitive decline and Alzheimer's disease. *Commun Biol* **3**, 69 (2020).

52. Bárcena, C., *et al.* Healthspan and lifespan extension by fecal microbiota transplantation into progeroid mice. *Nat Med* **25**, 1234-1242 (2019).

53. Singh, P.P., Demmitt, B.A., Nath, R.D. & Brunet, A. The genetics of aging: a vertebrate perspective. *Cell* **177**, 200-220 (2019).

54. Valenzano, D.R., *et al.* The African turquoise killifish genome provides insights into evolution and genetic architecture of lifespan. *Cell* **163**, 1539-1554 (2015).

55. Seim, I., *et al.* Genome analysis reveals insights into physiology and longevity of the Brandt's bat Myotis brandtii. *Nat Commun* **4**, 2212 (2013).

56. Abegglen, L.M., *et al.* Potential mechanisms for cancer resistance in elephants and comparative cellular response to DNA damage in humans. *JAMA* **314**, 1850-1860 (2015).

57. Sahm, A., *et al.* Higher gene expression stability during aging in long-lived giant mole-rats than in short-lived rats. *Aging (Albany NY)* **10**, 3938-3956 (2018).

58. Melzer, D., Pilling, L.C. & Ferrucci, L. The genetics of human ageing. *Nat Rev Genet* **21**, 88-101 (2020).

59. Yu, C.E., *et al.* Positional cloning of the Werner's syndrome gene. *Science* **272**, 258-262 (1996).

60. Croteau, D.L., Popuri, V., Opresko, P.L. & Bohr, V.A. Human RecQ helicases in DNA repair, recombination, and replication. *Annu Rev Biochem* **83**, 519-552 (2014).

61. Merideth, M.A., *et al.* Phenotype and course of Hutchinson-Gilford progeria syndrome. *N Engl J Med* **358**, 592-604 (2008).

62. Hennekam, R.C. Hutchinson-Gilford progeria syndrome: review of the phenotype. *Am J Med Genet A* **140**, 2603-2624 (2006).

63. Eriksson, M., *et al.* Recurrent de novo point mutations in lamin A cause Hutchinson-Gilford progeria syndrome. *Nature* **423**, 293-298 (2003).

64. De Sandre-Giovannoli, A., *et al.* Lamin a truncation in Hutchinson-Gilford progeria. *Science* **300**, 2055 (2003).

65. Goldman, R.D., *et al.* Accumulation of mutant lamin A causes progressive changes in nuclear architecture in Hutchinson-Gilford progeria syndrome. *Proc Natl Acad Sci U S A* **101**, 8963-8968 (2004).

66. Ashapkin, V.V., Kutueva, L.I., Kurchashova, S.Y. & Kireev, II. Are there common mechanisms between the Hutchinson-Gilford progeria syndrome and natural aging? *Front Genet* **10**, 455 (2019).

67. Scaffidi, P. & Misteli, T. Lamin A-dependent nuclear defects in human aging. *Science* **312**, 1059-1063 (2006).

68. Pendás, A.M., *et al.* Defective prelamin A processing and muscular and adipocyte alterations in Zmpste24 metalloproteinase-deficient mice. *Nat Genet* **31**, 94-99 (2002).

69. Varga, R., *et al.* Progressive vascular smooth muscle cell defects in a mouse model of Hutchinson-Gilford progeria syndrome. *Proc Natl Acad Sci U S A* **103**, 3250-3255 (2006).

70. Osorio, F.G., *et al.* Splicing-directed therapy in a new mouse model of human accelerated aging. *Sci Transl Med* **3**, 106ra107 (2011).

71. Dorado, B., *et al.* Generation and characterization of a novel knockin minipig model of Hutchinson-Gilford progeria syndrome. *Cell Discov* **5**, 16 (2019).

72. Wang, F., *et al.* Generation of a Hutchinson-Gilford progeria syndrome monkey model by base editing. *Protein Cell* (2020).

73. Osorio, F.G., Obaya, A.J., López-Otín, C. & Freije, J.M. Accelerated ageing: from mechanism to therapy through animal models. *Transgenic Res* **18**, 7-15 (2009).

74. Osorio, F.G., *et al.* Cell autonomous and systemic factors in progeria development. *Biochem Soc Trans* **39**, 1710-1714 (2011).

75. Varela, I., *et al.* Accelerated ageing in mice deficient in Zmpste24 protease is linked to p53 signalling activation. *Nature* **437**, 564-568 (2005).

76. Mariño, G., *et al.* Premature aging in mice activates a systemic metabolic response involving autophagy induction. *Hum Mol Genet* **17**, 2196-2211 (2008).

77. Espada, J., *et al.* Nuclear envelope defects cause stem cell dysfunction in premature-aging mice. *J Cell Biol* **181**, 27-35 (2008).

78. Mariño, G., *et al.* Insulin-like growth factor 1 treatment extends longevity in a mouse model of human premature aging by restoring somatotroph axis function. *Proc Natl Acad Sci U S A* **107**, 16268-16273 (2010).

79. Osorio, F.G., *et al.* Nuclear lamina defects cause ATM-dependent NF-kappaB activation and link accelerated aging to a systemic inflammatory response. *Genes Dev* **26**, 2311-2324 (2012).

80. Fong, L.G., *et al.* Prelamin A and lamin A appear to be dispensable in the nuclear lamina. *J Clin Invest* **116**, 743-752 (2006).

81. Harhouri, K., *et al.* An overview of treatment strategies for Hutchinson-Gilford Progeria syndrome. *Nucleus* **9**, 246-257 (2018).

82. Xu, S. & Jin, Z.G. Hutchinson-Gilford progeria syndrome: cardiovascular pathologies and potential therapies. *Trends Biochem Sci* **44**, 561-564 (2019).

83. Toth, J.I., *et al.* Blocking protein farnesyltransferase improves nuclear shape in fibroblasts from humans with progeroid syndromes. *Proc Natl Acad Sci U S A* **102**, 12873-12878 (2005).

84. Glynn, M.W. & Glover, T.W. Incomplete processing of mutant lamin A in Hutchinson-Gilford progeria leads to nuclear abnormalities, which are reversed by farnesyltransferase inhibition. *Hum Mol Genet* **14**, 2959-2969 (2005).

85. Yang, S.H., *et al.* Blocking protein farnesyltransferase improves nuclear blebbing in mouse fibroblasts with a targeted Hutchinson-Gilford progeria syndrome mutation. *Proc Natl Acad Sci U S A* **102**, 10291-10296 (2005).

86. Mallampalli, M.P., Huyer, G., Bendale, P., Gelb, M.H. & Michaelis, S. Inhibiting farnesylation reverses the nuclear morphology defect in a HeLa cell model for Hutchinson-Gilford progeria syndrome. *Proc Natl Acad Sci U S A* **102**, 14416-14421 (2005).

87. Capell, B.C., *et al.* Inhibiting farnesylation of progerin prevents the characteristic nuclear blebbing of Hutchinson-Gilford progeria syndrome. *Proc Natl Acad Sci U S A* **102**, 12879-12884 (2005).

88. Fong, L.G., *et al.* A protein farnesyltransferase inhibitor ameliorates disease in a mouse model of progeria. *Science* **311**, 1621-1623 (2006).

89. Yang, S.H., *et al.* A farnesyltransferase inhibitor improves disease phenotypes in mice with a Hutchinson-Gilford progeria syndrome mutation. *J Clin Invest* **116**, 2115-2121 (2006).

90. Yang, S.H., Qiao, X., Fong, L.G. & Young, S.G. Treatment with a farnesyltransferase inhibitor improves survival in mice with a Hutchinson-Gilford progeria syndrome mutation. *Biochim Biophys Acta* **1781**, 36-39 (2008).

91. Capell, B.C., *et al.* A farnesyltransferase inhibitor prevents both the onset and late progression of cardiovascular disease in a progeria mouse model. *Proc Natl Acad Sci U S A* **105**, 15902-15907 (2008).

92. Gordon, L.B., *et al.* Clinical trial of a farnesyltransferase inhibitor in children with Hutchinson-Gilford progeria syndrome. *Proc Natl Acad Sci U S A* **109**, 16666-16671 (2012).

93. Gordon, L.B., *et al.* Impact of farnesylation inhibitors on survival in Hutchinson-Gilford progeria syndrome. *Circulation* **130**, 27-34 (2014).

94. Gordon, L.B., *et al.* Association of lonafarnib treatment vs no treatment with mortality rate in patients with Hutchinson-Gilford progeria syndrome. *JAMA* **319**, 1687-1695 (2018).

95. Varela, I., *et al.* Combined treatment with statins and aminobisphosphonates extends longevity in a mouse model of human premature aging. *Nat Med* **14**, 767-772 (2008).

96. Gordon, L.B., *et al.* Clinical trial of the protein farnesylation inhibitors lonafarnib, pravastatin, and zoledronic acid in children with Hutchinson-Gilford progeria syndrome. *Circulation* **134**, 114-125 (2016).

97. Cao, K., *et al.* Rapamycin reverses cellular phenotypes and enhances mutant protein clearance in Hutchinson-Gilford progeria syndrome cells. *Sci Transl Med* **3**, 89ra58 (2011).

98. Cenni, V., *et al.* Autophagic degradation of farnesylated prelamin A as a therapeutic approach to lamin-linked progeria. *Eur J Histochem* **55**, e36 (2011).

99. Ramos, F.J., *et al.* Rapamycin reverses elevated mTORC1 signaling in lamin A/C-deficient mice, rescues cardiac and skeletal muscle function, and extends survival. *Sci Transl Med* **4**, 144ra103 (2012).

100. Choi, J.C., *et al.* Temsirolimus activates autophagy and ameliorates cardiomyopathy caused by lamin A/C gene mutation. *Sci Transl Med* **4**, 144ra102 (2012).

101. Liao, C.Y., *et al.* Rapamycin reverses metabolic deficits in lamin A/C-deficient mice. *Cell Rep* **17**, 2542-2552 (2016).

102. Liu, B., *et al.* Resveratrol rescues SIRT1-dependent adult stem cell decline and alleviates progeroid features in laminopathy-based progeria. *Cell Metab* **16**, 738-750 (2012).

103. Bárcena, C., *et al.* Methionine restriction extends lifespan in progeroid mice and alters lipid and bile acid metabolism. *Cell Rep* **24**, 2392-2403 (2018).

104. Villa-Bellosta, R. Dietary magnesium supplementation improves lifespan in a mouse model of progeria. *EMBO Mol Med*, e12423 (2020).

105. Huang, S., *et al.* Correction of cellular phenotypes of Hutchinson-Gilford progeria cells by RNA interference. *Hum Genet* **118**, 444-450 (2005).

106. Scaffidi, P. & Misteli, T. Reversal of the cellular phenotype in the premature aging disease Hutchinson-Gilford progeria syndrome. *Nat Med* **11**, 440-445 (2005).

107. Lee, J.M., *et al.* Modulation of LMNA splicing as a strategy to treat prelamin A diseases. *J Clin Invest* **126**, 1592-1602 (2016).

108. Liu, G.H., *et al.* Targeted gene correction of laminopathy-associated LMNA mutations in patient-specific iPSCs. *Cell Stem Cell* **8**, 688-694 (2011).

109. Doudna, J.A. & Charpentier, E. Genome editing. The new frontier of genome engineering with CRISPR-Cas9. *Science* **346**, 1258096 (2014).

110. Cong, L., *et al.* Multiplex genome engineering using CRISPR/Cas systems. *Science* **339**, 819-823 (2013).

111. Ran, F.A., *et al.* Genome engineering using the CRISPR-Cas9 system. *Nat Protoc* **8**, 2281-2308 (2013).

112. Abudayyeh, O.O., *et al.* RNA targeting with CRISPR-Cas13. *Nature* **550**, 280-284 (2017).

113. Gaudelli, N.M., *et al.* Programmable base editing of A*T to G*C in genomic DNA without DNA cleavage. *Nature* **551**, 464-471 (2017).

114. Anzalone, A.V., *et al.* Search-and-replace genome editing without double-strand breaks or donor DNA. *Nature* **576**, 149-157 (2019).

115. Amoasii, L., *et al.* Single-cut genome editing restores dystrophin expression in a new mouse model of muscular dystrophy. *Sci Transl Med* **9**(2017).

116. Humbert, O., *et al.* Therapeutically relevant engraftment of a CRISPR-Cas9-edited HSC-enriched population with HbF reactivation in nonhuman primates. *Sci Transl Med* **11**(2019).

117. Jain, A., *et al.* CRISPR-Cas9-based treatment of myocilin-associated glaucoma. *Proc Natl Acad Sci U S A* **114**, 11199-11204 (2017).

118. Yang, Y., *et al.* A dual AAV system enables the Cas9-mediated correction of a metabolic liver disease in newborn mice. *Nat Biotechnol* **34**, 334-338 (2016).

119. Gao, X., *et al.* Treatment of autosomal dominant hearing loss by in vivo delivery of genome editing agents. *Nature* **553**, 217-221 (2018).

120. Treaster, S.B., *et al.* Superior proteome stability in the longest lived animal. *Age (Dordr)* **36**, 9597 (2014).

121. Pyo, J.O., *et al.* Overexpression of Atg5 in mice activates autophagy and extends lifespan. *Nat Commun* **4**, 2300 (2013).

122. Walker, G.A. & Lithgow, G.J. Lifespan extension in C. elegans by a molecular chaperone dependent upon insulin-like signals. *Aging Cell* **2**, 131-139 (2003).

123. Freilich, R., Arhar, T., Abrams, J.L. & Gestwicki, J.E. Protein-protein interactions in the molecular chaperone network. *Acc Chem Res* **51**, 940-949 (2018).

124. Soti, C. & Csermely, P. Chaperones and aging: role in neurodegeneration and in other civilizational diseases. *Neurochem Int* **41**, 383-389 (2002).

125. Schopf, F.H., Biebl, M.M. & Buchner, J. The HSP90 chaperone machinery. *Nat Rev Mol Cell Biol* **18**, 345-360 (2017).

126. Collins, G.A. & Goldberg, A.L. The logic of the 26S proteasome. *Cell* **169**, 792-806 (2017).

127. Hegde, A.N., Smith, S.G., Duke, L.M., Pourquoi, A. & Vaz, S. Perturbations of ubiquitin-proteasome-mediated proteolysis in aging and Alzheimer's disease. *Front Aging Neurosci* **11**, 324 (2019).

128. Meyer-Schwesinger, C. The ubiquitin-proteasome system in kidney physiology and disease. *Nat Rev Nephrol* **15**, 393-411 (2019).

129. Gilda, J.E. & Gomes, A.V. Proteasome dysfunction in cardiomyopathies. *J Physiol* **595**, 4051-4071 (2017).

130. Pérez, V.I., *et al.* Protein stability and resistance to oxidative stress are determinants of longevity in the longest-living rodent, the naked mole-rat. *Proc Natl Acad Sci U S A* **106**, 3059-3064 (2009).

131. Chondrogianni, N., Petropoulos, I., Franceschi, C., Friguet, B. & Gonos, E.S. Fibroblast cultures from healthy centenarians have an active proteasome. *Exp Gerontol* **35**, 721-728 (2000).

132. Shah, J.J. & Orlowski, R.Z. Proteasome inhibitors in the treatment of multiple myeloma. *Leukemia* **23**, 1964-1979 (2009).

133. Moreau, P.*, et al.* Bortezomib, thalidomide, and dexamethasone with or without daratumumab before and after autologous stem-cell transplantation for newly diagnosed multiple myeloma (CASSIOPEIA): a randomised, open-label, phase 3 study. *Lancet* **394**, 29-38 (2019).

134. Kaushik, S. & Cuervo, A.M. The coming of age of chaperone-mediated autophagy. *Nat Rev Mol Cell Biol* **19**, 365-381 (2018).

135. Madeo, F., Zimmermann, A., Maiuri, M.C. & Kroemer, G. Essential role for autophagy in life span extension. *J Clin Invest* **125**, 85-93 (2015).

136. Alfaro, I.E.*, et al.* Chaperone mediated autophagy in the crosstalk of neurodegenerative diseases and metabolic disorders. *Front Endocrinol (Lausanne)* **9**, 778 (2018).

137. Kon, M.*, et al.* Chaperone-mediated autophagy is required for tumor growth. *Sci Transl Med* **3**, 109ra117 (2011).

138. Gomes, L.R., Menck, C.F.M. & Cuervo, A.M. Chaperone-mediated autophagy prevents cellular transformation by regulating MYC proteasomal degradation. *Autophagy* **13**, 928-940 (2017).

139. Walter, P. & Ron, D. The unfolded protein response: from stress pathway to homeostatic regulation. *Science* **334**, 1081-1086 (2011).

140. Meusser, B., Hirsch, C., Jarosch, E. & Sommer, T. ERAD: the long road to destruction. *Nat Cell Biol* **7**, 766-772 (2005).

141. Khaminets, A.*, et al.* Regulation of endoplasmic reticulum turnover by selective autophagy. *Nature* **522**, 354-358 (2015).

142. Brown, M.K. & Naidoo, N. The endoplasmic reticulum stress response in aging and age-related diseases. *Front Physiol* **3**, 263 (2012).

143. Duran-Aniotz, C.*, et al.* IRE1 signaling exacerbates Alzheimer's disease pathogenesis. *Acta Neuropathol* **134**, 489-506 (2017).

144. Cubillos-Ruiz, J.R., Bettigole, S.E. & Glimcher, L.H. Tumorigenic and immunosuppressive effects of endoplasmic reticulum stress in cancer. *Cell* **168**, 692-706 (2017).

145. Taylor, R.C., Berendzen, K.M. & Dillin, A. Systemic stress signalling: understanding the cell non-autonomous control of proteostasis. *Nat Rev Mol Cell Biol* **15**, 211-217 (2014).

146. Bejarano, E.*, et al.* Connexins modulate autophagosome biogenesis. *Nat Cell Biol* **16**, 401-414 (2014).

147. Takeuchi, T.*, et al.* Intercellular chaperone transmission via exosomes contributes to maintenance of protein homeostasis at the organismal level. *Proc Natl Acad Sci U S A* **112**, E2497-2506 (2015).

148. Goetzl, E.J.*, et al.* Altered lysosomal proteins in neural-derived plasma exosomes in preclinical Alzheimer disease. *Neurology* **85**, 40-47 (2015).

149. Agosta, F., Weiler, M. & Filippi, M. Propagation of pathology through brain networks in neurodegenerative diseases: from molecules to clinical phenotypes. *CNS Neurosci Ther* **21**, 754-767 (2015).

150. Hassan, W.M., Merin, D.A., Fonte, V. & Link, C.D. AIP-1 ameliorates beta-amyloid peptide toxicity in a Caenorhabditis elegans Alzheimer's disease model. *Hum Mol Genet* **18**, 2739-2747 (2009).

151. Osorio, F.G.*, et al.* Loss of the proteostasis factor AIRAPL causes myeloid transformation by deregulating IGF-1 signaling. *Nat Med* **22**, 91-96 (2016).

152. Osorio, F.G., Freije, J.M. & López-Otín, C. The novel tumor suppressor AIRAPL regulates IGF1R proteostasis. *Cell Cycle* **15**, 873-874 (2016).

153. Santiago-Fernández, O., Osorio, F.G. & López-Otín, C. Proteostasis alterations in myeloproliferative neoplasms: Oncogenic relevance and therapeutic opportunities. *Exp Hematol* **44**, 574-577 (2016).

154. Mahmoudi, S., Xu, L. & Brunet, A. Turning back time with emerging rejuvenation strategies. *Nat Cell Biol* **21**, 32-43 (2019).

155. de Cabo, R., Carmona-Gutierrez, D., Bernier, M., Hall, M.N. & Madeo, F. The search for antiaging interventions: from elixirs to fasting regimens. *Cell* **157**, 1515-1526 (2014).

156. Lamming, D.W., Ye, L., Sabatini, D.M. & Baur, J.A. Rapalogs and mTOR inhibitors as anti-aging therapeutics. *J Clin Invest* **123**, 980-989 (2013).

157. Li, J., Kim, S.G. & Blenis, J. Rapamycin: one drug, many effects. *Cell Metab* **19**, 373-379 (2014).

158. Majumder, S., Richardson, A., Strong, R. & Oddo, S. Inducing autophagy by rapamycin before, but not after, the formation of plaques and tangles ameliorates cognitive deficits. *PLoS One* **6**, e25416 (2011).

159. Madeo, F., Carmona-Gutierrez, D., Kepp, O. & Kroemer, G. Spermidine delays aging in humans. *Aging (Albany NY)* **10**, 2209-2211 (2018).

160. Kulkarni, A.S., Gubbi, S. & Barzilai, N. Benefits of metformin in attenuating the hallmarks of aging. *Cell Metab* **32**, 15-30 (2020).

161. Baur, J.A. & Sinclair, D.A. Therapeutic potential of resveratrol: the in vivo evidence. *Nat Rev Drug Discov* **5**, 493-506 (2006).

162. Lagouge, M., *et al.* Resveratrol improves mitochondrial function and protects against metabolic disease by activating SIRT1 and PGC-1alpha. *Cell* **127**, 1109-1122 (2006).

163. Campos, J.C., *et al.* Exercise prevents impaired autophagy and proteostasis in a model of neurogenic myopathy. *Sci Rep* **8**, 11818 (2018).

164. Jamart, C., *et al.* Modulation of autophagy and ubiquitin-proteasome pathways during ultra-endurance running. *J Appl Physiol (1985)* **112**, 1529-1537 (2012).

165. He, C., *et al.* Exercise-induced BCL2-regulated autophagy is required for muscle glucose homeostasis. *Nature* **481**, 511-515 (2012).

166. Brunquell, J., Morris, S., Snyder, A. & Westerheide, S.D. Coffee extract and caffeine enhance the heat shock response and promote proteostasis in an HSF-1-dependent manner in Caenorhabditis elegans. *Cell Stress Chaperones* **23**, 65-75 (2018).

167. Fernández del Río, L., Gutiérrez-Casado, E., Varela-López, A. & Villalba, J.M. Olive oil and the hallmarks of aging. *Molecules* **21**, 163 (2016).

168. McCay, C.M., Maynard, L.A., Sperling, G. & Barnes, L.L. Retarded growth, life span, ultimate body size and age changes in the albino rat after feeding diets restricted in calories: four figures. *J Nutr* **18**, 1-13 (1939).

169. Galluzzi, L., Pietrocola, F., Levine, B. & Kroemer, G. Metabolic control of autophagy. *Cell* **159**, 1263-1276 (2014).

170. Longo, V.D. & Mattson, M.P. Fasting: molecular mechanisms and clinical applications. *Cell Metab* **19**, 181-192 (2014).

171. Nencioni, A., Caffa, I., Cortellino, S. & Longo, V.D. Fasting and cancer: molecular mechanisms and clinical application. *Nat Rev Cancer* **18**, 707-719 (2018).

172. Raffaghello, L., *et al.* Starvation-dependent differential stress resistance protects normal but not cancer cells against high-dose chemotherapy. *Proc Natl Acad Sci U S A* **105**, 8215-8220 (2008).

173. Lee, C., *et al.* Fasting cycles retard growth of tumors and sensitize a range of cancer cell types to chemotherapy. *Sci Transl Med* **4**, 124ra127 (2012).

174. Sun, P., *et al.* Fasting inhibits colorectal cancer growth by reducing M2 polarization of tumor-associated macrophages. *Oncotarget* **8**, 74649-74660 (2017).

175. Caffa, I., *et al.* Fasting potentiates the anticancer activity of tyrosine kinase inhibitors by strengthening MAPK signaling inhibition. *Oncotarget* **6**, 11820-11832 (2015).

176. Lu, Z., *et al.* Fasting selectively blocks development of acute lymphoblastic leukemia via leptin-receptor upregulation. *Nat Med* **23**, 79-90 (2017).

177. Sanjana, N.E., Shalem, O. & Zhang, F. Improved vectors and genome-wide libraries for CRISPR screening. *Nat Methods* **11**, 783-784 (2014).

178. Ran, F.A., *et al.* In vivo genome editing using Staphylococcus aureus Cas9. *Nature* **520**, 186-191 (2015).

179. Li, H. & Durbin, R. Fast and accurate long-read alignment with Burrows-Wheeler transform. *Bioinformatics* **26**, 589-595 (2010).

180. Li, H., *et al.* The Sequence Alignment/Map format and SAMtools. *Bioinformatics* **25**, 2078-2079 (2009).

181. Gnerre, S., *et al.* High-quality draft assemblies of mammalian genomes from massively parallel sequence data. *Proc Natl Acad Sci U S A* **108**, 1513-1518 (2011).

182. Boetzer, M., Henkel, C.V., Jansen, H.J., Butler, D. & Pirovano, W. Scaffolding pre-assembled contigs using SSPACE. *Bioinformatics* **27**, 578-579 (2011).

183. English, A.C., *et al.* Mind the gap: upgrading genomes with Pacific Biosciences RS long-read sequencing technology. *PLoS One* **7**, e47768 (2012).

184. Simao, F.A., Waterhouse, R.M., Ioannidis, P., Kriventseva, E.V. & Zdobnov, E.M. BUSCO: assessing genome assembly and annotation completeness with single-copy orthologs. *Bioinformatics* **31**, 3210-3212 (2015).

185. Zdobnov, E.M., *et al.* OrthoDB v9.1: cataloging evolutionary and functional annotations for animal, fungal, plant, archaeal, bacterial and viral orthologs. *Nucleic Acids Res* **45**, D744-D749 (2017).

186. Trapnell, C., Pachter, L. & Salzberg, S.L. TopHat: discovering splice junctions with RNA-Seq. *Bioinformatics* **25**, 1105-1111 (2009).

187. Quesada, V., Velasco, G., Puente, X.S., Warren, W.C. & López-Otín, C. Comparative genomic analysis of the zebra finch degradome provides new insights into evolution of proteases in birds and mammals. *BMC Genomics* **11**, 220 (2010).

188. de la Rosa, J., *et al.* Prelamin A causes progeria through cell-extrinsic mechanisms and prevents cancer invasion. *Nat Commun* **4**, 2268 (2013).

189. Sullivan, T., *et al.* Loss of A-type lamin expression compromises nuclear envelope integrity leading to muscular dystrophy. *J Cell Biol* **147**, 913-920 (1999).

190. Kotterman, M.A. & Schaffer, D.V. Engineering adeno-associated viruses for clinical gene therapy. *Nat Rev Genet* **15**, 445-451 (2014).

191. Yin, H., Kauffman, K.J. & Anderson, D.G. Delivery technologies for genome editing. *Nat Rev Drug Discov* **16**, 387-399 (2017).

192. Hamczyk, M.R., *et al.* Vascular smooth muscle-specific progerin expression accelerates atherosclerosis and death in a mouse model of Hutchinson-Gilford progeria syndrome. *Circulation* **138**, 266-282 (2018).

193. Tollis, M., *et al.* The Agassiz's desert tortoise genome provides a resource for the conservation of a threatened species. *PLoS One* **12**, e0177708 (2017).

194. Muller, P.A. & Vousden, K.H. p53 mutations in cancer. *Nat Cell Biol* **15**, 2-8 (2013).

195. Alföldi, J., *et al.* The genome of the green anole lizard and a comparative analysis with birds and mammals. *Nature* **477**, 587-591 (2011).

196. Wang, Z., *et al.* The draft genomes of soft-shell turtle and green sea turtle yield insights into the development and evolution of the turtle-specific body plan. *Nat Genet* **45**, 701-706 (2013).

197. Zhao, Y., *et al.* Codon 104 variation of p53 gene provides adaptive apoptotic responses to extreme environments in mammals of the Tibet plateau. *Proc Natl Acad Sci U S A* **110**, 20639-20644 (2013).

198. Ørsted, D.D., Bojesen, S.E., Tybjaerg-Hansen, A. & Nordestgaard, B.G. Tumor suppressor p53 Arg72Pro polymorphism and longevity, cancer survival, and risk of cancer in the general population. *J Exp Med* **204**, 1295-1301 (2007).

199. Hegde, M.L., *et al.* Prereplicative repair of oxidized bases in the human genome is mediated by NEIL1 DNA glycosylase together with replication proteins. *Proc Natl Acad Sci U S A* **110**, E3090-3099 (2013).

200. MacRae, S.L., *et al.* DNA repair in species with extreme lifespan differences. *Aging (Albany NY)* **7**, 1171-1184 (2015).

201. Shinmura, K., *et al.* Abnormal expressions of DNA glycosylase genes NEIL1, NEIL2, and NEIL3 are associated with somatic mutation loads in human cancer. *Oxid Med Cell Longev* **2016**, 1546392 (2016).

202. Daley, J.M., Chiba, T., Xue, X., Niu, H. & Sung, P. Multifaceted role of the Topo IIIalpha-RMI1-RMI2 complex and DNA2 in the BLM-dependent pathway of DNA break end resection. *Nucleic Acids Res* **42**, 11083-11091 (2014).

203. Hudson, D.F., *et al.* Loss of RMI2 increases genome instability and causes a Bloom-like syndrome. *PLoS Genet* **12**, e1006483 (2016).

204. Pace, P., *et al.* Ku70 corrupts DNA repair in the absence of the Fanconi anemia pathway. *Science* **329**, 219-223 (2010).

205. Kragelund, B.B., Weterings, E., Hartmann-Petersen, R. & Keijzers, G. The Ku70/80 ring in non-homologous end-joining: easy to slip on, hard to remove. *Front Biosci (Landmark Ed)* **21**, 514-527 (2016).

206. Cremona, C.A., *et al.* Extensive DNA damage-induced sumoylation contributes to replication and repair and acts in addition to the mec1 checkpoint. *Mol Cell* **45**, 422-432 (2012).

207. Ye, J., *et al.* TRF2 and apollo cooperate with topoisomerase 2alpha to protect human telomeres from replicative damage. *Cell* **142**, 230-242 (2010).

208. Wang, Y., Ghosh, G. & Hendrickson, E.A. Ku86 represses lethal telomere deletion events in human somatic cells. *Proc Natl Acad Sci U S A* **106**, 12430-12435 (2009).

209. Ribes-Zamora, A., Indiviglio, S.M., Mihalek, I., Williams, C.L. & Bertuch, A.A. TRF2 interaction with Ku heterotetramerization interface gives insight into c-NHEJ prevention at human telomeres. *Cell Rep* **5**, 194-206 (2013).

210. Beyret, E., *et al.* Single-dose CRISPR-Cas9 therapy extends lifespan of mice with Hutchinson-Gilford progeria syndrome. *Nat Med* **25**, 419-422 (2019).

211. López-Mejía, I.C., *et al.* Antagonistic functions of LMNA isoforms in energy expenditure and lifespan. *EMBO Rep* **15**, 529-539 (2014).

212. Suzuki, K., *et al.* Precise in vivo genome editing via single homology arm donor mediated intron-targeting gene integration for genetic disease correction. *Cell Res* **29**, 804-819 (2019).

213. Anzalone, A.V., Koblan, L.W. & Liu, D.R. Genome editing with CRISPR-Cas nucleases, base editors, transposases and prime editors. *Nat Biotechnol* **38**, 824-844 (2020).

214. Levy, J.M., *et al.* Cytosine and adenine base editing of the brain, liver, retina, heart and skeletal muscle of mice via adeno-associated viruses. *Nat Biomed Eng* **4**, 97-110 (2020).

215. Seim, I., *et al.* The transcriptome of the bowhead whale Balaena mysticetus reveals adaptations of the longest-lived mammal. *Aging (Albany NY)* **6**, 879-899 (2014).

216. Kastenhuber, E.R. & Lowe, S.W. Putting p53 in context. *Cell* **170**, 1062-1078 (2017).

217. Vázquez, J.M., Sulak, M., Chigurupati, S. & Lynch, V.J. A zombie LIF gene in elephants is upregulated by TP53 to induce apoptosis in response to DNA damage. *Cell Rep* **24**, 1765-1776 (2018).

218. Ashur-Fabian, O., *et al.* Evolution of p53 in hypoxia-stressed Spalax mimics human tumor mutation. *Proc Natl Acad Sci U S A* **101**, 12236-12241 (2004).

219. Quesada, V., *et al.* Giant tortoise genomes provide insights into longevity and age-related disease. *Nat Ecol Evol* **3**, 87-95 (2019).

220. Corti, P., *et al.* Globin X is a six-coordinate globin that reduces nitrite to nitric oxide in fish red blood cells. *Proc Natl Acad Sci U S A* **113**, 8538-8543 (2016).

221. Hendriks, I.A., *et al.* Uncovering global SUMOylation signaling networks in a site-specific manner. *Nat Struct Mol Biol* **21**, 927-936 (2014).

222. Kaessmann, H. Origins, evolution, and phenotypic impact of new genes. *Genome Res* **20**, 1313-1326 (2010).

223. Evdokimov, A., *et al.* Naked mole rat cells display more efficient excision repair than mouse cells. *Aging (Albany NY)* **10**, 1454-1473 (2018).

224. Woodhead, A.D., Satlow, R.B. & Grist, E. DNA repair and longevity in three species of cold-blooded vertebrates. *Exp Gerontol* **15**, 301-304 (1980).